Spring 5-17-2013

Regulation of the Target of Rapamycin Signaling Pathway in Saccharomyces cerevisiae

Tammy Pracheil
University of New Orleans, New Orleans, tmprache@my.uno.edu

Regulation of the Target of Rapamycin Signaling Pathway in *Saccharomyces cerevisiae*

A Dissertation

Submitted to the Faculty of
The University of New Orleans
In Partial Fulfillment of the Requirements
For the Degree of

Doctor of Philosophy
In
Chemistry

by

Tammy Marie Pracheil

B.S., University of New Orleans, New Orleans, LA 2008
M.S., University of New Orleans, New Orleans, LA 2012

May 17, 2013

To my family,

for all of their love

and support

Acknowledgements

First and foremost, I would like to thank my mentor, Dr. Zhengchang Liu for introducing me to the Department of Chemistry's PhD program and encouraging me to join his lab to conduct research towards my dissertation. His guidance both in my research and in my development as a professional has been invaluable and has challenged me to become the scientist I am today. I would also like to thank my current and former committee members, Dr. Wendy Schluchter, Dr. Bernard Rees, Dr. Mark Trudell, Dr. Richard Cole (former), Dr. Bruce Gibbs (former), and Dr. Ananthakrishnan Sankaranarayanan (former) for their advice and feedback. I would also like to thank Dr. Mary Clancy for additional experimental guidance working with Yeast. I would like to thank the late Dr. John Savage for his letter of recommendation for my acceptance into the Chemistry Department's PhD program and for his always humorous lunch time conversations which frequently included how incredibly slow the elevator in the biology building was. He will be greatly missed.

To all of my former and current lab mates, thank you for your willingness to aid me in my research whenever possible, but more importantly, thank you for your friendship.

I would like to thank my parents whom I undoubtedly attribute my talents to for their unconditional love and support, and my sister for her friendship and encouragement as I worked through the difficult times towards completing this dissertation.

To my boyfriend, Derrick, I want to thank you with all of my heart for sticking by my side for all of these years and being there for me whenever I needed you.

Table of Contents

Publications

Pracheil, T. Thorton, J. Liu, Z. TORC2 Signaling is Antagonized by Protein Phosphatase 2A and the Far Complex in *Saccharomyces cerevisiae*. *Genetics*, 2012 Apr; 190(4):1325-39.

Zhang, F. Pracheil, T. Thorton, J. Liu, Z. Adenosine Triphosphate (ATP) is a Candidate Signaling Molecule in the Mitochondria-to-Nucleus Retrograde Response Pathway. *Genes* 2013, *4*(1):86-100.

Pracheil, T. Liu, Z. Tiered Assembly of the Yeast Far3-7-8-9-10-11 Complex at the Endoplasmic Reticulum. *The Journal of Biological Chemistry* (in revision)

List of Figures and Tables

List of Abbreviations

1N	haploid
2N	diploid
5-FOA	5-fluoroorotic acid
Amp^R	ampicillin-resistance gene
ATP	adenosine triphosphate
CCM3	cerebral cavernous malformation 3
CTTNBP2	cortactin-binding protein 2
CWI	cell wall integrity
DNA	deoxyribonucleic acid
DTT	dithiothreitol
ER	endoplasmic reticulum
FAT	(FRAP, ATM, TTRAP) domain
FRB	(FKBP12-rapamycin binding) domain
GAP	GTPase activating protein
GDP	guanosine diphosphate
GEF	GDP-GTP exchange factor
GFP	green fluorescent protein
GTP	guanosine triphosphate
HEAT	(Huntington, Elongation factor 3, protein phosphatase 2A, TOR1) domain
IL-2	interleukin 2
IPTG	isopropyl β-D-1-thiogalactopyranoside
MAP	mitogen activated protein

PCR	polymerase chain reaction
PIKK	phosphatidylinositol kinase-related protein kinase
PMSF	phenylmethylsulfonyl fluoride
PP2A	protein phosphatase 2A
RFP	red fluorescent protein
RNA	ribonucleic acid
RP	ribosomal protein
SD (YNBD)	yeast nitrogen base with dextrose
SDS-PAGE	sodium dodecyl sulfate polyacrylamide gel electrophoresis
SLMAP	sarcolemmal membrane-associated protein
STRIP	striatin interacting protein
STRIPAK	striatin interacting phosphatase and kinase
TCA	trichloroacetic acid
TOR	target of rapamycin
TORC	target of rapamycin complex
YNBcasD	yeast nitrogen base with casamino acids and dextrose
YPD	yeast nitrogen base with peptone and dextrose
λ-PPase	lambda protein phosphatase

Nomenclature: *LST8* (upper case italic: wild-type gene); *lst8* (lower case italic: mutant of a gene); Lst8 (first letter upper case, the rest lower case: gene product/protein); lst8 (lower case: mutant of protein); Δ behind the gene indicates an entire gene deletion.

Abstract

An integrative, biochemical, genetic, and molecular biology approach utilizing gene manipulation, gene knock outs, plasmid based protein expression, and *in vivo* protein localization of fluorescence tagged proteins was employed to determine the function of an essential protein, Lst8, in TORC1 and TORC2 signaling and a previously uncharacterized complex, the Far3-7-8-9-10-11 complex (Far complex) in the budding yeast, *Saccharomyces cerevisiae*. Mutations in *SAC7* and *FAR11* suppressed lethality of both *lst8Δ* and *tor2-21* mutations but not TORC1 inactivation, suggesting that the essential function of Lst8 is linked only to TORC2.

Far11, a component of a six-member complex, was found to interact with Tpd3 and Pph21, conserved components of Protein Phosphatase 2A (PP2A) via co-immunoprecipitation. Mutations in *FAR11* and *RTS1,* which encodes a PP2A regulatory B subunit, restore phosphorylation to the TORC2 substrate Slm1 in a *tor2-21* mutant. These data suggest that TORC2 signaling is antagonized by Far11-dependent PP2A activity.

To characterize the assembly of the Far complex *in vivo*, intracellular localization of the Far complex was examined by fluorescence microscopy. It was found that the Far

complex localizes to the endoplasmic reticulum (ER). The data show that Far9 and Far10 are tail-anchored proteins that localize to the ER first and recruit a Far8-Far7-Far3 pre-complex. Far11 is found at the ER only when all other Far proteins are assembled at the ER. Surprisingly, ER localization is required for the Far Complex's role TORC2 signaling because deletion of the tail-anchor domain of Far9 results in partial bypass of the *tor2-21* mutant growth defect at 37 ˚C.

Keywords: Lst8; Far11; Yeast; protein phosphatase 2A; rapamycin; TOR signaling

CHAPTER I. INTRODUCTION

1.1. *Saccharomyces cerevisiae*: Baker's Yeast as a Model Organism

Saccharomyces cerevisiae or Baker's yeast is one of the most studied eukaryotes. From its applications in baking and brewing to its versatility as a model organism in the laboratory, the study of this organism continues to produce valuable information relevant to both the scientific/medical community and breweries alike. In 1996, the entire genome, approximately 12000bp or 6000 genes was sequenced (46). The following year, Botstein et al. estimated that 31% of all yeast gene products had mammalian counterparts, a number which they felt was actually much greater due to the fact that the majority of the mammalian genome had yet to be sequenced (18). This sparked the use of Baker's yeast as a model organism for the studies of mammalian pathways.

Yeast have the ability to exist as either diploids (2N) or haploids (1N) and can reproduce both sexually and asexually (6). Figure 1 summarizes the yeast cell cycle. Baker's yeast reproduce asexually through the mitotic cell cycle, a highly regulated process also known as budding where a small bud forms on the parent cell. Briefly, during progression through the mitotic cell cycle, genetic information is replicated during the S and G2 phase. Replicated DNA, organelles, and cytoplasm are then divided amongst the parent and daughter cell and the daughter cell grows until its size

approximately matches the parent cell during the M phase. At the end of the M phase, cytokinesis splits the two into separate cells and both cells enter G1 phase. Cell cycle progression is highly regulated and many signaling pathways target cell cycle progression by inhibiting progression from G1 to S phase to prevent cell proliferation in response to various signaling cues.

Haploid lab strains characteristically produce one of two mating pheromones: a-factor, and α-factor. a-type yeast cells produce a-factor and α-type cells produce α-factor. Each type cell has receptors for the opposite type factor such that when cells are in the presence of mating factor of the opposite type, cell cycle progression is halted at the G1 phase and polarized cell growth begins in the direction of the mating factor. Polarized cell growth continues until two cells of opposite mating type are able to fuse forming a new diploid cell (6).

The fate of diploid cells depends on nutrient availability. Under rich growth conditions, diploid cells will continue through the mitotic cell cycle. However, under stressful or nutrient deplete conditions diploid cells will switch to sexual reproduction or meiosis to produce new haploid cells or spores by undergoing sporulation (6, 111). Yeast geneticists widely take advantage of this unique versatility in ploidy to create specific mutant cell lines by mating haploids of certain genotypes, sporulating the

resulting diploid and selecting spores that contain the desired genotypes. This makes yeast an invaluable tool for genetic studies of conserved pathways whereby in other organisms necessary mutants are unobtainable. Yeast have the capacity to contain genetic information on plasmids. The power of yeast genetics becomes apparent when essential genes are expressed on plasmids and transformed into diploid cells heterozygous for the essential gene. When these cells are sporulated, it is possible to obtain a haploid strain that lacks the essential gene in the genome yet are sustained due to the presence of the essential gene on the plasmid. These strains are then able to be manipulated to identify mutations that allow for loss of the plasmid and by association the essential gene.

Furthermore, the usefulness of Baker's yeast as a single cellular model organism parallels that of bacterial systems in that yeast cells can be grown in a matter of days, are non-pathogenic, easily amplifiable and able to be cryogenically stored indefinitely. These characteristics paired with its conservation of eukaryotic system make Baker's yeast a highly convenient model organism.

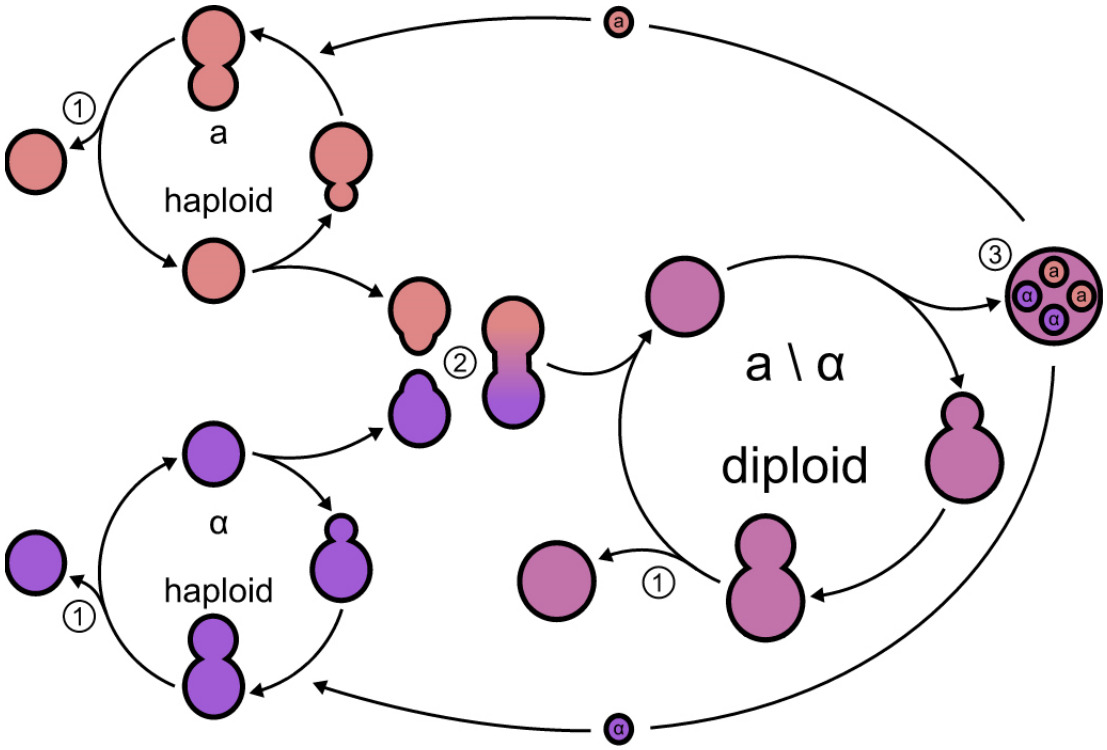

Figure 1. Stages of the yeast life cycle.

Schematic diagram of the haploid and diploid life cycles of budding yeast.

1.2. The TOR Signaling Pathway

Target of rapamycin (TOR) is a phosphatidylinositol kinase-related protein kinase (PIKK) that controls eukaryotic cell growth and proliferation in response to nutrient conditions (40, 62, 125). TOR, first identified in yeast and subsequently in mammalian cells, is inhibited by the complex of rapamycin, an immunosuppressant macrolide, and the immunophilin FKBP12, a peptidylprolyl *cis-trans* isomerase. Rapamycin, by inhibiting TOR, serves as an immunosuppressant, an inhibitor of restenosis, and a potential chemotherapeutic agent for cancer treatment (99, 104, 107, 116, 125).

1.2.1 The TOR Complexes

TORs are large protein kinases (~280 kD) conserved in most, if not all, eukaryotes (125). Fungal species may possess two TOR kinases while higher eukaryotes possess only one. The TOR kinase consists of HEAT (**H**untington, **E**longation factor 3, protein phosphatase 2**A**, **T**OR1) repeats at the amino-terminal half of the protein, a FAT (FRAP, ATM, TTRAP) domain, an FRB (FKBP12-rapamycin binding) domain, a kinase domain, and an FATC domain (Fig. 2). The TOR kinase exists in multi-protein complexes, which have been purified in yeast and mammals. There exist two distinctive TOR kinase complexes in yeast: a rapamycin-sensitive TOR Complex 1 (TORC1) (consisting of Tor1

or Tor2, Lst8, Kog1, and Tco89) and a rapamycin-insensitive TOR Complex 2 (TORC2) (consisting of Tor2, Lst8, Avo1, Avo2, Avo3, and Bit61) (Fig. 2A and 2B) (81, 94, 121). Of the two branches TORC1 has been studied the most. Both complexes are partially conserved in mammals: mTORC1 complex contains raptor, a Kog1 ortholog; mTORC2 contains rictor and mSin1, orthologs of yeast Avo3 and Avo1, respectively. GβL, the mammalian ortholog of yeast Lst8, exists in both mTORC1 and mTORC2 (41, 63, 64, 69, 70, 98, 130). TOR is a central controller of cell growth in yeast by sensing and responding to changes in nutrient conditions (100). Physiological processes regulated by TOR are also partially conserved: TORC1/mTORC1 positively regulates anabolic processes including ribosome biogenesis and protein translation while inhibiting catabolic processes such as autophagy; TORC2/mTORC2 is involved in the organization of the actin cytoskeleton (Fig. 2) (11, 57, 58, 83, 84, 102, 103, 117, 125, 133).

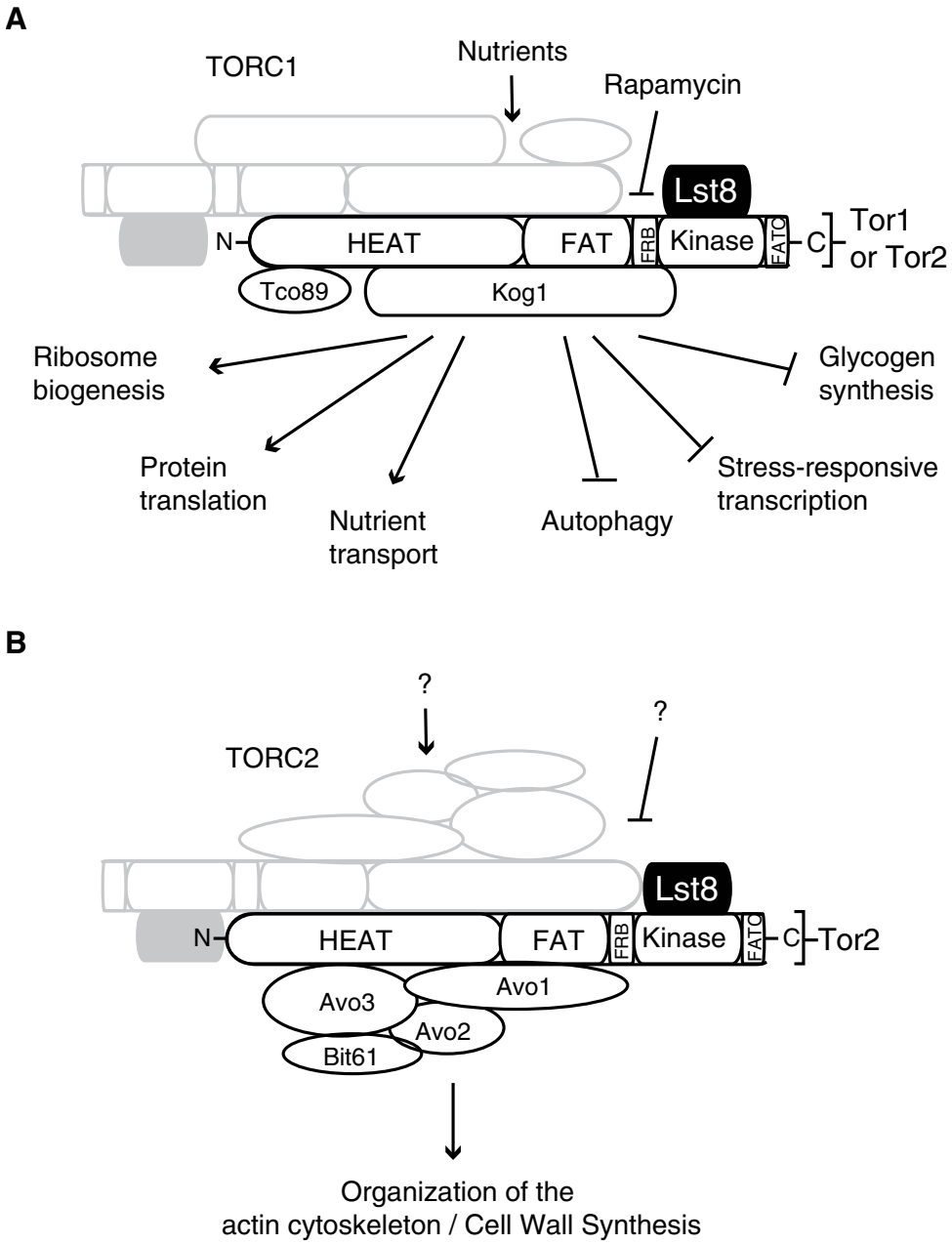

Figure 2. TOR Complex 1 (TORC1) and TOR Complex 2 (TORC2) of budding yeast.

(A) TORC1 is consisted of Tor1 or Tor2, Kog1, Lst8, and Tco89. Depicted are domains of TOR, HEAT, FAT, FRB, kinase, and FATC. Rapamycin, in complex with FKBP12 (not shown), inhibits TOR through its binding to the FRB domain of TOR. TORC1 senses nutrient signals and promotes anabolic processes including ribosome biogenesis, protein translation, and nutrient transport while inhibiting catabolic processes like autophagy, stress-responsive transcription, and glycogen synthesis.

(B) TORC2 is consisted of Tor2p, Lst8p, Avo1-3p, and Bit61p. TORC2 is involved in the regulation of the actin cytoskeleton.

1.2.2 TORC2 signaling and the Cell Wall Integrity Pathway

All eukaryotic cells must balance the regulation of several important pathways in order to maintain a healthy state of growth. In yeast, one example of such is the regulation of the Cell Wall Integrity (CWI) Pathway. Integrity of the yeast cell wall is required for cell shape and stability as well as budding to produce daughter cells to ensure proliferation of the cell line (26, 29) Constant remodeling of the cell enables cell expansion during normal vegetative growth and morphology changes in response to mating pheromone (54). Because water can freely enter cells, turgor pressure can build in the cell. The cell wall must be rigid in some areas while pliable in others to enable the cell to take on shapes other than perfect spheres and not rupture in hypo-osmotic environments. For this, an internal actin cytoskeleton is utilized to direct cell wall expansion to a particular area (32). The CWI pathway is a signaling pathway in which signals received from a family of cell surface sensors are transmitted to a Rho1/2p GTPase switch, comprised of the Rho GTPases, Rho1 and Rho2, the Rho GDP-GTP exchange factors (GEF) Rom2 and Tus1, and the Rho GTPase activating protein (Rho GAP) Sac7 (11, 57, 58, 102, 130) (Fig. 3). Activated Rho1/2 transmit this signal by activating the Pkc1-activated mitogen-activated protein (MAP) kinase cascade (56). The Pkc1-activated MAP cascade consists of Pkc1, Bck1, redundant Mkk1 and Mkk2, and

Slt2. In the current model, activated Pkc1 phosphorylates Bck1 which phosphorylates Mkk1 and Mkk2 that in turn phosphorylate Slt2. Phosphorylated Slt2 then phosphorylates downstream targets to activate synthesis of the cell wall (reviewed in (43)). While the CWI Pathway has been extensively characterized there is some dispute over whether it functions in a parallel or a linear pathway with the Target of Rapamycin (TOR) signaling pathway.

The rapamycin-insensitive TORC2 mediates organization of the actin cytoskeleton through activation of the same Rho1/2 GTPase switch as in the CWI pathway. How TORC2 signals to the Rho1/2 GTPase switch is not well understood and might involve three recently identified TORC2 substrates, Slm1/2 and Ypk2 (5, 37). Activation of Rho1 and the Pck1-Bck1-Mkk1/2-Mpk1cell integrity pathway can restore cell growth to *tor2* mutant cells (11, 57, 58, 102). Cell wall defects, induced by treating cells with small amounts of SDS or by mutations compromising cell wall synthesis can also suppress a *tor2* mutation possibly by activating cell wall integrity signaling via Rho1, which requires both Rom2 and Tus1, another GEF for Rho1 (101). Therefore, TORC2 signaling and the CWI pathway likely converge to regulate organization of the actin cytoskeleton (Fig. 4). Apart from its role in organizing the cytoskeleton, it is not known what other pathways this complex may regulate, and no one knows what regulates TORC2 signaling.

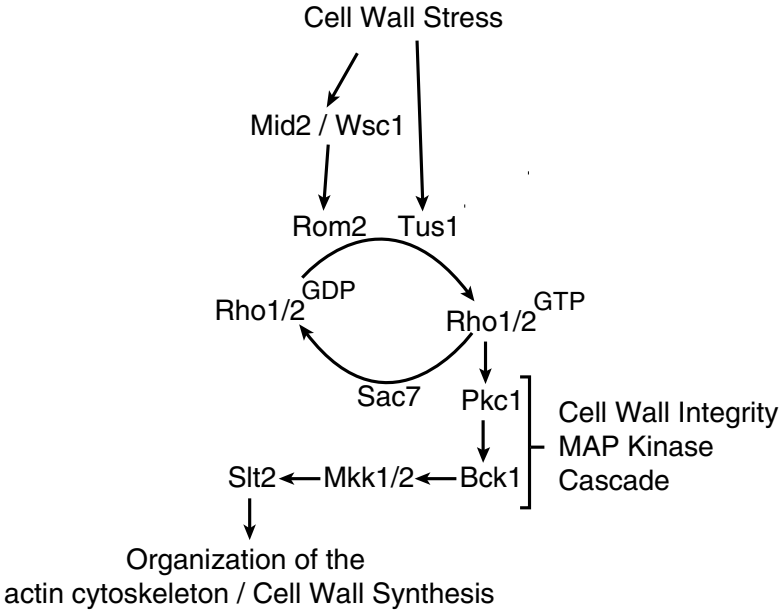

Figure 3. Diagram of the Cell Wall Integrity pathway.

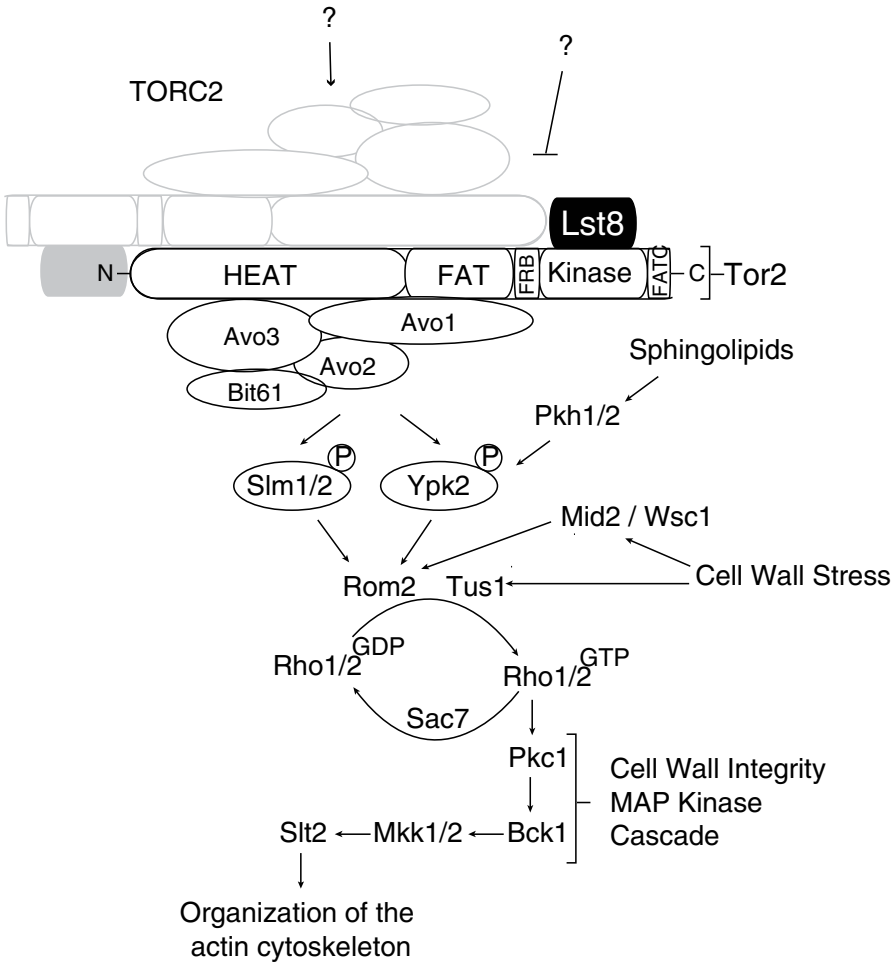

Figure 4. The TORC2 signaling pathway converges with the CWI pathway.

TORC2 is involved in the regulation of the actin cytoskeleton through the activation of a Rho1/2 GTPase switch, consisted of the Rho GTPases, Rho1 and Rho2, the Rho GDP-GTP exchange factor (Rho GEF) Rom2, and the Rho GTPase activating protein (Rho GAP) Sac7. TORC2 may signal to the Rho1/2 GTPase switch via phosphorylation of Slm1/2 and Ypk2.

1.2.3 Lst8: an essential component of both TOR complexes

Lst8 is essential for cell viability in *S. cerevisiae* (97). It is still unknown whether the essential function of Lst8 is linked to TORC1, TORC2, or both. In TORC2, Lst8 binds to the C-terminal kinase domain of Tor2, independent of Avo1/2/3, and Lst8 depletion destabilizes interaction between Tor2 and Avo2 or Avo3 (126). Lst8 is also required for full Tor2 kinase activity *in vitro* and its depletion leads to defective polarization of the actin cytoskeleton similar to *tor2* mutations (81, 126). However, although over-expression of *MSS4* (encoding a PI-4-P 5 kinase), *RHO2*, *ROM2*, or members of the cell integrity pathway, *PKC1*, *MKK1*, or *BCK1* suppresses both *tor2* temperature-sensitive (*tor2-21*) and *avo1* mutations (57, 58, 81), these suppressors have been reported to be unable to suppress an *lst8* mutation (81), raising the question whether the essential function of Lst8 is linked to TORC2. On the other hand, the role of Lst8 in TORC1 is also largely unknown.

1.2.4 Cellular localization of the TOR complexes

Earlier studies on the localization of components of the TOR complexes led to a variety of conclusions about the identity of membranes with which components of the TOR complexes are associated (23, 25, 72, 94, 121). What was clear from these studies is that TORC1 and TORC2 associate with membrane structures. Several recent reports on

the localization of TOR components suggest that TORC2 is predominantly found as punctate structures at the plasma membrane while TORC1 dynamically associates with the vacuolar membrane (3). Discrepancy of these localization data may be partly due to dynamic associations of TORC1 and TORC2 with different membrane structures in response to changes in nutrient conditions.

1.3 Rapamycin and its clinical applications

The namesake of TOR signaling, rapamycin, is a macrolide that was first discovered in 1975 on the island of Rapa Nui, Easter Island. Rapamycin, pictured in Figure 5, was originally identified as an antifungal produced by the bacterium *Streptomyces hygroscopicus* mainly against *Candida albicans, Microsporum gypseum* and *Trichophyton granulosum (*120*).* It was later found to have immunosuppressive and antiproliferative properties and this is its major use today. Rapamycin acts as an immunosuppressive agent by inhibiting the response to interleukin 2 (IL-2), preventing activation of T and B cells (86). Once inside the cell, rapamycin binds to cytosolic FKBP12, encoded for in yeast by the gene *FPR1,* which then binds to the FRB domain of the Tor kinases in TORC1. For reasons unknown, rapamycin-FKBP12 does not inhibit TORC2, possibly due to inability to bind to the FRB domain of the Tor kinase in this complex (81).

The immunosuppressant rapamycin marketed under the name Sirolimus or Rapamune by Pfiser, has low toxicity towards kidneys due to its mechanism of action making it useful to treat patients with kidney transplants to avoid transplant rejection. However, since rapamycin also has antiproliferative effects, a side effect is impaired wound healing; therefore, it is typically not administered until several weeks after surgery (86). Another clinical use for rapamycin takes advantage of its antiproliferative property to prevent restenosis or re-narrowing of blood vessels in patients who received coronary stents coated with rapamycin polymer. The polymer coating allows for slow release of the drug to prevent restenosis over time (118).

Renal transplant patients are at a high risk for developing Kaposi's sarcomas because treatment with immunosuppressants after surgery can weaken the immune system that normally combat the formation of this type of tumor. Because rapamycin inhibited the progression of dermal Kaposi's sarcomas in patients who had renal transplants, it is currently being investigated as an anticancer drug (112). For example, derivatives of rapamycin such as temsirolimus and everolimus are being tested for their effects on cancers such as glioblastoma multiforme and mantle cell lymphoma (44, 95). Combining doxorubicin and rapamycin is also being studied in mice to treat cancers that become resistant to chemotherapeutic drugs like doxorubicin due to increased Akt

signaling. Rapamycin is proposed to block Akt signaling rendering these cells sensitive to chemotherapy once again (114, 123).

Rapamycin has also shown promise in treating an array of other disorders including autism and Alzheimer's in a mouse model as well tuberous sclerosis complex in clinical trials (35, 110). It is being investigated in HIV, autosomal dominant polycystic kidney disease, and progeria, a rare aging disorder that accelerates the aging process typically leading to an early death in patients' teenage years (13, 31, 91). Rapamycin treatment mimics nutrient starvation and leads to an increase in lifespan in both yeast and mouse models however this use is not recommended for humans due to its toxicity at high doses (55, 92). The variety of applications for rapamycin stresses the importance of TOR signaling. Yet, much remains to be understood about this signaling pathway. Therefore, the study of TOR signaling particularly the lesser understood TORC2 signaling branch could uncover novel therapeutic targets for the treatment of these diseases and others yet to be linked to TOR signaling.

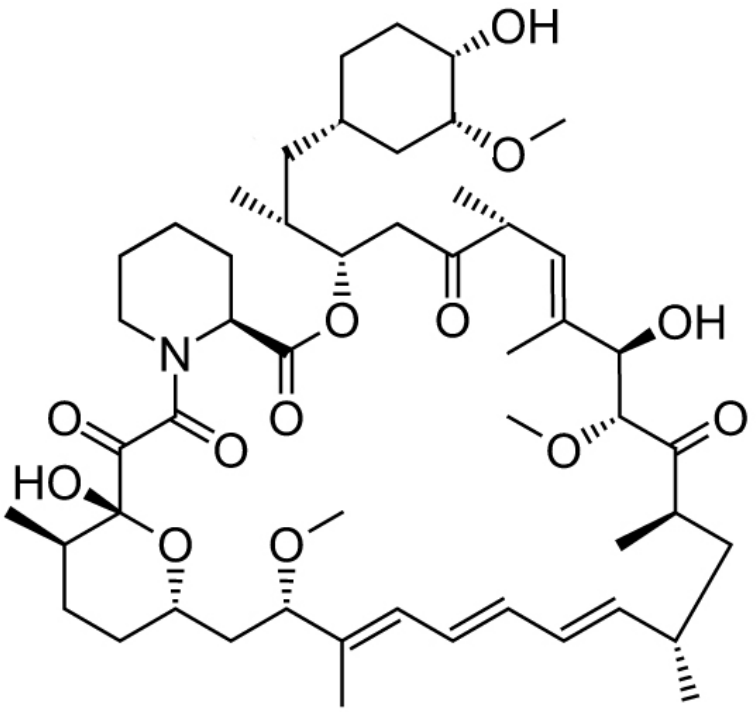

Figure 5. The structure of rapamycin.

1.4 Specific Goals

Many studies on the TOR signaling pathway have provided invaluable insights into the regulation and function of this pathway. While TOR signaling is an extensively studied pathway, the majority of studies done were on the TORC1 signaling branch. Much remains unknown about the regulation and possible novel functions of the TORC2 signaling branch. Besides Tor2, Lst8 is the only other essential component of both TOR signaling complexes. I have addressed two questions. First, the function of Lst8 in these two complexes is unknown and whether the essential function of Lst8 is through its action in TORC1 or TORC2 or both remains a mystery. Solving this mystery could provide insights into the essential function of Lst8 in TOR signaling. It is not possible to study the effect of losing an essential gene because cells will die in the absence of that gene product. Therefore, I addressed the following question: Are there mutations that will allow cells to survive without Lst8? Identification of such mutants would allow further studies to be performed on the mutants to address the first question. Second, identification of such mutants could present novel regulators of TOR signaling. If they exist, how do Lst8 bypass mutants enable cells to survive without Lst8? Answering this question could greatly expand the current knowledge of this signaling pathway and could even link pathways to TOR signaling that were not

known to be involved before, providing possible novel therapeutic targets for regulating this pathway in many of the associated diseases.

CHAPTER 2.
TORC2 SIGNALING IS ANTAGONIZED BY PROTEIN PHOSPHATASE 2A AND THE FAR3-7-8-9-10-11 COMPLEX

2.1. Summary

The target of rapamycin (TOR) kinase, a central regulator of eukaryotic cell growth, exists in two essential, yet distinct TOR kinase complexes in the budding yeast *Saccharomyces cerevisiae*: rapamycin-sensitive TORC1 and rapamycin-insensitive TORC2. Lst8, a component of both TOR complexes, is essential for cell viability. However, it is unclear whether the essential function of Lst8 is linked to TORC1, TORC2, or both. To that end, I carried out a genetic screen to isolate *lst8* deletion suppressor mutants. Here I report that mutations in *SAC7* and *FAR11* suppress lethality of *lst8Δ* and TORC2-deficient (*tor2-21*) mutations but not TORC1 inactivation, suggesting that the essential function of Lst8 is linked only to TORC2. More importantly, characterization of *lst8Δ* bypass mutants reveals a role for Protein Phosphatase 2A (PP2A) in the regulation of TORC2 signaling. I show that Far11, a member of the Far3-7-8-9-10-11 complex involved in pheromone induced cell cycle arrest, interacts with Tpd3 and Pph21, conserved components of PP2A, and deletions of components of the Far3-7-8-9-10-11 complex and PP2A rescue growth defects in *lst8Δ* and *tor2-21* mutants. Additionally,

loss of the regulatory B' subunit of PP2A Rts1 or Far11 restores phosphorylation to the TORC2 substrate Slm1 in a *tor2-21* mutant. Mammalian Far11 orthologs, FAM40A/B, exist in a complex with PP2A known as STRIPAK, suggesting conserved functional association of PP2A and Far11. Antagonism of TORC2 signaling by PP2A-Far11 represents a novel regulatory mechanism for controlling spatial cell growth of yeast.

2.2. Introduction

The target of rapamycin (TOR) kinase is a phosphatidylinositol kinase-related protein kinase that controls eukaryotic cell growth and proliferation in response to nutrient conditions (62, 125, 132). The TOR kinase is inhibited by the complex of rapamycin and Fpr1, a peptidyl-prolyl *cis-trans* isomerase. The TOR kinase is conserved in eukaryotes. Unlike fungal species, which may possess two TOR kinases, higher eukaryotes such as humans possess only one. The TOR kinase exists in multi-protein complexes, which have been purified from many different eukaryotic systems. There exist two distinct TOR kinase complexes. In yeast, rapamycin-sensitive TORC1 consists of Tor1 or Tor2, Lst8, Kog1, and Tco89, and rapamycin-insensitive TORC2 consists of Tor2, Lst8, Avo1, Avo2, Avo3, and Bit61 (81, 94, 121). Both complexes are partially conserved in mammals: mTORC1 contains the yeast Kog1 ortholog raptor, while

mTORC2 contains mSin1 and rictor, orthologs of yeast Avo1 and Avo3, respectively; GβL, the ortholog of yeast Lst8, exists in both mTORC1 and mTORC2 (132).

TOR regulates cell growth by sensing and responding to changes in nutrient conditions (100). TORC1 has an essential function involving the regulation of cell growth that is carried out when either Tor1 or Tor2 is in the complex. Under favorable growth conditions, TORC1 promotes cell growth by maintaining robust ribosome biogenesis (83, 84, 133). When TORC1 is inactive, there is a dramatic down-regulation of general protein translation, an up-regulation of autophagy, accumulation of the storage carbohydrate glycogen, increased sorting and turnover of amino acid permeases, and activation of stress-responsive transcription factors via nuclear translocation (125). TOR inhibition via rapamycin treatment activates a subset of stress-responsive transcription factors (8, 22, 25, 27, 106). Rapamycin treatment can also lead to reduced gene expression, including those encoding ribosomal proteins (RP) (125).

TORC2 has a separate essential function that is Tor2-specific, which involves cell cycle-dependent polarization of the actin cytoskeleton (28). TORC2 mediates the organization of the actin cytoskeleton through the activation of a Rho1/2p GTPase switch, comprised of the Rho GTPases, Rho1 and Rho2, the Rho GDP-GTP exchange factor Rom2, and the Rho GTPase activating protein Sac7. Activated GTP-bound Rho1

activates Pkc1, which activates the cell wall integrity pathway MAP kinase cascade, Bck1-Mkk1/2-Mpk1. Activation of Rho1 and the cell wall integrity pathway restores cell growth and actin polarization to *tor2* mutant cells. *sac7* mutations suppress TORC2-deficiency by increasing the levels of GTP-bound Rho1. How TORC2 mediates the organization of the actin cytoskeleton is unclear and might involve three TORC2 substrates: Slm1, Slm2 and Ypk2 (4, 5, 37, 66, 115).

Lst8 is essential for cell viability in *S. cerevisiae* (97). It is unknown whether the essential function of Lst8 is linked to TORC1, TORC2, or both. In TORC2, Lst8 binds to the C-terminal kinase domain of Tor2, independent of Avo1/2/3, and Lst8 depletion destabilizes the interaction between Tor2 and Avo2 or Avo3 (126). Lst8 is also required for full Tor2 kinase activity *in vitro* and its depletion leads to depolarized actin cytoskeleton similar to *tor2* mutations (81, 126). Overexpression of *MSS4*, encoding a phosphatidylinositol-4-phosphate 5-kinase, *RHO1/2*, *ROM2*, *PKC1*, *MKK1*, or *BCK1* suppresses *tor2* and *avo1* mutations (57, 58, 81), however, these suppressors were reported to be unable to suppress an *lst8* mutation (81). The question remains whether the essential function of Lst8 is linked to TORC2, and the role of Lst8 in TORC1 is largely unknown.

Here, I provide evidence that the essential function of Lst8 is linked to TORC2, but not TORC1. I show that components of the Far3-7-8-9-10-11 complex, which have been implicated in pheromone-induced cell cycle arrest, vacuolar protein sorting, and cell fitness, negatively regulate TORC2 signaling. I find that Far11 interacts with protein phosphatase 2A and that mutations in the PP2A-Rts1 subcomplex suppress TORC2-deficiency. I propose that the Far3-7-8-9-10-11 complex and PP2A-Rts1 antagonize TORC2 signaling by promoting dephosphorylation of TORC2 substrates.

2.3. Materials and methods

2.3.1. Strains, plasmids, and growth media and growth conditions

Yeast strains and plasmids used in this study are listed in Table 2 and 3 or Appendix Table 1 and 2, respectively. Yeast cells were grown at 30 °C or 37 °C in SD (0.67% yeast nitrogen base plus 2% dextrose), YNBcasD (SD medium plus 1% casamino acids), Ura Leu drop-out (SD plus CSM without uracil and leucine, Bio101), or YPD (1% yeast extract, 2% peptone, 2% dextrose) medium as indicated in the text and in the figure legends. For *lst8Δ* bypass assays, SD medium with or without 1 g/L 5-Fluroorotic acid was used to select for growth of cells that have lost *URA3* plasmids. When necessary, amino acids, adenine, and/or uracil were added to the growth medium at standard concentrations to cover auxotrophic requirements (2).

2.3.2. Transposon mutagenesis

lst8Δ mutant bypass genetic screens were conducted using transposon mutagenesis as described (77). Briefly, *ade2Δ lst8Δ* cells carrying plasmid pRS412-LST8 were used for transposon mutagenesis; after mutagenesis, cells were plated on YPD medium to select for colonies which were red or sectoring indicating loss of the pRS412-LST8 plasmid. Putative *lst8Δ* bypass mutants were confirmed to be recessive, single-gene mutations using standard yeast genetic techniques. Determination of transposon insertion sites were carried out as described (20). Briefly, a recovery plasmid encoding the Ampicillin-resistance gene (Amp^R) and *URA3* was integrated into the transposon integration site of the *leb1* and *leb2* mutants by homologous recombination and transformants were selected on uracil-dropout medium. Genomic DNA was then isolated, digested with EcoRI and ligated with T4 DNA ligase. Ligation products were transformed into bacteria and Amp^R transformants were selected for on LB Broth supplemented with ampicillin. Transposon integration sites were determined by sequencing of the recovered plasmids.

2.3.3. Northern Blotting

Total cellular RNAs were isolated using hot phenol method as described (45). Cells were grown in appropriate medium to ~OD_{600} 0.6 and collected for isolation of

total cellular RNA. ^{32}P-labeled probes against *RPL3*, *RPS6a*, and *ACT1* were used to probe mRNA immobilized on nylon membranes. PhosphorImager was used to record signals of the RNA transcripts. Experiments were repeated at least twice.

2.3.4. Cellular extract preparation, immunoblotting, and immunoprecipitation

Total cellular protein extracts were prepared by disrupting yeast cells in extraction buffer (1.85N NaOH-7.5% β-mercaptoethanol) followed by precipitation with trichloroacetic acid (TCA) as described (129). Phosphatase treatment of total cellular proteins was conducted as described (79). For co-immunoprecipitation experiments, cellular lysates were prepared in IP buffer (50 mM Tris-HCl pH 7.6, 150 mM NaCl, 0.5% Triton X-100, and protease inhibitors). Cell extracts (~3 mg proteins) were incubated at 4 °C for 1 h with anti-myc antibody (9E10, Roche), after which 30 μl of a 50% slurry of protein G-Sepharose (Roche) was added to each sample and the samples were further incubated at 4 °C for 2 h. Washed immunoprecipitates bound to the sepharose beads were released by boiling in 1X SDS-PAGE loading buffer. The released immune complexes were analyzed by Western blotting. myc- and HA-tagged proteins were probed with anti-myc antibody and anti-HA antibody (3F10, Roche), respectively. Chemiluminescence images of Western blots were captured using the Bio-Rad Chemi-Doc photo documentation system (Bio-Rad). Experiments were repeated at least twice.

2.3.5. Actin staining and GFP fluorescence microscopy

The actin cytoskeleton was visualized in rhodamine phalloidin-stained, formaldehyde-fixed cells, as described (2). Overnight cultures were diluted to ~OD 0.1 and allowed to grow at 30 °C for 2 h and then switched to 37 °C for 3 h before formaldehyde was added to a final concentration of 3.7%. After fixing for 1 h, 1mL of fixed cells were collected, washed in PBS buffer and stained with rhodamine phalloidin conjugate (Invitrogen) and visualized by fluorescence microscopy. GFP fluorescence of GFP-tagged proteins was analyzed in cells grown to log phase. Fluorescence images of rhodamine phalloidin-labeled actin structures and GFP-tagged proteins were acquired with a Photometrics Coolsnap fx CCD camera and Metamorph Imaging Software and processed using ImageJ (NIH) and Adobe Photoshop. Experiments were repeated at least twice.

2.3.6. Preparation of recombinant 6xHis-tagged Slm1

PCR-amplified *SLM1* coding sequence was cloned into the SacI and XhoI sites of pET24a vector (Novagen). The resultant plasmid was transformed into BL21(DE3) competent cells (Novagen) and expression of 6xHis-tagged Slm1 was induced by adding 1 mM IPTG to bacterial cultures grown at 20 °C for 16 h. Recombinant C-terminal 6xHis-tagged Slm1 was purified under native conditions using Ni-NTA

agarose beads (Qiagen) as described in the product instruction manual. 14 mg Slm1-His6 was obtained from 1 L induced culture. Experiments were repeated at least twice.

2.3.7. In vitro kinase assay of Slm1 phosphorylation by Tor2-HA

Yeast strains expressing 3xHA-tagged Tor2 were grown overnight to mid-log phase and cellular lysates were prepared in lysis buffer (50 mM Tris-HCl, pH 7.6, 150 mM NaCl, 1% Triton X-100, and protease inhibitors) by vortexing with glass beads. Cell extracts (~3 mg proteins) were incubated with 100 μl protein A-agarose beads (Roche) at 4 °C for 1 h to remove nonspecific binding proteins. Precleared cell lysates were then incubated with 16 μg anti-HA antibody (12CA5, Roche) for 1 h, after which 40 μL of a 50% slurry of protein A-agarose beads was added to each sample and the samples were further incubated at 4 °C for 1 h. Precipitates were washed twice with 1ml lysis buffer, twice with 1ml wash buffer (50 mM Tris-HCl, pH 7.6, 300 mM NaCl, and protease inhibitors), and once with 1ml kinase buffer (20 mM Tris-HCl pH 7.6, 50 mM NaCl, 5 mM $MgCl_2$, 1mM PMSF). After the final wash, beads were resuspended in 25 μL of kinase buffer plus 1 mM dithiothreitol (DTT). The reaction was initiated by adding 25 μL reaction mixture (kinase buffer with 1 mM DTT, 0.4 mM ATP, 5μCi of [γ-^{32}P]-ATP (PerkinElmer), 5 μg recombinant Slm1-His6). After incubation for 30 minutes at 30°C, the reaction was terminated by adding 25ul 3x SDS gel-loading buffer (150 mM Tris-

HCl, pH 6.8, 6% SDS, 30% glycerol, 0.3% bromophenol blue) and 8.5ul 1 M DTT and boiling for 4 minutes. 20 μl samples were fractionated by SDS–PAGE on 7.5% polyacrylamide gels in triplicate, with one dried for detecting ^{32}P-incorporation in Slm1 by autoradiography (Molecular PhosphorImager FX, Bio-Rad), one stained by Coomassie Blue for detecting 6xHis-tagged Slm1, and one processed for Western blotting for detecting HA-Tor2. A mock treatment experiment was conducted using anti-HA immunoprecipitates from cells expressing non-tagged Tor2. Experiments were repeated at least twice.

2.4. Results

2.4.1. Mutations in SAC7 and FAR11 suppress lethality due to an lst8Δ mutation

To gain insights into the essential function of Lst8, I conducted a genetic screen to search for mutations that allow cells to survive without Lst8 by employing an *ade2* colony sectoring assay (Fig. 1D). This assay takes advantage of a buildup of purine precursors in the vacuole, which results in colonies that appear red in *ade2* mutant cells. I utilized a previously constructed *Tn3::lacZ::LEU2* mutagenesis library (20) to introduce mutations in an *lst8Δ ade2Δ* mutant carrying plasmid pRS412-LST8 (*CEN LST8 ADE2*) and screened for red or sectoring *lst8Δ* bypass (*leb*) mutant cells on YPD medium, which had lost or were in the process of losing the pRS412-LST8 plasmid. Of approximately

30,000 *Leu*$^+$ transformants, 49 viable solid red or sectoring colonies were selected for further analysis. Of the 49, 11 colonies were pure red. Crossing to an *ade1Δ* strain resulted in non-complementation of the red phenotype in one of the 11 pure red colonies indicating that the red phenotype was due to a mutation in *ADE1* and not the loss of the pRS412-LST8 plasmid. Whereas, crossing to an *ade2Δ* strain resulted in non-complementation of the red phenotype in the remaining 10 pure red colonies indicating that the red phenotype is due to a mutation in *ADE2* or loss of the pRS412-LST8 plasmid. However, wild-type *LST8* was found by PCR to be present in all 11 pure red colonies, which were deemed false positives. The remaining 38 sectoring colonies were analyzed similarly and the red sectoring phenotype of one was due to an *ADE1* mutation while 35 were due to mutations in *ADE2*. PCR genotyping confirmed the absence of pRS412-*LST8* in the remaining two mutants, termed *leb1* and *leb2*. In these two *leb* mutants, the *lst8Δ* bypass phenotype was found to co-segregate with *Leu*$^+$ after crossing to an *lst8Δ leu2 ade2Δ pRS412-LST8* strain of the opposite mating type and tetrads were dissected, indicating that the transposon insertion had produced the mutant phenotype. Figure 1A shows that, in contrast to wild-type cells, *leb1* and *leb2* mutants form both red and sectoring colonies, indicating loss of the pRS412-LST8 plasmid.

I identified the transposon insertion site in the *leb1* and *leb2* mutants by plasmid rescue and sequencing of the recovered plasmids as described by Burns et al. (1994) and summarized in Figure 1E. The transposon insertion sites in the *leb1* and *leb2* mutants were found to be in the open reading frames of *SAC7* and *FAR11*, respectively. Consistently, Figure 1B-C shows that wild-type *SAC7* and *FAR11* on a centromeric plasmid can complement *leb1* and *leb2* mutations, respectively. Furthermore, a *sac7Δ* or *far11Δ* mutation in an *lst8Δ ade2Δ pRS412-LST8* strain also led to *lst8Δ* bypass (loss of pRS412-LST8 is indicated by the red colony phenotype in Figure 2A).

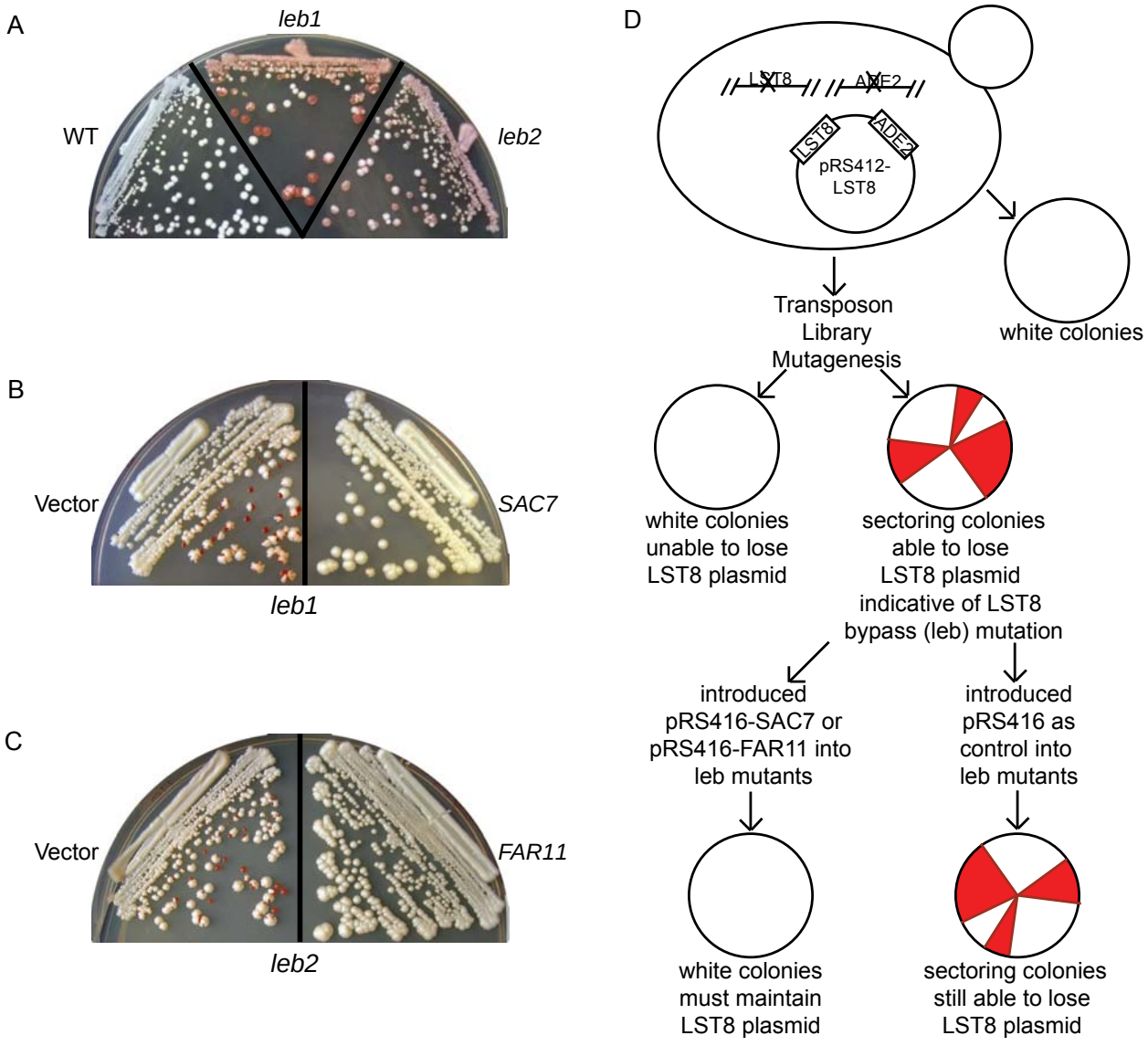

Figure 1. Mutations in *SAC7* and *FAR11* bypass *lst8Δ*.

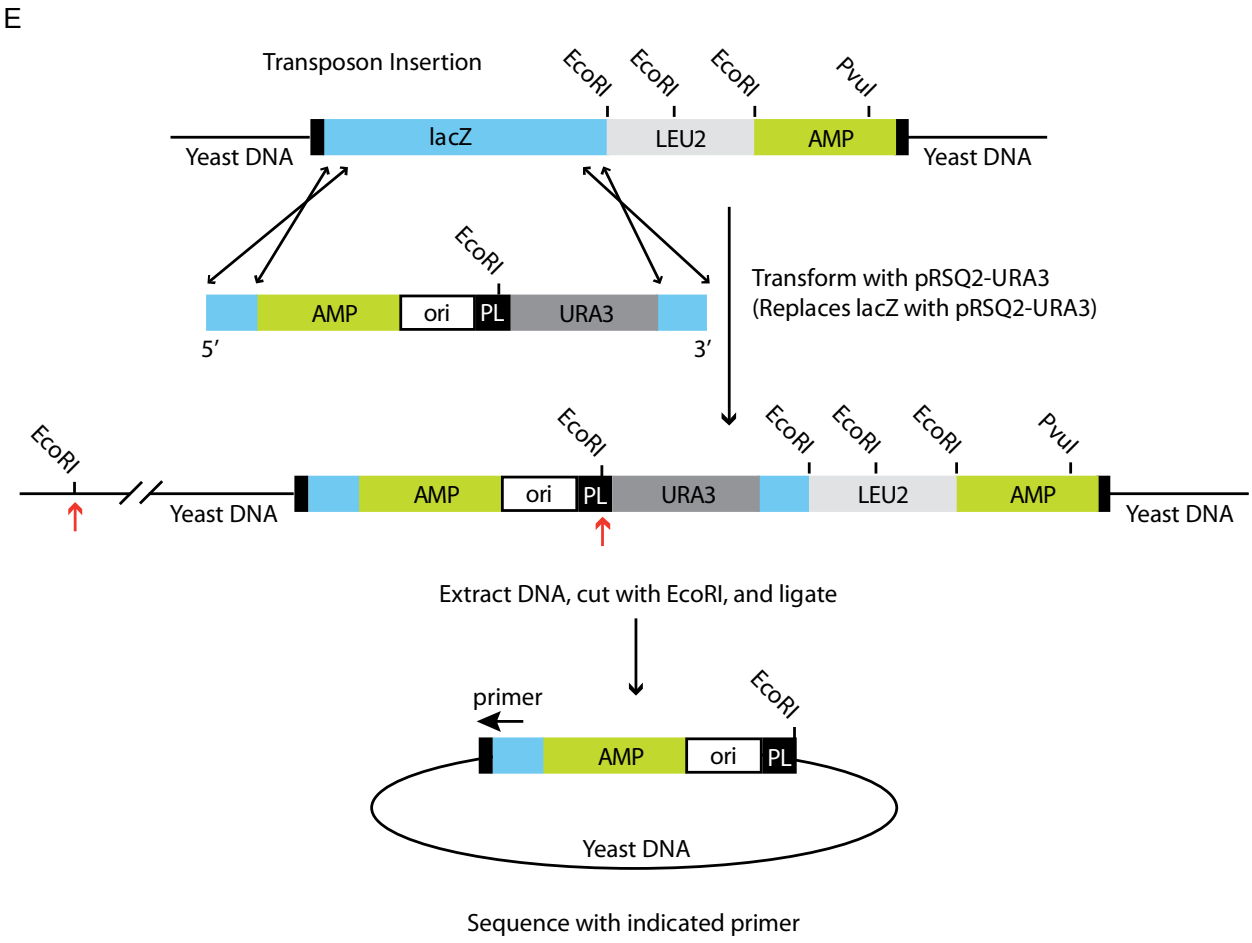

Figure 1 (cont.)

(A) Isolation of *lst8Δ* bypass (*leb*) mutants using *ade2*-based colony sectoring assay.

Wild-type (*lst8Δ ade2Δ*) (ZLY3081) and isogenic *leb1* (TPY104) and *leb2* (TPY103) mutant

cells carrying a centromeric plasmid encoding *ADE2* and *LST8* (pZL1255) were streaked on YPD medium.

(B) *SAC7* complements a *leb1* mutation. *leb1* mutant cells (*lst8Δ ade2Δ leb1*) carrying pRS412-LST8 and either pRS416 empty vector (Vector) or pRS416-SAC7 (*SAC7*, pZL2422) were grown on YNBcasD medium supplemented with adenine.

(C) *FAR11* complements a *leb2* mutation. *leb2* (*lst8Δ ade2Δ leb2*) mutant cells carrying pRS412-LST8 and either pRS416 empty vector (Vector) or pRS416-FAR11 (*FAR11*, pZL2550) were grown on YNBcasD medium supplemented with adenine.

(D) Diagram of colony sectoring assay

(E) Scheme for recovering and identifying the location of a transposon insertion within the yeast genome. Sequence obtained can be compared to the *Saccharomyces* Genome Database to identify location of insertion. Adapted from the *TRIPLES* database

2.4.2. sac7Δ and far11Δ mutants are sensitive to rapamycin

Whether the essential function of Lst8 is linked to TORC1, TORC2, or both has yet to be determined. I tested the ability of *sac7Δ* and *far11Δ* mutations to suppress TORC1 inactivation by rapamycin treatment and TORC2-deficiency due to a temperature-sensitive *tor2-21* mutation. An *fpr1Δ* mutation enables cells to grow in the presence of rapamycin, however, *far11Δ lst8Δ*, *far11Δ* (*far11Δ lst8Δ pRS412-LST8*), *sac7Δ lst8Δ* and *sac7Δ* (*sac7Δ lst8Δ pRS412-LST8*) cells were unable to grow on YPD medium supplemented with 200 nM rapamycin (Fig. 2A), demonstrating that these two *lst8Δ* bypass mutations do not suppress a severe or complete loss of TORC1 activity. Consistently, *sac7Δ* and f*ar11Δ* mutations failed to restore cell growth to *tor1Δ tor2-21* double mutants grown at 37 °C, which have defects in the function of both TORC1 and TORC2 (Appendix Fig. A1 and (102)). In contrast, *sac7Δ* and *far11Δ* mutations restored cell growth to a *tor2-21* mutant grown at 37 °C, which causes a specific defect in only TORC2 (Fig. 3C and 4C), consistent with previous findings that *sac7Δ* suppresses a *tor2-21* mutation (102). These data suggest that the essential function of Lst8 may be linked to TORC2, but not TORC1.

It is conceivable that *lst8Δ* may result in a partial loss of TORC1 activity, which is not sufficient to support cell growth but is not severe enough to prevent *sac7Δ* and

far11Δ mutations from restoring partial cell growth to *lst8Δ* mutant cells. To test this possibility, I tested the sensitivity of wild type, *fpr1Δ*, *sac7Δ*, and *far11Δ* mutant cells to lower concentrations of rapamycin (Appendix Fig. A2). It has been reported that *sac7Δ* and *far11Δ* mutant strains in the BY4741 background are hypersensitive to treatment with 10 nM rapamycin (128). In the presence of <10 nM rapamycin, a *far11Δ* mutant in the BY4741 background has been reported to grow better than wild-type cells (60). I analyzed cell growth in the presence of 2-20 nM rapamycin and found that *sac7Δ* resulted in hypersensitivity to rapamycin treatment. A *far11Δ* mutant, in contrast, grew slightly better than wild-type cells when treated with 3 and 5 nM rapamycin. In the presence of 7-20 nM rapamycin, however, *far11Δ* cells no longer grew better than wild-type cells. In my strain background, treatment of wild-type cells with 10 nM rapamycin likely reduces TORC1 activity to just below the threshold that supports cell growth. My observations that *sac7Δ* and *far11Δ* bypass *lst8Δ* but not treatment with 10 nM rapamycin strongly suggest that the essential function of lst8 is not linked to TORC1.

To further corroborate my hypothesis that Lst8 is not essential for TORC1 activity, the effect of *lst8Δ* on the expression of genes encoding ribosomal proteins (RP), which is positively regulated by TORC1, was examined. Utilizing *sac7Δ* to obtain a viable *lst8Δ* mutant, the expression of two RP genes, *RPL3* and *RPS6A*, encoding the L3 protein of the large (60S) ribosomal subunit and the S6 protein of the small (40S)

ribosomal subunit, respectively, was compared in *LST8 sac7Δ* versus *lst8Δ sac7Δ* mutant cells by Northern blot analysis. As expected, TORC1 inactivation due to rapamycin treatment inhibited expression of both *RPL3* and *RPS6A* (Fig. 2B). In contrast, *lst8Δ* only mildly reduced the expression of *RPL3* and *RPS6A*, suggesting that *lst8Δ* does not lead to severe loss of TORC1 activity.

2.4.3. lst8Δ causes mislocalization of Bit61 and Avo3, but not Kog1

Recent research has demonstrated that the TORC1 components are located on intracellular membranes with a concentration on the vacuolar membrane while TORC2 components appear as punctate spots at the plasma membrane (3, 10, 12, 113, 121). It has been proposed that plasma membrane localization of TORC2 is essential for cell viability (10). Isolation of *lst8Δ* mutant suppressors allowed me to examine the role of Lst8 in the cellular localization of TOR complex components. GFP fluorescence was analyzed in *sac7Δ far11Δ* double and *sac7Δ far11Δ lst8Δ* triple mutants expressing GFP-tagged TORC1 component Kog1 and TORC2 components Bit61 and Avo3. As previously reported, Bit61 and Avo3 localized to the plasma membrane as punctate spots in wild-type *LST8* cells (Fig. 2C) (10). An *lst8Δ* mutation, however, largely abolished punctate plasma membrane localization of Bit61 and Avo3. In contrast, *lst8Δ* did not affect localization of Kog1 to the vacuolar membrane (Figure 2C). These

findings are consistent with my hypothesis that the essential function of Lst8 is linked to TORC2, but not TORC1, and further suggest that Lst8 is required for proper cellular localization of TORC2.

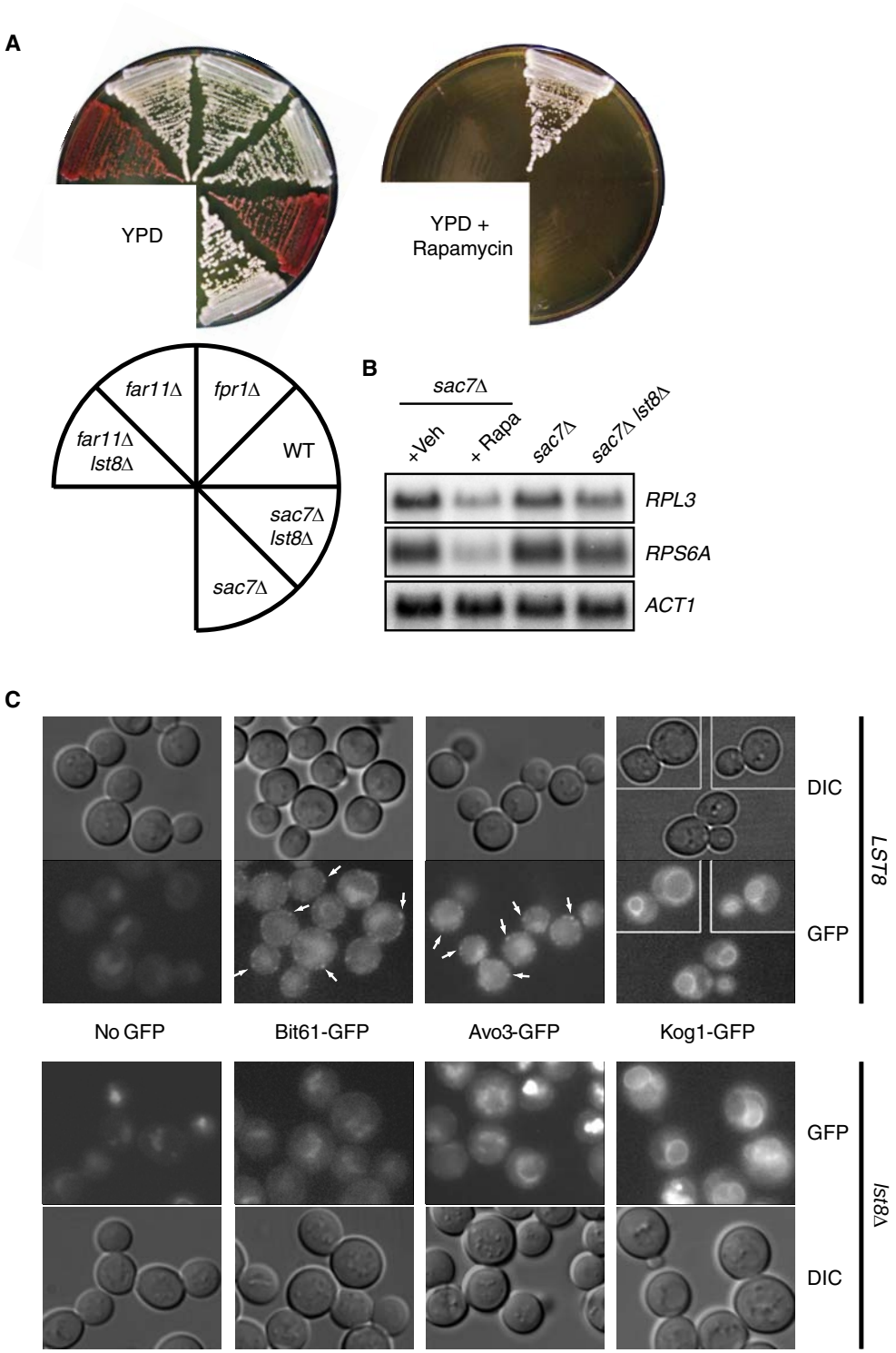

Figure 2. TORC1 function is not grossly affected in an *lst8Δ* mutant.

(A) *sac7Δ* and *far11Δ* mutations do not confer resistance to rapamycin. Wild type (ZLY423) and isogenic mutant cells as indicated (*far11Δ lst8Δ* TPY115; *far11Δ*, TPY114; *fpr1Δ*, TPY122; *sac7Δ lst8Δ*, ZLY2405; *sac7Δ*, ZLY2404) were grown on YPD medium with or without 200 nM rapamycin. The lack of a pRS412-LST8 plasmid results in the *far11Δ lst8Δ* and *sac7Δ lst8Δ* double mutant cells having a red phenotype.

(B) *lst8Δ* has little effect on the expression of *RPL3* and *RPS6A*. Expression of *RPL3*, *RPS6A* and *ACT1* in *sac7Δ* mutant cells (ZLY2404) treated with drug vehicle (+Veh) or 200 nM rapamycin (+Rapa), *sac7Δ* single (ZLY2404) and *sac7Δ lst8Δ* double (ZLY2845) mutant cells were analyzed by Northern blotting as described in Materials and Methods.

(C) *lst8Δ* causes mislocalization of Bit61 and Avo3, but not Kog1. Wild-type *LST8* (*LST8 sac7Δ far11Δ*) and *lst8Δ* mutant (*lst8Δ sac7Δ far11Δ*) cells expressing no GFP-tagged proteins (TPY1264, TPY1266), Bit61-GFP (TPY358, TPY366), Avo3-GFP (TPY369, TPY407), or Kog1-GFP (TPY371, TPY413) were grown in SD medium and observed by bright field (DIC) and GFP fluorescence microscopy. GFP fluorescence images were captured and processed using the same parameters. Arrows indicate punctate plasma membrane localization of Bit61 and Avo3. Background signals in cells expressing no GFP-tagged proteins, especially in the *lst8Δ* mutant strain, are due to autofluorescence caused by an *ade2* mutation.

2.4.4. Mutations of the Far3-7-8-9-10-11 Complex bypass lst8Δ and tor2-21 mutations

Far11 has been shown to be involved in cell cycle arrest in response to mating pheromone in a multi-protein complex with Far3, Far7, Far8, Far9, and Far10 (59, 68). Interactions among these six Far proteins are based mostly on yeast two-hybrid assays (68, 73); however, Far3 has been reported to interact with Far11 by coimmunoprecipitation. I generated strains coexpressing HA-tagged Far11 and myc-tagged Far7, Far8, Far9, Far10, and Far11 under the control of their respective endogenous promoters to test whether Far11 interacts with Far7, Far8, Far9, Far10 or itself by coimmunoprecipitation. *FAR11-HA* was found to be functional by its ability to complement a *far11Δ* mutation using the colony-sectoring assay described for Figure 1C (Appendix Fig. A3). myc-tagged Far proteins are functional as described previously (68). Far11-HA in cell lysates prepared for coimmunoprecipitation exists as two bands on Western blots (Fig. 3A). The faster mobility form of Far11-HA is likely to be a proteolytically truncated form of Far11 since Far11-HA exists as a single band on Western blots when the total cellular proteins were prepared by disrupting cells in the presence of 1.85N NaOH-7.5% β-mercaptoethanol and followed by precipitation with trichloroacetic acid (Appendix Fig. A4). myc-tagged proteins were precipitated from cell lysates using anti-myc antibody. Figure 3A shows that Far11-HA

coimmunoprecipitates with myc-tagged Far7, Far8, Far9, Far10, but not Far11, demonstrating that Far11 interacts with other Far proteins *in vivo*.

Since Far11 is part of a multi-protein complex, it is possible that the entire complex is involved in TORC2 signaling. I examined whether mutations of the Far complex bypass *lst8Δ* and *tor2-21* as well. *lst8Δ farΔ* double mutants each carrying a centromeric plasmid encoding *LST8* and *URA3* (*[CEN URA LST8]*) were grown on SD medium without or with 5-fluoroorotic acid (5-FOA), which selects for cells that have lost the *URA3* plasmid. Based on their relative growth in the presence of 5-FOA, mutations in *FAR3, FAR7, FAR8, FAR9, FAR10,* and *FAR11* bypass *lst8Δ* to varying degrees: *far11> far8/9> far3/7> far10* (Fig. 3B). *farΔ* mutations were subsequently found to suppress a *tor2-21* mutation at 37 °C (Fig. 3C). The *tor2-21* suppression phenotypes of *far3*, *far7*, *far8*, *far9*, *far10*, and *far11* mutations largely mirror that of their respective *lst8Δ* bypass (Fig. 3B and C), indicating that the function of Lst8 is tightly linked to TORC2.

Far9 and Far10 are homologous proteins with 31% sequence identity and 47% sequence similarity, yet they have different *lst8Δ* and *tor2-21* suppression phenotypes. I generated a *tor2-21 far9Δ far10Δ* triple mutant and found that its growth was only marginally better than the *tor2-21 far9Δ* double mutant (Appendix Fig. A5), indicating that of the two, Far9 plays the primary role in TORC2 signaling.

It is unclear whether an *lst8Δ* or *tor2-21* mutation leads to complete loss of TORC2 activity. Deletion of *TOR2*, encoding the only TOR kinase in TORC2, abolishes TORC2 activity. To test whether *far11Δ* bypasses *tor2Δ*, spores of tetrads from *FAR11/far11 TOR2/tor2Δ::kanMX4* diploid cells were assessed for viability. All tetrads produced at most two viable spores, none of which were geneticin-resistant (*kanXM4* confers geneticin resistance) (Appendix Fig. A6). Since *FAR11* and *TOR2* are not located on the same chromosome, 25% of spores should have the genotype *tor2Δ::kanMX4 far11Δ.* Failure to obtain viable geneticin-resistant spores indicates that *far11Δ* is unable to bypass *tor2Δ*. Similarly, I found that *far11Δ* failed to bypass *avo1Δ* or *avo3Δ* (Appendix Fig. A6). Since *far11Δ* is able to suppress *lst8Δ* and *tor2-21* mutations, it is likely that *lst8Δ* and *tor2-21* mutations do not completely abolish TORC2 activity and that *far11Δ* can restore growth to cells with a severe loss, but not a total loss of TORC2 activity.

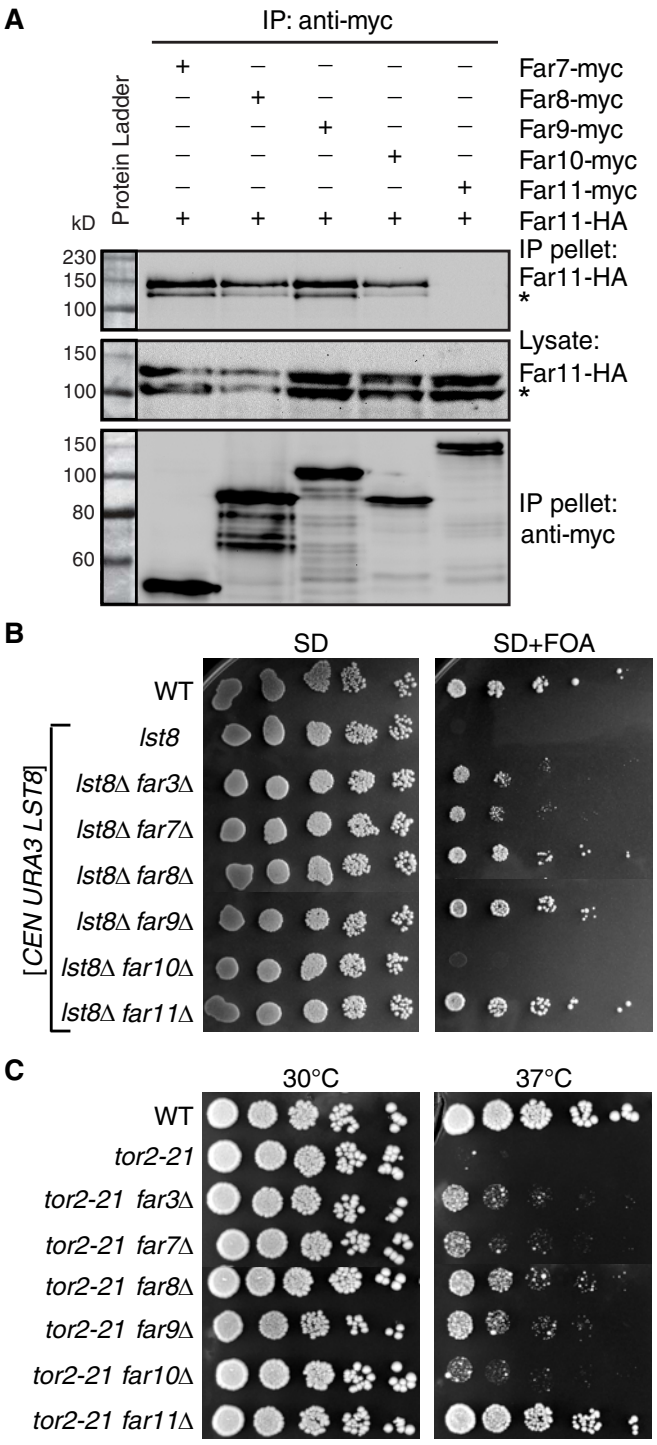

Figure 3. Mutations in *FAR3, FAR7, FAR8, FAR9, FAR10,* and *FAR11* bypass *lst8Δ* and *tor2-21* mutant phenotypes.

(A) Far11-HA interacts with myc-tagged Far7, Far8, Far9, and Far10. Cell lysates of strains TPY978 (Far7-myc), TPY981 (Far8-myc), TPY1001 (Far9-myc), TPY1002 (Far10-myc), and TPY1003 (Far11-myc) coexpressing Far11-HA (pZL2762) were subjected to immunoprecipitation with anti-myc antibody. HA- and myc-tagged proteins were detected by Western blotting. * denotes a likely truncation product of Far11-HA.

(B) Mutations in *FAR3*, *FAR7*, *FAR8*, *FAR9*, *FAR10*, and *FAR11* bypass *lst8Δ*. Serial dilutions of wild-type (RBY231) and isogenic mutant cells (*lst8Δ*, RBY223; *lst8Δ far3Δ*, MOY142; *lst8Δ far7Δ*, MOY145; *lst8Δ far8Δ*, MOY146; *lst8Δ far9Δ*, MOY169; *lst8Δ far10Δ*, MOY149; *lst8Δ far11Δ*, MOY150) carrying a centromeric plasmid encoding *URA3* and *LST8* (pZL339) as indicated were grown on SD medium without or with 5-FOA.

(C) Mutations in *FAR3*, *FAR7*, *FAR8*, *FAR9*, *FAR10*, and *FAR11* suppress *tor2-21* at 37 °C. Serial dilutions of indicated cells (WT, SH100; *tor2-21*, SH121; *tor2-21 far3Δ*, TPY157; *tor2-21 far7Δ*, TPY147; *tor2-21 far8Δ*, TPY213; *tor2-21 far9Δ*, TPY207; *tor2-21 far10Δ*, TPY151; *tor2-21 far11Δ*, TPY116) were grown on YPD medium at 30 °C and 37 °C for 3-4 days.

2.4.5. sac7Δ and far11Δ additively suppress tor2-21

TORC2 is involved in the organization of the actin cytoskeleton. A *tor2-21* mutant shows depolarization of the actin cytoskeleton and several *tor2-21* suppressors can restore actin polarization to *tor2-21* mutant cells (102). I compared actin structures in wild-type, *tor2-21*, *tor2-21 sac7Δ*, and *tor2-21 far11Δ* mutant cells to establish whether actin polarization defects caused by a *tor2-21* mutation could be restored by a *far11Δ* mutation. As expected, a *sac7Δ* mutation restored polarization of the actin cytoskeleton in *tor2-21* mutant cells grown at 37 °C (Fig. 4A). Similarly, a *far11Δ* mutation restored polarization of actin structures in *tor2-21* mutant cells grown at 37 °C (Fig. 4B). A recent genome-wide study of genetic interactions in yeast showed that *far11Δ* restored actin polarization to *tsc11-1* (*avo3-1*) mutant cells (7). Together, these data establish that Far11 negatively regulates TORC2-mediated polarization of the actin cytoskeleton.

Similar phenotypes of *far11Δ* and *sac7Δ* mutations prompted me to determine whether they act through the same molecular mechanism. Accordingly, I compared the growth of a *tor2-21 sac7Δ far11Δ* triple mutant to wild-type, *tor2-21*, *tor2-21 sac7Δ*, and *tor2-21 far11Δ* mutants at 30 °C versus 37 °C. Figure 4C shows that while all strains grew equally well at 30 °C, the *tor2-21 sac7Δ far11Δ* mutant grew better than either the *tor2-21*

far11Δ or the *tor2-21 sac7Δ* mutant at 37 °C, indicating that *far11Δ* and *sac7Δ* have additive effects in suppressing *tor2-21*. To examine whether *sac7Δ* and *far11Δ* have an additive effect in suppressing an actin depolarization defect in *tor2-21* mutant cells, I determined the percentage of cells with polarized actin cytoskeleton in wild-type and isogenic *tor2-21*, *tor2-21 sac7Δ, tor2-21 far11Δ, tor2-21 sac7Δ far11Δ* mutant cells. Table 1 shows that the effect of *sac7Δ* and *far11Δ* on the restoration of actin structure polarization is additive. Sac7 and Rom2 have opposing roles in mediating TORC2 function and it has been proposed that Tor2 activates Rho1 via Rom2 (102). Therefore, to determine whether *tor2-21* suppression by *far11Δ* is Rom2-dependent, I introduced a *rom2Δ* mutation into the *tor2-21 far11Δ* mutant. Figure 4D shows that a *rom2Δ* mutation greatly reduced the *tor2-21* suppression phenotype of a *far11Δ* mutation at 37 °C but did not abolish it, suggesting that *far11Δ* suppression of TORC2-deficiency is not entirely dependent on the Rom2-mediated Rho1/2 GTPase switch.

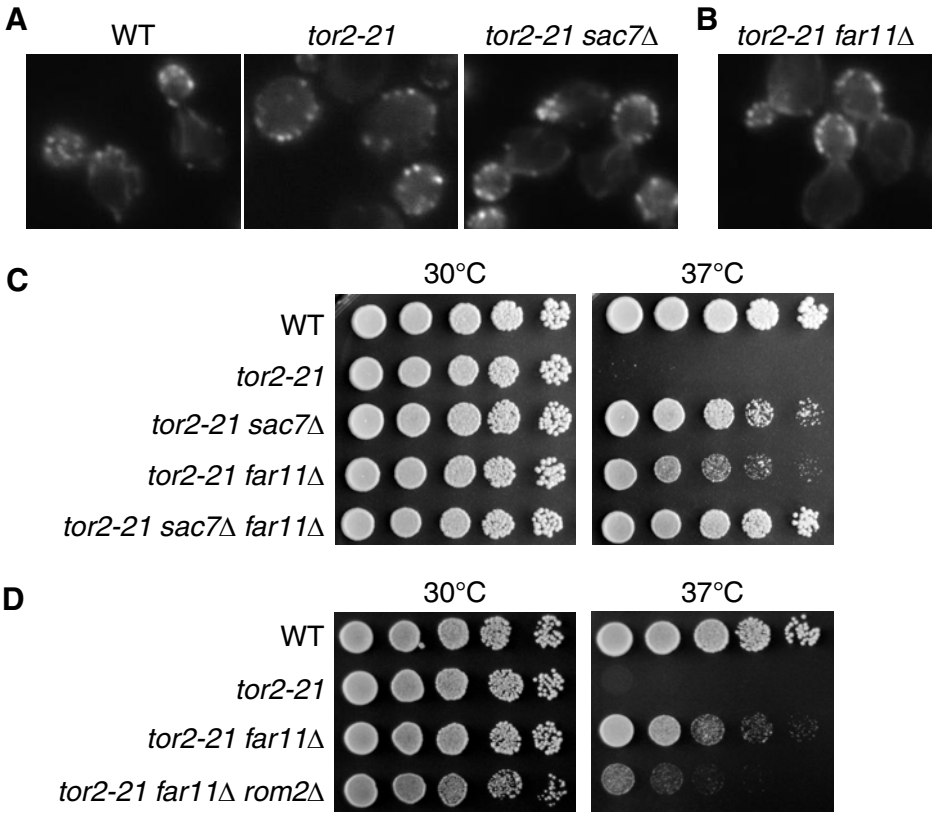

Figure 4. *sac7Δ* and *far11Δ* additively suppress *tor2-21*.

(A-B) Mutations in *SAC7* and *FAR11* restore polarization of the actin cytoskeleton to *tor2-21* mutant cells grown at 37 °C. Actin structures in indicated cells (WT, SH100; *tor2-21*, SH121; *tor2-21 sac7Δ*, TPY110; *tor2-21 far11Δ* TPY116) were detected by staining with rhodamine phalloidin as described in Materials and Methods.

(C) *sac7Δ* and *far11Δ* have an additive effect in suppressing *tor2-21*. Serial dilutions of indicated cells (WT, SH100; *tor2-21*, SH121; *tor2-21 sac7Δ*, TPY110; *tor2-21 far11Δ* TPY311;

tor2-21 sac7Δ far11Δ, TPY301) were grown on YPD medium at 30 °C and 37 °C for 2-3 days.

(D) *far11Δ* suppression of *tor2-21* is partially dependent on *ROM2*. Serial dilutions of indicated cells (WT, SH100; *tor2-21*, SH121; *tor2-21 far11Δ* TPY311; *tor2-211 far11Δ rom2Δ*, TPY680) were grown on YPD medium at 30 °C and 37 °C.

Table 1. Quantitative analysis of polarization of the actin cytoskeleton.

Strain	# cells imaged	# polarized cells	% polarized cells
Wild-type	474	357	75.3%
tor2-21	424	89	21.0%
tor2-21 sac7Δ	504	267	53.0%
tor2-21 far11Δ	461	240	52.1%
tor2-21 sac7Δ far11Δ	451	318	70.5%

2.4.6. Far11 interacts with Tpd3 and Pph21, components of PP2A

The data so far raise the question: How does the Far3-7-8-9-10-11 complex mediate TORC2 signaling? The human ortholog of yeast Far11 exists in the human STRIPAK complex, which also contains components of PP2A (48). The Far11 ortholog in *Drosophila* has also been reported to interact with PP2A in the dSTRIPAK complex (96). Therefore, I tested whether Far11 in yeast also exists in a complex with PP2A. In yeast, the heterotrimeric PP2A phosphatase consists of the regulatory A subunit Tpd3, the regulatory B subunit Cdc55 or B' subunit Rts1, and one of the two homologous and functionally redundant catalytic C subunits Pph21 or Pph22 (34). Among approximately 75 proteins that genetically or biochemically interact with Far11 in various genome-wide gene/protein interaction studies (*Saccharomyces Genome Database*), Tpd3 has been found to interact with Far11 by yeast two-hybrid analysis (119). The significance of this interaction remains unknown.

To establish the interaction between Far11 and PP2A in yeast, lysates from cells coexpressing 3x HA-tagged Far11 and 3x myc-tagged Tpd3 or Pph21 were subjected to immunoprecipitation using anti-myc antibody. *TPD3-myc* and *PPH21-myc* constructs were found to be functional by their ability to rescue growth defects of *tpd3Δ* and *pph21/22Δ* mutants respectively (Appendix Fig. A7). No Far11-HA was detected in the

IP pellet from cells expressing Far11-HA alone. In contrast, Far11-HA was recovered in the IP pellet from cells coexpressing Tpd3-myc, and to a lesser extent, from cells coexpressing Pph21-myc (Fig. 5A) likely because C-terminal tagging of Pph21 perturbs methylation at its C-terminus required for PP2A complex stability (122). These findings establish that Far11 interacts with PP2A phosphatase.

2.4.7. Defects in PP2A-Rts1 bypass lst8Δ and tor2-21 mutations

To investigate whether PP2A is involved in TORC2 signaling, I examined whether mutations in PP2A components bypass *lst8Δ*. I analyzed the growth of an *lst8Δ tpd3Δ* double mutant, an *lst8Δ rts1Δ* double mutant, an *lst8Δ cdc55Δ* double mutant, and an *lst8Δ pph21Δ pph22Δ* triple mutant each carrying a centromeric plasmid encoding *URA3* and *LST8* on SD medium without or with 5-FOA. *tpd3Δ, rts1Δ,* and *pph21/22Δ* mutations, but not a *cdc55Δ* mutation, were able to bypass *lst8Δ* (Fig. 5B and C), indicated by their ability or inability to grow in the presence of 5-FOA, suggesting that reduced activity in the PP2A-Rts1 subcomplex results in *lst8Δ* bypass. I then tested whether *rts1Δ* and *tpd3Δ* mutations suppress *tor2-21*. Figure 5D shows that *rts1Δ* suppresses a *tor2-21* mutation by restoring cell growth at 37 °C. A *tpd3Δ* mutation led to temperature-sensitive growth defects in the *TOR2* wild-type strain used in my study; therefore, I could not assay *tor2-21* suppression by *tpd3Δ*. These findings indicate that

mutations in genes encoding components of the PP2A-Rts1 subcomplex suppress TORC2-deficiency.

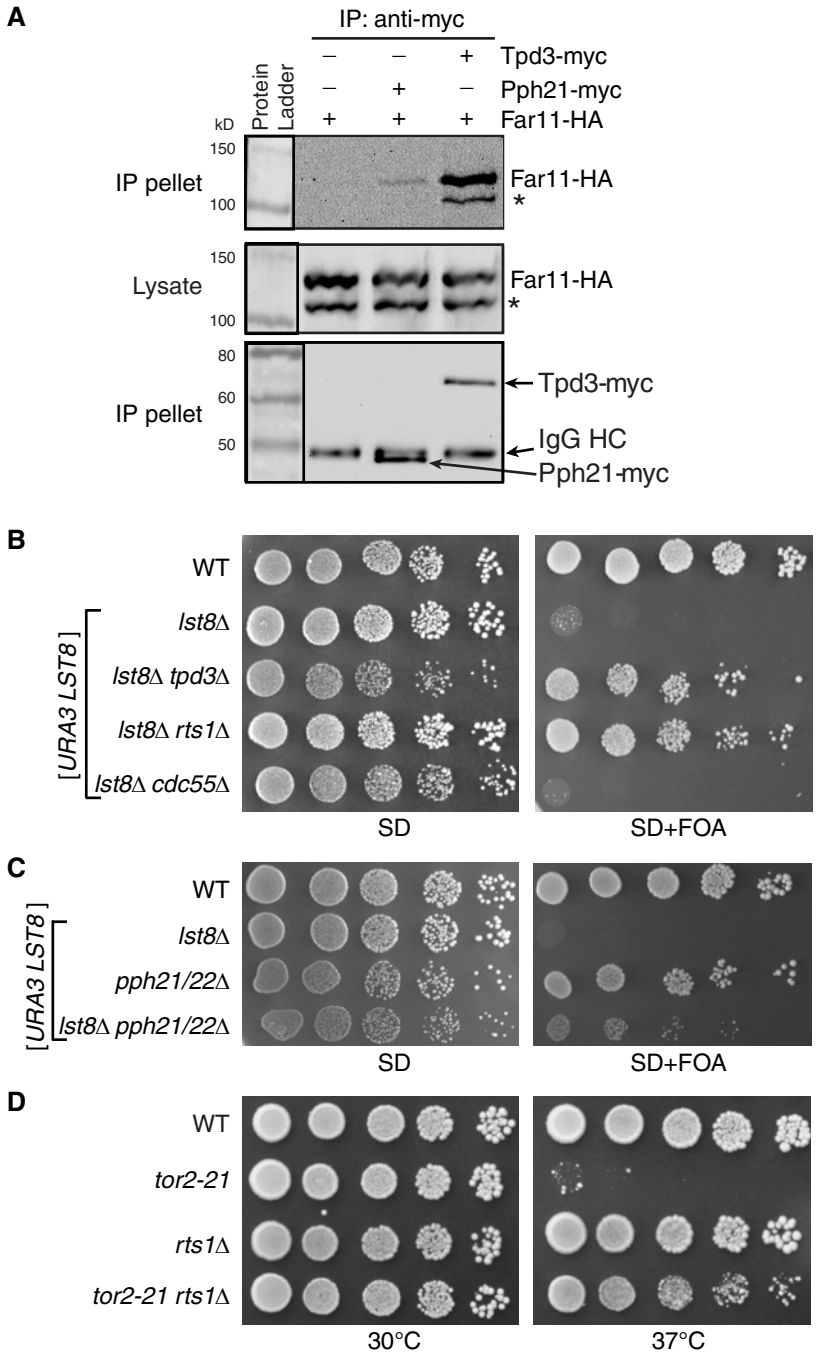

Figure 5. Mutations in *TPD3, RTS1* and *PPH21/22* suppress TORC2 deficiency.

(A) Far11-HA interacts with Tpd3-myc and Pph21-myc. Cell lysates of *far11Δ* mutant cells (BY4741 *far11*) expressing Far11-HA only (pZL2762), *tpd3Δ far11Δ* double mutant cells (TPY633) coexpressing Far11-HA and Tpd3-myc (pTP242), and *pph21/22Δ far11Δ* triple mutant cells coexpressing Far11-HA and Pph21-myc (pTP244) were subject to immunoprecipitation with anti-myc antibody. IgG HC indicates the heavy chain of the anti-myc antibody used for Co-IP. * denotes a likely truncation product of Far11.

(B) Mutations in *TPD3* and *RTS1* bypass *lst8Δ*. Serial dilutions of wild-type (WT, RBY231), *lst8Δ* (RBY223), *lst8Δ tpd3Δ* (TPY625), *lst8Δ rts1Δ* (TPY648), and *lst8Δ cdc55Δ* mutant (TPY732) cells carrying a centromeric plasmid encoding *LST8* (*[URA3 LST8]*, pZL339) were grown on SD medium without or with 5-FOA.

(C) A *pph21/22Δ* double mutation bypasses *lst8Δ*. Serial dilutions of wild-type cells (WT, BY4741) carrying an empty vector pRS416, *lst8Δ* single (BY4741 *lst8*), *pph21/22Δ* double (BY4741 *pph21*/22) and *lst8Δ pph21/22Δ* triple (TPY622) mutant cells carrying a plasmid encoding *LST8* (pZL339) were tested for growth as described for panel B.

(D) An *rts1Δ* mutation suppresses *tor2-21* at 37 °C. Serial dilutions of wild-type (SH100), *tor2-21* (SH121), *rts1Δ* (TPY665), and *tor2-21 rts1Δ* (TPY601) cells were grown on YPD medium at 30 °C and 37 °C.

2.4.8. far11Δ and rts1Δ restore phosphorylation of Slm1 in a tor2-21 mutant

One known function of TORC2 is its role in the organization of the actin cytoskeleton possibly by phosphorylating Slm1, Slm2, and Ypk2. The data above show that *far11Δ*, *sac7Δ* and *rts1Δ* mutations suppress a *tor2-21* mutation and that Far11 interacts with PP2A. Therefore, I tested the possibility that Far11 may mediate dephosphorylation of Slm1, Slm2, and/or Ypk2 via PP2A by evaluating the phosphorylation states of Slm1, Slm2, and Ypk2 in wild-type, *tor2-21*, *tor2-21 far11Δ*, *tor2-21 sac7Δ*, and *tor2-21 rts1Δ* mutant cells each expressing Slm1-HA, Slm2-HA, or Ypk2-HA from their respective endogenous promoters. Ypk2 and Slm2's phosphorylation states did not differ between the wild-type and the *tor2-21* mutant grown at 37 °C (Appendix Fig. A8). Therefore, Ypk2 and Slm2 were not studied further. Consistent with previous reports on the phosphorylation state of GFP-tagged Slm1 (5), Figure 6A shows that Slm1-HA is phosphorylated: lambda protein phosphatase (λ PPase) treatment resulted in increased levels of the faster mobility forms of Slm1-HA with concomitant reduced levels of the slower mobility forms of Slm1-HA; phosphatase inhibitors largely abolished the effect of λ PPase treatment. As reported previously, Figure 6B shows that Slm1 is dephosphorylated in *tor2-21* mutant cells grown at 37 °C (5). Remarkably, *far11Δ*, but not *sac7Δ*, restored Slm1-HA phosphorylation to *tor2-21*

mutant cells grown at 37 °C (Fig. 6B), implicating Far11 in Slm1 dephosphorylation and suggesting that suppression of TORC2-deficiency by a *sac7Δ* mutation takes place downstream of Slm1. Furthermore, Slm1-HA was phosphorylated in *tor2-21 rts1Δ* mutant cells grown at 37 °C (Fig. 6C). These data suggest that Far11-PP2A-Rts1 may antagonize TORC2 activity and decrease the levels of the phosphorylated form of the TORC2 substrate Slm1.

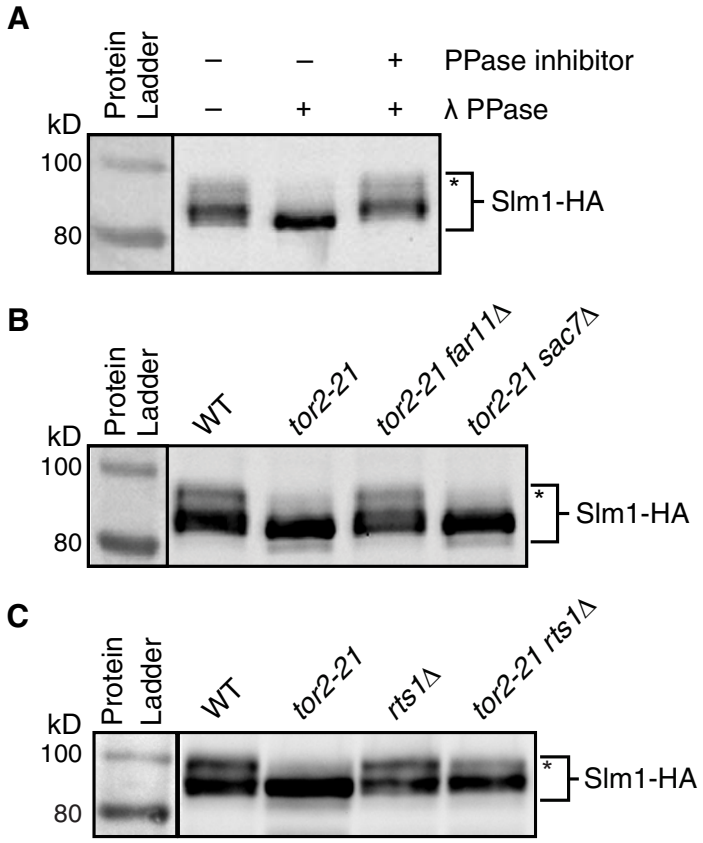

Figure 6. Mutations in *RTS1* and *FAR11,* but not *SAC7,* restore SLM1 phosphorylation in *tor2-21* mutant cells.

(A) Slm1-HA is phosphorylated. Cell lysates from wild-type cells (SH100) expressing Slm1-HA (pTP311) were prepared and treated with lambda protein phosphatase (λPPase) with or without phosphatase inhibitors as described in Materials and Methods. Slm1-HA was detected by Western blotting. * indicates phosphorylated Slm1.

(B) A mutation in *FAR11*, but not in *SAC7*, restores Slm1 phosphorylation in *tor2-21* mutant cells grown at 37 °C. Indicated cells (WT, SH100; *tor2-21*, SH121; *tor2-21 far11Δ*,

TPY116; *tor2-21 sac7Δ*, TPY110) expressing Slm1-HA were grown in YNBcasD medium at 30 °C to mid-log phase and switched to 37 °C for 3h before cellular proteins were processed for Western blotting.

(C) An *rts1Δ* mutation restores Slm1 phosphorylation in *tor2-21* mutant cells grown at 37 °C. Indicated cells (WT, SH100; *tor2-21*, SH121; *rts1Δ*, TPY665; *tor2-21 rts1Δ*, TPY601) expressing Slm1-HA were analyzed for Slm1-HA phosphorylation as described for panel B.

2.4.9. Effects of sac7Δ and far11Δ mutations on Tor2 kinase activity

Sac7 has been proposed to function downstream of TORC2. The genetic data suggest that Far11-PP2A-Rts1 antagonizes TORC2 signaling. It is possible that Far11-PP2A-Rts1 may function downstream of TORC2 and promote dephosphorylation of TORC2 substrates. It is also likely that Far11-PP2A-Rts1 may function upstream of TORC2 and negatively impact TORC2 activity. To differentiate between these two possibilities, the activity of immunopurified Tor2 with a N-terminal 3xHA tag from wild-type and isogenic *far11Δ* mutant cells was determined in an *in vitro* kinase assay using Slm1 as a substrate. Slm1 has been reported to be a TORC2 substrate in *in vitro* kinase assays (5, 37). For the assays, recombinant 6xHis-tagged Slm1was added to kinase reactions with immunopurified HA-Tor2 and [γ-^{32}P]-ATP. Figure 7 shows that *far11Δ* has no significant effect on kinase activity of immunopurified HA-Tor2, suggesting that Far11 functions at a site downstream of TORC2.

Similarly, I performed an *in vitro* kinase assay using HA-Tor2 from *sac7Δ* mutant cells. Surprisingly, *sac7Δ* slightly increases kinase activity of immunopurified HA-Tor2 (Fig. 7). Mutations in *SAC7* have been proposed to activate Rho1, which in turn activates Pkc1 and the cell wall integrity MAP kinase cascade. Increased activity of Tor2 in *sac7Δ* mutant cells suggests positive feedback regulation in TORC2 signaling.

Differential effects of *sac7Δ* and *far11Δ* mutations on Tor2 kinase activity further support the notion that Sac7 and Far11 mediate TORC2 signaling through different mechanisms.

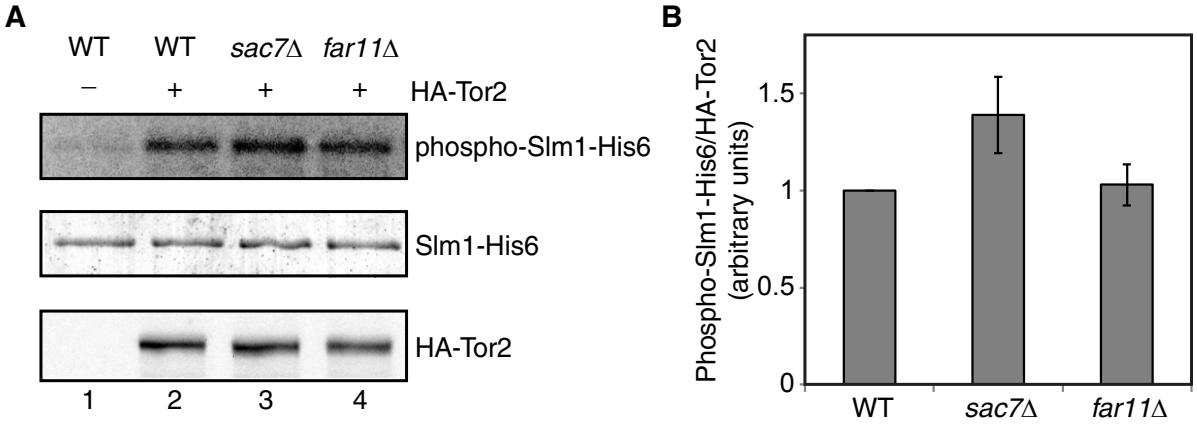

Figure 7. *In vitro* phosphorylation of Slm1 by immunopurified HA-Tor2.

(A) Wild-type (SW70) and isogenic *sac7Δ* (TPY1246) and *far11Δ* (TPY1249) cells expressing N-terminal 3xHA-tagged Tor2 from the *TOR2* genomic locus were grow in YPD medium. Slm1-His6 phosphorylation assays by HA-Tor2 were conducted as described in Materials and Methods. Phospho-Slm1-His6 was detected by autoradiography. Total Slm1-His6 and HA-Tor2 in the assays were detected by Coomassie Blue staining and immunoblotting, respectively. The result of a mock kinase assay using cell lysates from wild-type cells expressing native, nontagged Tor2 (TB50a) was included in lane 1.

(B) The amount of phospho-Slm1-His6 was normalized to that of HA-Tor2 and graphed. Kinase assays were performed with HA-Tor2 from two independent cell lysates and the error bar indicates the standard deviation.

2. 5. Discussion

Lst8 is an essential protein that exists in both TOR kinase complexes. I found that mutations in genes encoding the PP2A-Rts1 subcomplex and the Far3-7-8-9-10-11 complex bypass *lst8Δ* and TORC2-deficiency. Analysis of these mutants led me to propose that the essential function of Lst8 is linked to TORC2. The Far3-7-8-9-10-11 complex components are partially conserved in *Drosophila* and mammals, and have been reported to interact with PP2A phosphatase in the STRIPAK complex. I showed that the Far3-7-8-9-10-11 complex and PP2A negatively regulate TORC2 signaling possibly by mediating dephosphorylation of the TORC2 substrate Slm1, depicted by the proposed model in Figure 8. My results not only demonstrate that the essential function of Lst8 is only linked to TORC2, but more importantly, reveal a novel link between the two major signaling protein complexes PP2A and TORC2.

2.5.1. The essential function of Lst8 is linked to TORC2, but not TORC1

Yeast Lst8 has been reported to be important for TORC2 complex integrity *in vivo* and Tor2 kinase activity *in vitro* (126). Underlying its importance in TORC2 activity, the presence of Lst8 in TORC2 has been reported in multiple organisms including yeast, slime mold, worms, flies, and mammals (28). Consistently, my data demonstrate that the essential function of Lst8 is linked to TORC2. Delocalization of Bit61 and Avo3 from

punctate structures at the plasma membrane in *lst8Δ* mutant cells likely results from compromised TORC2 integrity in the absence of Lst8, indicating that Lst8 is also required for proper localization of the TORC2 complex.

Lst8 interacts with the kinase domain of Tor2 in yeast TORC2 (126). Since *far11Δ* bypasses *lst8Δ* and *tor2-21*, but not *tor2Δ*, *avo1Δ*, and *avo3Δ*, my data suggest that neither *lst8Δ* nor the temperature-sensitive *tor2-21* mutation leads to total loss of TORC2 activity. This possibility helps explain my observation that *far11Δ* and *rts1Δ* can restore Slm1 phosphorylation to *tor2-21* mutant cells at the restrictive temperature: If *tor2-21* led to total loss of TORC2 activity and consequent loss of Slm1 phosphorylation, PP2A inactivation could not restore Slm1 phosphorylation unless other protein kinases also phosphorylate Slm1. In this scenario, TORC2 would share a redundant function with the other putative kinase in phosphorylating Slm1 and may have another essential function separate from its kinase activity, for example, by maintaining interactions with other proteins to conduct downstream signaling.

Three TORC2 substrates in yeast are Slm1, Slm2, and Ypk2. A constitutively active Ypk2 mutant can restore growth to *tor2Δ* mutant cells, leading to the proposal that the essential function of TORC2 is mainly linked to Ypk2 phosphorylation (28, 66). There is strong evidence that functionally redundant Slm1 and Slm2 are essential

substrates of TORC2. Firstly, Slm1 has been reported to interact with TORC2 and to be phosphorylated by TORC2 (5, 37). Secondly, TORC2-dependent phosphorylation of Slm1 seems to correlate with its plasma membrane association (5). Slm1 contains a PH domain that binds to multiply phosphorylated phosphoinositides and is required for Slm1's plasma membrane localization (37), and putative loss of plasma membrane association of Slm1/2 leads to cell death. Thirdly, a *sac7Δ* mutation suppresses both a *tor2-21* mutation and a *slm1Δ slm2Δ* double mutation, and the actin cytoskeleton is depolarized in both *slm1/2* and *tor2-21* mutant cells. Although I could not test whether phosphorylation of Slm2 and Ypk2 in a *tor2-21* mutant is restored by *far11* and *rts1* mutations, it is likely that due to mutations in Far11-PP2A, increased phosphorylation of Slm1, Slm2, and/or Ypk2 leads to cell viability in TORC2-deficient cells.

The presence of Lst8 in TORC1 is conserved from yeast to mammals. In yeast, Lst8 localizes not only to the TORC1 compartment at the vacuolar membrane, but also to the TORC2 compartment as punctate structures at the plasma membrane (10). Similar to its interaction with Tor2 in TORC2, in yeast and humans, Lst8 interacts with the Tor1 kinase domain in the TORC1 complex (1, 70). Therefore, the observation that Lst8 is not required for TORC1-dependent expression of genes encoding ribosomal proteins and Kog1 localization at the vacuolar membrane is surprising, raising the question: Is Lst8 required for TORC1 activity at all? Missense mutations in *LST8* increase the expression

of a subset of TORC1-target genes (25, 45). Therefore, Lst8 is likely to be required for optimal TORC1 activity, but an *lst8Δ* mutation may not reduce TORC1 activity severely enough to lead to cell death. In mammals, the role of Lst8 in mTORC1 is unclear. mLst8 knockdown in human immortalized cell lines suggested that mLst8 is important for mTORC1 activity (70). Later in mice, mLst8 was found to be important for mTORC2, but not mTORC1 function during mouse development (50). The discrepancy could be attributed to the differences between a developing mouse embryo and an immortalized human cell line. However, the conclusions concerning the role of Lst8 in both yeast and mouse are similar: the essential function of Lst8 is linked to TORC2 but not TORC1.

2.5.2. Far3-7-8-9-10-11-PP2A as a negative regulator of TORC2 signaling

One of the important findings presented here is a negative regulatory role of the Far3-7-8-9-10-11 complex and PP2A in TORC2 signaling. Considering the extensive studies on PP2A and TORC2, it is surprising that, to my knowledge, this study may represent the first to present a direct genetic interaction between TORC2 and PP2A. More importantly, my data mirror a recent study in *Drosophila* demonstrating that the *Drosophila* Far complex works in concert with PP2A in the regulation of a different kinase pathway, the Hippo signaling pathway (96). Thus, PP2A regulation by the Far protein complex appears to be evolutionarily conserved. In a proteomics study, the

yeast Far11 orthologs, Fam40A and Fam40B (STRIP1/2) were isolated in the STRIPAK complex, which also contains components of PP2A. Interestingly, *far11Δ* leads to the strongest suppression of TORC2-deficiency, and among the six Far proteins, Far11 is the most conserved. Far9 and Far10 are homologous proteins and their *Drosophila* and mammalian orthologs show limited sequence homology, mostly in an FHA domain, which is known to interact with phosphothreonine epitopes on target proteins (33). Far8 shows very limited sequence homology to striatin (48). The question remains: How does the Far3-7-8-9-10-11 complex affect PP2A activity? Interaction between Far11 and Tpd3, the scaffolding subunit of PP2A suggests that the Far complex may directly regulate PP2A by either targeting the TORC2 substrate Slm1 and/or mediating PP2A activity. Unlike slow cell growth phenotypes due to a *tpd3Δ* single or a *pph21/22Δ* double mutation, mutations in *FAR3, FAR7, FAR8, FAR9, FAR10,*and *FAR11* have little or no growth defects, suggesting that the Far complex is not integral to PP2A activity. In both the *Drosophila* study and this one, mutations in PP2A and/or Far components of the STRIPAK complex lead to increased phosphorylation of target proteins. Thus, it is possible that the Far complex might target certain substrates to PP2A.

This study demonstrates that Far11-PP2A-Rts1 modulates Slm1 phosphorylation by counteracting the kinase activity of TORC2, providing a molecular mechanism to explain how mutations in *FAR11* and genes encoding PP2A-Rts1 components might

suppress TORC2-deficiency. The calcineurin phosphatase also mediates Slm1 dephosphorylation and counteracts TORC2 signaling (19, 30, 87). It was further shown that mutations in *cnb1*, encoding the regulatory subunit of calcineurin, suppress an *avo3* temperature-sensitive mutation (4). It remains to be determined whether a *cnb1* mutation restores phosphorylation of Slm1 to TORC2-deficient cells. Ypk2 is another essential effector of TORC2. Mutations in calcineurin could potentially restore phosphorylation of Ypk2 in *avo3* mutant cells, thereby suppressing the *avo3* temperature-sensitive growth phenotype. Furthermore, in a genome-wide study on genetic interactions in yeast, mutations in *PPG1*, encoding a PP2A-like phosphatase, also suppress TORC2-deficiency (7). Therefore, it is likely that these phosphatases may work together to mediate TORC2 signaling.

Various genetic screens in fungi have isolated mutations in the Far complex. In *Neurospora crassa*, a mutation in *ham-2*, the ortholog of yeast *FAR11* leads to defects in hyphal fusion (127). In *Sordaria macrospora,* mutations in *PRO22*, encoding the yeast Far11 ortholog, generate a novel type of sterile mutant with a defect in ascogonial septum formation (15). In yeast, mutations in *FAR9*/*VPS64* and *FAR11*/*YNL127w* result in vacuolar sorting defects (16), and mutations in *FAR3*, *FAR7*, *FAR8*, *FAR10*, and *FAR11* create long-lived mutants (36). In all of these studies, the underlying mechanisms are unknown. In light of my findings, it is possible that these disparate

phenotypes are due to the perturbation of PP2A activity and/or TORC2 signaling in these mutants.

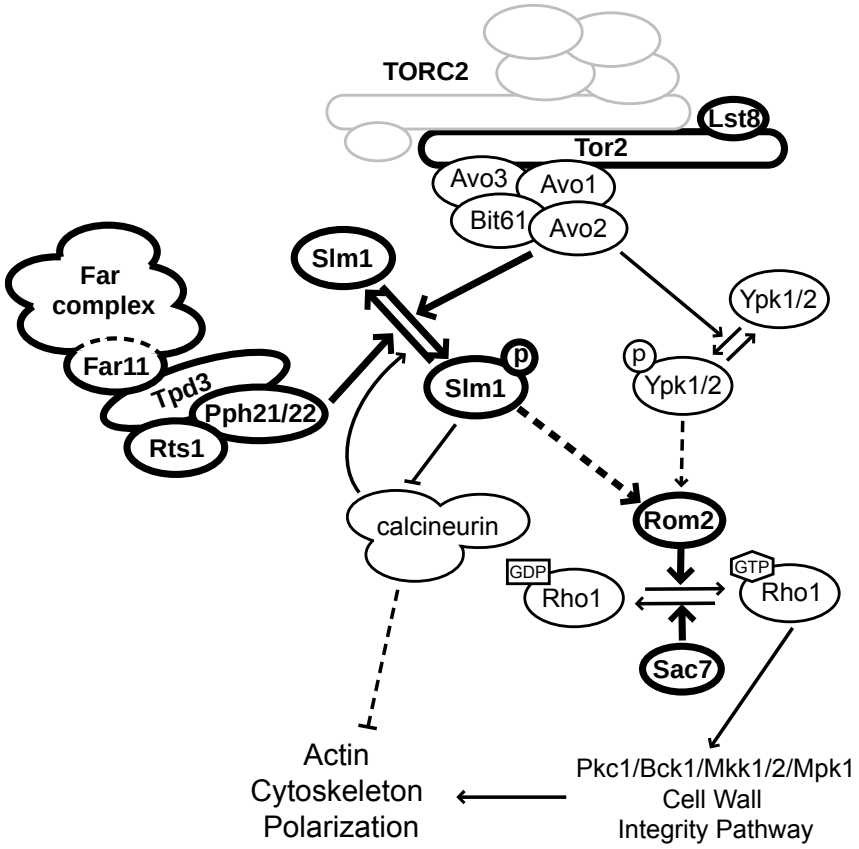

Figure 8. A model for the regulation of TORC2 signaling by the Far3-7-8-9-10-11 complex and PP2A-Rts1.

TORC2 regulates the organization of the actin cytoskeleton via phosphorylation of Slm1 and Ypk1/2. Far3-7-8-9-10-11-PP2A-Rts1 antagonizes TORC2 signaling by promoting Slm1 dephosphorylation. Proteins in bold were analyzed in this study.

Table 2. *S. cerevisiae* strains used in Chapter 2.

Strain	Genotype	Source	Application
ZLY2254	*MATa ura3Δ0 leu2Δ0 his3Δ1 met15Δ0 lst8::kanMX4 ade2Δ::HIS3 [pRS412-LST8]*	This study	
ZLY3081 (WT)	*MATα ura3Δ0 leu2Δ0 his3Δ1 met15Δ0 lst8::kanMX4 ade2Δ::HIS3 [pRS412-LST8]*	This study	Fig. 1
TPY104 (*leb1*)	*MATα ura3Δ0 leu2Δ0 his3Δ1 met15Δ0 lst8::kanMX4 ade2Δ::HIS3 leb1::Tn3::LEU2 [pRS412-LST8]*	This study	Fig. 1
TPY103 (*leb2*)	*MATα ura3Δ0 leu2Δ0 his3Δ1 met15Δ0 lst8::kanMX4 ade2Δ::HIS3 leb2::Tn3::LEU2 [pRS412-LST8]*	This study	Fig. 1
ZLY423 (WT)	*MATa ade2-1 ura3 his3-11,15 leu2 lst8::LEU2 [pRS412-LST8]*	This study	Fig. 2A
TPY115 (*far11 lst8*)	*MATa ade2-1 ura3 his3-11,15 leu2 lst8::LEU2 far11::kanMX4*	This study	Fig. 2A
TPY114 (*far11*)	*MATa ade2-1 ura3 his3-11,15 leu2 lst8::LEU2 far11::kanMX4 [pRS412-LST8]*	This study	Fig. 2A
TPY122 (*fpr1*)	*MATa ade2-1 ura3 his3-11,15 leu2 lst8::LEU2 fpr1::kanMX4 [pRS412-LST8]*	This study	Fig. 2A
ZLY2405 (*sac7 lst8*)	*MATa ade2-1 ura3 his3-11,15 leu2 lst8::LEU2 sac7::kanMX4*	This study	Fig. 2A
ZLY2404 (*sac7*)	*MATa ade2-1 ura3 his3-11,15 leu2 lst8::LEU2 sac7::kanMX4 [pRS412-LST8]*	This study	Fig. 2A-B
ZLY2845 (*sac7 lst8*)	*MATa ade2-1 ura3 his3-11,15 leu2 lst8::LEU2 sac7::kanMX4 [pRS412]*	This study	Fig. 2B
TWY680	*MATa AVO3-GFP::kanR ura3 trp1 leu2 his3 ade2 can1-100*	(10)	
TWY696	*MATa BIT61-GFP::HIS ura3 trp1 leu2 his3 ade2 can1-100*		
TWY748	*MATa KOG1-GFP::HIS ura3 trp1 leu2 his3 ade2 can1-100*		
TPY1264 (WT, no GFP)	*MATa sac7::kanMX4 far11::TRP1 ura3 leu2 his3 ade2 trp1 can1-100*	This study	Fig. 2C
TPY1266 (lst8, no GFP)	*MATa sac7::HIS3 far11::TRP1 lst8::LEU2 ura3 leu2 his3 ade2 trp1*	This study	Fig. 2C

	can1-100		
TPY369 (*AVO3-GFP*)	*MATa AVO3-GFP::kanR ura3 trp1 leu2 his3 ade2 can1-100 sac7::HIS3 far11::TRP1*	This study	Fig. 2
TPY407 (*lst8 AVO3-GFP*)	*MATa AVO3-GFP::kanR ura3 trp1 leu2 his3 ade2 can1-100 sac7::HIS3 far11::TRP1 lst8::LEU2*	This study	Fig. 2
TPY358 (*BIT61-GFP*)	*MATa BIT61-GFP::HIS ura3 trp1 leu2 his3 ade2 can1-100 sac7::kanMX4 far11::TRP1*	This study	Fig. 2C
TPY366 (*lst8 BIT61-GFP*)	*MATa BIT61-GFP::HIS ura3 trp1 leu2 his3 ade2 can1-100 sac7::kanMX4 far11::TRP1 lst8::LEU2*	This study	Fig. 2C
TPY371 (*KOG1-GFP*)	*MATa KOG1-GFP::HIS ura3 trp1 leu2 his3 ade2 can1-100 sac7::kanMX4 far11::TRP1*	This study	Fig. 2C
TPY413 (*lst8 KOG1-GFP*)	*MATa KOG1-GFP::HIS ura3 trp1 leu2 his3 ade2 can1-100 sac7::kanMX4 far11::TRP1 lst8::LEU2*	This study	Fig. 2C
SY2227	*MATa ade1-1 leu2-2,113 trp1 ura3-52 bar1 HIS3::pFUS1::HIS3 mfa2-Δ1::FUS1-lacZ rad16::pGAL1::STE4*	(68)	
SY4078	SY2227 *FAR7-myc13-KAN <pSL2771>*		
SY4079	SY2227 *FAR8-myc13-KAN <pSL2771>*		
SY4080	SY2227 *FAR9-myc13-KAN <pSL2771>*		
SY4081	SY2227 *FAR10-myc13-KAN <pSL2771>*		
SY4082	SY2227 *FAR11-myc13-KAN <pSL2771>*		
TPY978	SY2227 *FAR7-myc13-KAN [pRS416-FAR11-HA]*	This study	Fig. 3A
TPY981	SY2227 *FAR8-myc13-KAN [pRS416-FAR11-HA]*	This study	Fig. 3A
TPY1001	SY2227 *FAR9-myc13-KAN [pRS416-FAR11-HA]*	This study	Fig. 3A
TPY1002	SY2227 *FAR10-myc13-KAN [pRS416-FAR11-HA]*	This study	Fig. 3A
TPY1003	SY2227 *FAR11-myc13-KAN [pRS416-FAR11-HA]*	This study	Fig. 3A
RBY231 (WT)	*MATα ura3 leu2 lys2 [pRS416-LST8]*	This study	Fig. 3B,

			5B
RBY223 (*lst8*)	*MATα ura3 leu2 lys2 lst8::LEU2 [pRS416-LST8]*	This study	Fig. 3B, 5B
MOY142 (*lst8 far3*)	*MATα ura3 leu2 lys2 lst8::LEU2 far3::kanMX4 [pRS416-LST8]*	This study	Fig. 3B
MOY145 (*lst8 far7*)	*MATα ura3 leu2 lys2 lst8::LEU2 far7::kanMX4 [pRS416-LST8]*	This study	Fig. 3B
MOY146 (*lst8 far8*)	*MATα ura3 leu2 lys2 lst8::LEU2 far8::kanMX4 [pRS416-LST8]*	This study	Fig. 3B
MOY169 (*lst8 far9*)	*MATα ura3 leu2 lys2 lst8::LEU2 far9::kanMX4 [pRS416-LST8]*	This study	Fig. 3B
MOY149 (*lst8 far10*)	*MATα ura3 leu2 lys2 lst8::LEU2 far10::kanMX4 [pRS416-LST8]*	This study	Fig. 3B
MOY150 (*lst8 far11*)	*MATα ura3 leu2 lys2 lst8::LEU2 far11::kanMX4 [pRS416-LST8]*	This study	Fig. 3B
SH100 (WT)	*MATa leu2-3,112 ura3-52 rme1 trp1 his4 HMLa ade2 tor2::ADE2 [YCplac111::TOR2]*	(57)	Fig. 3C, 4, 5D, 6A, 6B, 6C, Table 1
SH121 (*tor2-21*)	*MATa leu2-3,112 ura3-52 rme1 trp1 his4 HMLa ade2 tor2::ADE2 [YCplac111::tor2-21]*		Fig. 3C, 4, 5D, 6B, 6C, Table 1
SH221 (*tor1 tor2-21*)	*MATa leu2-3,112 ura3-52 rme1 trp1 his3 HMLa ade2 tor1::HIS3 tor2::ADE2 [YCplac111::tor2-21]*		
TPY157 (*tor2-21 far3*)	SH121 *far3::kanMX4*	This study	Fig. 3C
TPY147 (*tor2-21 far7*)	SH121 *far7::kanMX4*	This study	Fig. 3C
TPY213 (*tor2-21 far8*)	SH121 *far8::kanMX4*	This study	Fig. 3C
TPY207 (*tor2-21 far9*)	SH121 *far9::kanMX4*	This study	Fig. 3C
TPY151 (*tor2-21 far10*)	SH121 *far10::kanMX4*	This study	Fig. 3C
TPY116 (*tor2-21 far11*)	SH121 *far11::kanMX4*	This study	Fig. 3C, 4C, 6B
TPY110 (*tor2-21 sac7*)	SH121 *sac7::kanMX4*	This study	Fig. 4A, 4C, 6B.

			Table 1
TPY311 (*tor2-21 far11*)	SH121 *far11::TRP1*	This study	Fig. 4C, 4D, Table 1
TPY301 (*tor2-21 sac7 far11*)	SH121 *sac7::kanMX4 far11::TRP1*	This study	Fig. 4C, Table 1
TPY680 (*tor2-21 far11 rom2*)	SH121 *rom2::kanMX4 far11::TRP1*	This study	Fig. 4D
BY4741	*MATa ura3 leu2 his3 met15*	Yeast Genome Deletion Project	
BY4741 *far11*	BY4741 *far11::kanMX4*		Fig. 5A
TPY633	BY4741 *tpd3::kanMX4 far11::HIS3*	This study	Fig. 5A
TPY632	BY4741 *pph21::kanMX4 pph22::kanMX4 far11::HIS3*	This study	Fig. 5A
TPY625 (*lst8 tpd3*)	*MATα ura3 leu2 lys2 lst8::LEU2 tpd3::kanMX4 [pRS416-LST8]*	This study	Fig. 5B
TPY648 (*lst8 rts1*)	*MATα ura3 leu2 lys2 lst8::LEU2 rts1::kanMX4 [pRS416-LST8]*	This study	Fig. 5B
TPY732 (*lst8 cdc55*)	*MATα ura3 leu2 lys2 lst8::LEU2 cdc55::kanMX4 [pRS416-LST8]*	This study	Fig. 5B
BY4741 (WT)	*MATa ura3 leu2 his3 met15 [pRS416]*	This study	Fig. 5C
BY4741 (*lst8*)	*MATa ura3 leu2 his3 met15 lst8::LEU2 [pRS416-LST8]*	This study	Fig. 5C
BY4741 (*pph21/22*)	*MATa ura3 leu2 his3 met15 pph21::kanMX4 pph22::kanMX4[pRS416-LST8]*	This study	Fig. 5C
TPY622 (*lst8 pph21/22*)	*MATa ura3 leu2 his3 met15 lst8::LEU2 pph21::kanMX4 pph22::kanMX4[pRS416-LST8]*	This study	Fig. 5C
TPY665 (*rts1*)	*MATa leu2-3,112 ura3-52 rme1 trp1 his4 HMLa ade2 tor2::ADE2 rts1::kanMX4 [YCplac111::TOR2]*	This study	Fig. 5D, 6C
TPY601 (*tor2-21 rts1*)	*MATa leu2-3,112 ura3-52 rme1 trp1 his4 HMLa ade2 tor2::ADE2 rts1::kanMX4 [YCplac111::tor2-21]*	This study	Fig. 5D, 6C
TB50a	*MATa leu2–3,112 ura3–52 trp1 his3 rme1 HMLa*	(126)	Fig. 7
SW70	*TB50a 3HA-TOR2*		Fig. 7
TPY1246	*TB50a 3HA-TOR2 sac7::HIS3*	This study	Fig. 7
TPY1249	*TB50a 3HA-TOR2 far11::TRP1*	This study	Fig. 7

Table 3. Plasmids used in Chapter 2

Plasmid	Description	Reference	Application
pZL2422	pRS416-SAC7	This study	Fig. 1
pZL2550	pRS416-FAR11	This study	Fig. 1
pZL1255	pRS412-LST8	This study	Fig. 2A-B
pZL2762	pRS416-FAR11-HA, expressing Far11 from its own promoter with a 3xHA tag at the C-terminus.	This study	Fig. 3A, 5A
pTP242	pRS415-ADH1-TPD3-myc, expressing Tpd3 from the ADH1 promoter with a 3xmyc tag at the C-terminus.	This study	Fig. 5A
pTP244	pRS415-PPH21-myc, expressing Pph21 from its own promoter with a 3xmyc tag at the C-terminus.	This study	Fig. 5A
pZL339	pRS416-LST8	(77)	Fig. 3B, 5B
pTP311	pRS416-SLM1-HA, expressing Slm1 from its own promoter with a 3xHA tag at the C-terminus.	This study	Fig. 6A
pTP377	pRS416-SLM2-HA, expressing Slm2 from its own promoter with a 3xHA tag at the C-terminus.	This study	Fig. 6
pTP271	pRS416-YPK2-HA, expressing Ypk2 from its own promoter with a 3xHA tag at the C-terminus.	This study	Fig. 6
pZL3031	pET24a-SLM1, expressing Slm1 with a C-terminal 6xHis tag under the control of an IPTG-inducible promoter.	This study	Fig. 7

CHAPTER 3. TIERED ASSEMBLY OF THE YEAST FAR3-7-8-9-10-11 COMPLEX AT THE ENDOPLASMIC RETICULUM

3.1. Summary

TOR (target of rapamycin) signaling is a conserved, essential pathway integrating nutritional cues with cell growth and proliferation. The TOR kinase exists in two distinct complexes, TORC1 and TORC2. It has been reported that protein phosphatase 2A (PP2A) and the Far3-7-8-9-10-11 complex (Far complex) negatively regulate TORC2 signaling in yeast. The Far complex, originally identified as factors required for pheromone-induced cell cycle arrest, and PP2A form the yeast counterpart of the STRIPAK complex, which was first isolated in mammals. The cellular localization of the Far complex has yet to be fully characterized. Here I show that the Far complex localizes to the endoplasmic reticulum (ER) by analyzing functional, GFP-tagged Far proteins in vivo. I found that Far9 and Far10, two homologous proteins each with a tail-anchor domain, localize to the ER in mutant cells lacking the other Far complex components. Far3, Far7, and Far8 form a subcomplex, which is recruited to the ER by Far9/10. The Far3-7-8 complex in turn recruits Far11 to the ER. Finally, I show that the tail-anchor domain of Far9 is required for its optimal function in TORC2 signaling. My

study reveals tiered assembly of the yeast Far complex at the ER and a function for Far complex's ER localization in TORC2 signaling.

3.2. Introduction

Protein phosphorylation plays important roles in many cellular processes. Protein phosphorylation is catalyzed by specific protein kinases and protein dephosphorylation is carried out by protein phosphatases. Thus, the phosphorylation state of proteins is finely controlled by the opposing activities of protein kinases and phosphatases. Multiple mechanisms exist to fine-tune the activity of these protein kinases and phosphatases through the regulation of their expression levels, their activity, cellular localization, and availability to substrates, among others. Recently, a large multi-protein complex known as the striatin-interacting phosphatase and kinase (STRIPAK) complex was found in mammals. STRIPAK contains PP2A catalytic and scaffolding subunits, striatins, the striatin-associated protein Mob3, two homologous novel proteins STRIP1 and STRIP2, members of the germinal center kinase III family of Ste20 kinases, and the Cerebral Cavernous Malformation 3 (CCM3) protein (48, 96). The STRIPAK assembly maintains mutually exclusive interactions with either the CTTNBP2 (cortactin-binding protein 2) proteins or a second subcomplex consisting of sarcolemmal membrane-associated protein (SLMAP) and two related coiled-coil

proteins SIKE and FGFR1OP2. The N-terminal region of CCM3 mediates heterodimerization with Ste20 kinases, and its C-terminal domain interacts with striatin (24, 39, 67, 75, 131), which also interacts with the regulatory and catalytic subunits of PP2A, thus bridging a kinase to a phosphatase. This arrangement likely facilitates the regulation of the activity of protein kinases by PP2A (47, 67). Both Striatin 3 and STRIP1 localize to the Golgi and depletion of either results in similar defects suggesting they perform similar functions in regulation of Golgi morphology and mitosis (42, 67). The SLMAP gene has several splice variants, encoding tail-anchored membrane proteins that associate with the sarcolemmal membrane in muscle cells, the endoplasmic reticulum and the mitochondrial membrane in non-muscle cells, and the centrosome and the outer nuclear envelope (21, 42, 52, 89, 124). SLMAP is required for myoblast fusion, centrosome function, and structural arrangement of the excitation-contraction coupling apparatus in cardiomyocytes (42, 51-53). Much remains to be determined about the role of STRIPAK components and the regulation and substrates of STRIPAK.

Orthologs of mammalian STRIPAK components have been reported to exist in many eukaryotes. The *Drosophila* STRIPAK complex has been reported to be involved in Hippo signaling by mediating phosphorylation of the Hippo kinase and the transcriptional activator Yorkie (96). In *Neurospora crassa*, orthologs of STRIPAK complex components are required for hyphal fusion (108, 127). In the ascomycete

Sordaria macrospora, the STRIPAK complex is required for sexual development and vegetative hyphal fusion (14, 15). In the fission yeast *Schizosaccharomyces pombe*, components of the STRIPAK complex localize to the mitotic spindle pole body in early mitosis and are required for the establishment of asymmetry of the septation initiation network, a conserved signaling pathway that is required for cytokinesis and mitotic transitions (42, 109).

In the budding yeast *Saccharomyces cerevisiae*, the STRIPAK complex has been reported to mediate pheromone signaling, the TORC2 signaling pathway, and the toxicity due to expression of human Caspase-10 in yeast (7, 68, 76, 93). The yeast STRIPAK complex contains Far3, Far7, Far8, Far9, Far10, Far11, Tpd3 (the A scaffolding subunit of PP2A), and Pph21/22 (the two redundant catalytic subunits of PP2A) (68, 73, 76, 93, 119). Far11 is an ortholog of human STRIP1/2; Far8 shares limited sequence similarity to human striatins; Far9 and Far10 are homologous tail-anchored proteins similar to human SLMAP (Table 1) (9, 48). Yeast cells secrete pheromones to induce cell cycle arrest to prepare for mating as part of the fungal life cycle (38). Mutations in *FAR* genes lead to increased resistance to pheromone-induced cell cycle arrest (59, 68), but the underlying mechanism is still unclear. TOR (target of rapamycin) kinases are conserved in eukaryotes and exist in two distinct multi-protein complexes, TORC1 and TORC2 (74, 80), and mutations in the yeast STRIPAK complex components lead to

suppression of cell lethality specifically due to TORC2-deficiency possibly by restoring phosphorylation of TORC2 substrates Slm1, Slm2, Ypk1 and Ypk2 (7, 37, 90, 93). The role of STRIPAK in human Caspase-10 induced toxicity in yeast likely results from promoting Atg13 dephosphorylation and subsequent activation of autophagy (65, 76).

In yeast, Far3, Far7, Far8, Far9, Far10 and Far11 have been reported to form a complex (68, 73, 93). However, it is unclear how these proteins assemble together to form the final complex, and identification of the cellular component of this complex could potentially provide insights into the mechanism of its function. Cellular localization of subsets of the Far complex components has been reported in three different studies, however the results were not consistent (9, 61, 76). A genome-wide study on the localization of yeast proteins found that Far3, Far7, and Far8 localize to the ER (61). In that study, Far9 was shown to be localized in the cytoplasm, Far10 localization was ambiguous, and there was no data on Far11. In another study, Beilharz et al. showed that Far9 localizes to the ER and that Far10 is found in clusters within the bounds of the ER (9). In the third reported study on the localization of Far proteins, Far11 was reported to co-localize with Chc1, a late-Golgi protein, Far3 with Cop1, an early Golgi protein, and Far9 with Sec13, an ER-to-Golgi protein that is located on ER-derived transport vesicles (76). To gain insights into how the Far proteins assemble into a complex and address the inconsistency in their cellular localization, I constructed

functional GFP-tagged Far proteins and analyzed their localization in various *far* mutants. My data show that all of the Far proteins localize in a tiered fashion at the endoplasmic reticulum and ER localization of Far9 is required for its optimal function in TORC2 signaling.

Table 1. Components of the STRIPAK complex in mammals and yeast

Description	Mammals	Yeast
PP2A A subunit	PR65A/PR65B	Tpd3
PP2A B‴ subunit	Striatin/ Striatin-3/ Striatin-4	Far8
PP2A C subunit	PP2A Cα and Cβ	Pph21, Pph22
Novel protein	STRIP1/STRIP2	Far11
Tail-anchored protein	SLMAP	Far9/Far10
Coiled-coil domain protein	SIKE, FGFR1OP2	Far3, Far7
Striatin-associated protein	Mob3	*Mob1*
Ste20 family kinase	STK24/STK25/Mst4	*Kic1*
Cavernous cerebral malformation protein 3	CCM3	?
Cortactin-binding protein 2	CTTNBP2	?

(Proteins in italics are orthologs of the respective mammalian proteins but have not yet been confirmed to be part of the yeast STRIPAK complex)

3.3. Materials and methods

3.3.1. Strains, plasmids, and growth media and growth conditions

Yeast strains and plasmids used in this study are listed in Table 2 and 3, respectively. Yeast cells were grown in SD (0.67% yeast nitrogen base plus 2% dextrose), YNBcasD (SD medium plus 1% casamino acids), or YPD (1% yeast extract, 2% peptone, 2% dextrose) medium at temperatures as indicated in the text and in the figure legends. When necessary, amino acids, adenine, and/or uracil were added to the growth medium at standard concentrations to cover auxotrophic requirements (2).

3.3.2. Cellular extract preparation and co-immunoprecipitation

Total cellular protein extracts were prepared by disrupting yeast cells in extraction buffer (1.85 N NaOH–7.5% β-mercaptoethanol) followed by precipitation with trichloroacetic acid as described (129). For co-immunoprecipitation experiments, cellular lysates were prepared in IP buffer (50 mM Tris-HCl pH 7.6, 150 mM NaCl, 0.5% Triton X-100, and protease inhibitors). Cell extracts (~3 mg proteins) were incubated at 4 °C for 1 h with anti-myc antibody (9E10, Roche) or anti-HA antibody (12CA5, Roche) as indicated, after which 30 μl of a 50% slurry of protein G-Sepharose (Roche) was added to each sample and the samples were further incubated at 4 °C for 2 h. Washed

immunoprecipitates bound to the Sepharose beads were released by boiling in 1X SDS-PAGE loading buffer. The released immune complexes were analyzed by SDS-PAGE and immunoblotting. myc, HA, and GFP-tagged proteins were probed with anti-myc antibody 9E10, high affinity anti-HA antibody 3F10 (Roche), and anti-GFP antibody B-2 (Santa Cruz Biotechnology, Inc), respectively. Chemiluminescence images of Western blots were captured using the Bio-Rad Chemi-Doc photo documentation system (Bio-Rad) and processed using Bio-Rad Quantity One software. Experiments were repeated at least twice.

3.3.3. Fluorescence microscopy

Fluorescence of GFP and RFP-tagged proteins was analyzed in live cells grown in SD medium to the mid-logarithmic growth phase by fluorescence microscopy. Cells were concentrated by centrifugation at 5000*g* for 2 minutes and fluorescence images were immediately captured using a Nikon Eclipse E800 microscope equipped with an HBO 100 W/2 mercury arc lamp, a Nikon Plan Fluor 100x objective lens, a Photometrics Coolsnap fx CCD camera, and a Nikon B-2E/C filter set (excitation light wavelengths 465-495 nm, emission light wavelengths 515-555 nm, dichromatic mirror cut-on wavelength 505 nm) for GFP images and a Y-2E/C filter set (excitation light wavelengths 540-580 nm, emission light wavelengths 600-660 nm, dichromatic mirror

cut-on wavelength 595 nm) for RFP images. Digital images were acquired using the Metamorph Imaging Software and processed using ImageJ (NIH) and Adobe Photoshop software. Experiments were repeated at least twice.

3.3.4. Pheromone response halo assay

Sensitivity to the mating pheromone α-factor was assayed by standard plate halo assays as previously described (59, 111). Briefly, 2 μg of α-factor was applied to a sterile filter paper disc placed onto a lawn of $1x10^6$ cells spread on a YNBcasD plate. Halo formation was documented after 3 days of cell growth. Experiments were repeated at least twice.

3.4. Results

3.4.1. GFP-tagged Far3, Far7, Far8, Far9, Far10, and Far11 localize to the Endoplasmic Reticulum

Elucidating the cellular localization of the Far Complex thus far has not been straight forward. Several studies report inconsistent data with the components of the Far complex localizing to different cellular compartments from one study to the next (9, 61, 76). Furthermore, none of the studies comprehensively analyzed the intracellular localization of all components of the complex. In all cases, fluorescent tags were fused to

each Far protein to localize each component. I considered two possibilities that could result in disparity of the cellular localization patterns of the Far proteins and designed the experiment to minimize these complications. First, the functionality of a protein can be inhibited by the addition of a tag. Therefore functionality of the fusion proteins should be determined. The functionality of the fusions of the previous studies was not indicated therefore, it is possible that if their functionalities were not tested and the fusions were not functional the proteins could show inconsistent cellular localizations. Another factor that could affect the localization of a fusion protein is the placement of the fluorescent tag. For instance, Far9 and Far10 contain a hydrophobic tail-anchor domain, and the addition of a fluorescent protein at the C-terminal end of Far9 and Far10 would affect their cellular localization. Therefore, differential cellular localization of Far9 and Far10 could be attributed to the position of the fluorescent protein tag such as in Lisa-Sanatmaria et al.'s study where the authors added a C-terminal CFP tag to Far9 and found Far9 to localize on transport vesicles between ER and the Golgi inconsistent with previous studies (9, 61). Accordingly, I generated N-terminal GFP-tagged Far9 and Far10 fusion constructs and C-terminal GFP-tagged Far3, Far7, Far8 and Far11 constructs on centromeric plasmids and determined their functionality and cellular localization. Expression of GFP-tagged Far3, Far7, Far8 and Far11 fusion proteins was under the control of their respective endogenous promoters. Expression of

GFP-tagged Far9 and Far10 was under the control of a stronger but still relatively weak promoter of *MKS1* (105) due to my initial observations that N-terminal GFP-tagged Far9 and Far10 under the control of their endogenous promoters did not yield enough signal to determine their cellular localization. To minimize potential interference of GFP with the functionality and thus localization of Far proteins, I also introduced a 10-alanine linker between the Far proteins and the GFP tag.

I first determined the functionality of GFP-tagged Far fusion proteins by a plate halo assay (Fig. 1A). Wild-type mating type **a** cells normally arrest cell growth around a paper disc infused with α-factor and create a cell-free zone in the shape of a halo. I generated *far3*, *far7*, *far8*, *far9*, *far10*, and *far11* single deletion mutants and found that they became resistant to α-factor-induced cell cycle arrest, which was manifested by increased cell growth around the disc containing α-factor, consistent with previous results (68). After these *far*Δ mutants were transformed with centromeric plasmids encoding respective wild-type *FAR* genes tagged with GFP, the resultant transformants now became as sensitive to α-factor as wild-type cells, indicating that GFP-tagged Far3, Far7, Far8, Far9, Far10, and Far11 proteins were all functional.

I next examined the cellular localization of the GFP-tagged Far proteins in their respective *far* deletion mutant strains. The right column of Figure 1B shows that all

exhibited localizations suggestive of perinuclear and periplasmic endoplasmic reticulum (ER) localization. To support this assumption, in cells expressing GFP-tagged Far proteins, I coexpressed C-terminal red fluorescent protein (RFP)-tagged Shr3, an ER-localized chaperone for packaging amino acid permeases into COPII-coated transport vesicles (71). Figure 1B shows that Shr3-RFP and each of the six Far-GFP fusion proteins colocalize, indicating that the Far complex localizes to the ER. I expressed GFP-tagged Far proteins in respective *far* deletion mutant strains of two other strain backgrounds, BY4741, which is derived from S288c, and SY2227 (68), and I found that in these strains, GFP-tagged Far proteins also localized to the ER (data not shown), indicating that ER localization of the Far complex is not strain dependent.

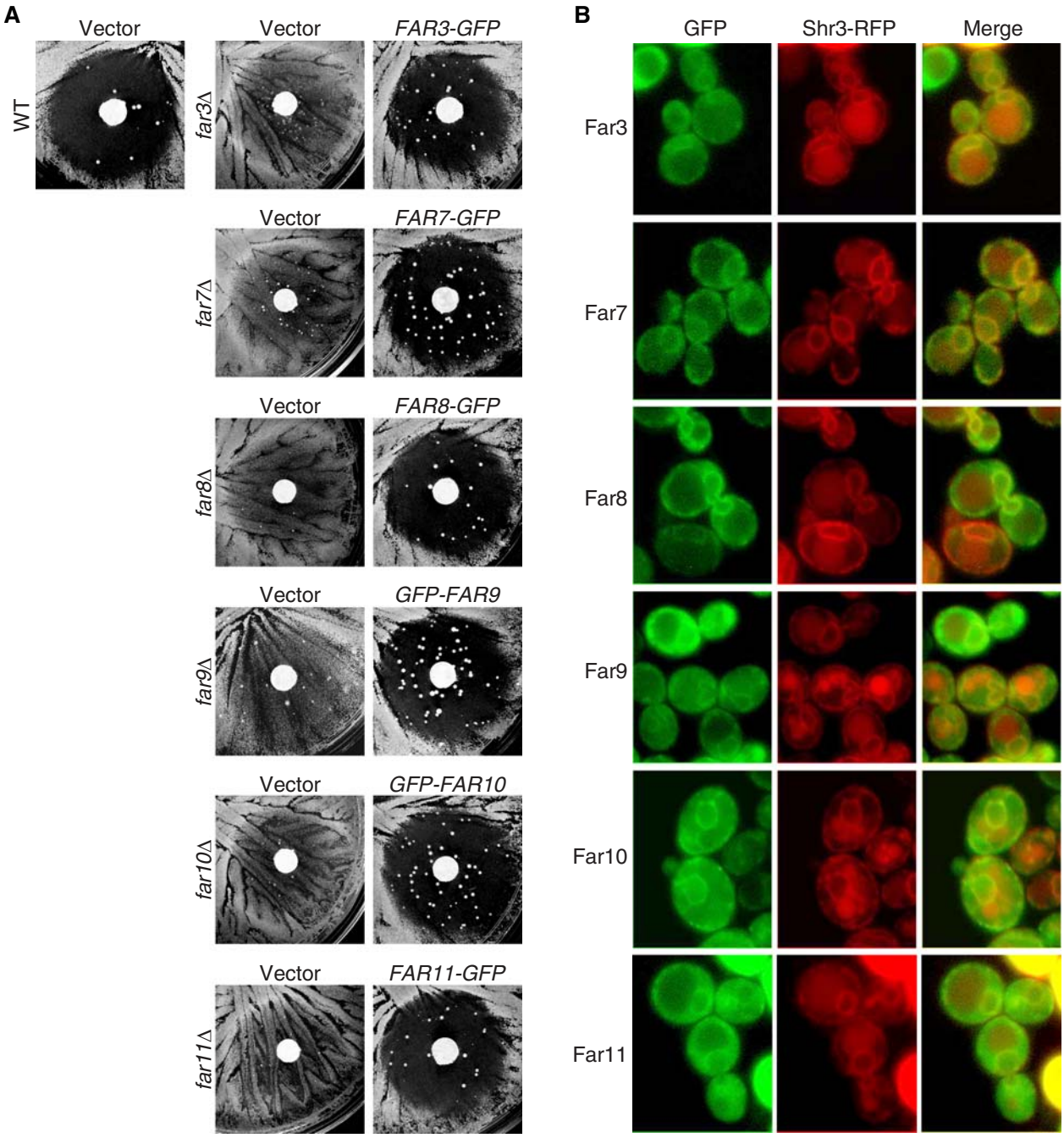

Figure 1. The Far3,7,8,9,10,11 complex localizes to the ER.

(A) GFP-tagged *FAR* constructs complement respective *far* deletion mutations by halo assay. Wild-type (WT, SY2227) and isogenic *far*Δ mutant cells (*far3*Δ, TPY1010; *far7*Δ, TPY1013; *far8*Δ, TPY1015; *far9*Δ, TPY1048; *far10*Δ, TPY1072; *far11*Δ, SY4064) carrying the empty vector pRS416 (Vector) or plasmids encoding respective *FAR-GFP* fusions (*FAR3-GFP*, pTP143; *FAR7-GFP*, pTP164; *FAR8-GFP*, pTP131; *GFP-FAR9*, pTP179; *GFP-FAR10*, pTP203; *FAR11-GFP*, pZL2564) were grown on YNBcasD medium in the presence of a paper filter disc containing α-factor as described in experimental procedures.

(B) Colocalization of GFP-tagged Far proteins with ER-localized Shr3-RFP. *far*Δ mutant cells (*far3*Δ, TPY157; *far7*Δ, TPY147; *far8*Δ, TPY213; *far9*Δ, TPY357; *far10*Δ, TPY151; *far11*Δ, TPY116) coexpressing respective GFP-tagged Far proteins as described for panel (A) and RFP-tagged Shr3 (pTP201) were grown in SD medium and observed by fluorescence microscopy. GFP and RFP fluorescence images were captured and processed using the same parameters for each channel. Vacuolar autofluorescence in the RFP channel was sometimes observed.

3.4.2. Far9 and Far10 localize to the ER independently of the other Far proteins

To better understand how the Far complex is organized on the ER, I sought to determine which Far protein(s) establishes a foothold on the ER. To this end, I analyzed the cellular localization of individual GFP-tagged Far proteins in a *far3/7/8/9/10/11Δ* sextuple mutant strain. Figure 2 shows that Far3-GFP, Far7-GFP, Far8-GFP, and Far11-GFP, when expressed individually in the sextuple mutant strain, did not exhibit ER localization, indicating that they were unable to localize to the ER in the absence of other Far complex components. In contrast, GFP-Far9 and GFP-Far10 fusion proteins could still localize to the ER in the sextuple mutant, indicating that Far9 and Far10 establish ER localization for the complex. Far9 and Far10 contain a tail-anchor domain at their C-termini. Therefore, it is not surprising that they may function as the ER anchor for the Far complex. Furthermore, the localization of Far9 and Far10 on the ER when expressed individually in the sextuple mutant suggests that these two homologous proteins do not require hetero-oligomerization for ER recruitment.

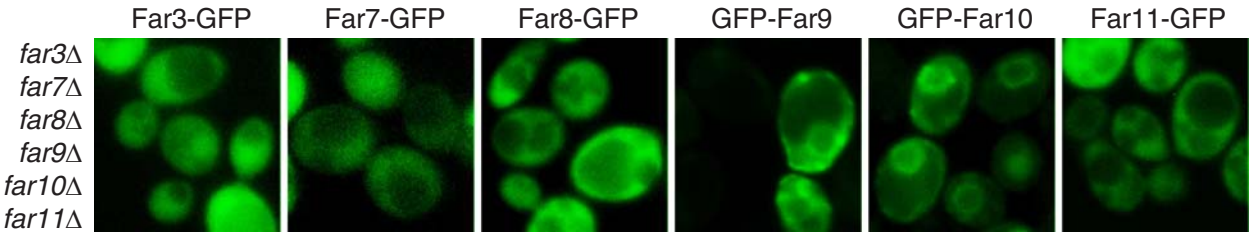

Figure 2. Far9 and Far10, but not Far3, Far7, Far8 or Far11, are able to localize to the ER in the absence of the other Far complex components.

Sextuple *farΔ* mutant cells (TPY845) expressing GFP-tagged Far proteins as indicated were grown in SD medium and observed by fluorescence microscopy.

3.4.3. Tiered assembly of the components of the Far complex at the ER

To further characterize the organization of the Far complex on the ER, I sought to determine the order in which the rest of the complex localizes to the ER. To achieve this, I determined whether ER localization of GFP-tagged Far3, Far7, Far8, or Far11 could be altered by the absence of just one of the other five Far complex components. Accordingly, I characterized the cellular localization of Far3-GFP in *far3Δ far7Δ*, *far3Δ far8Δ*, *far3Δ far9Δ*, *far3Δ far10Δ*, and *far3Δ far11Δ* double deletion mutant cells. Far3-GFP localization at the ER was abolished by *far7Δ*, *far8Δ*, *far9Δ*, and *far10Δ* mutations but still showed normal ER localization in a *far11Δ* mutant, indicating that ER localization of Far3-GFP requires Far7, Far8, Far9 and Far10, but not Far11 (Fig. 3A). Using the same strategy, I determined the cellular localization of Far7-GFP, Far8-GFP, and Far11-GFP in respective double deletion mutant cells. Likewise, ER localization of Far7-GFP and Far8-GFP was abolished by all respective *farΔ* mutations except a *far11Δ* mutation (Fig. 3B-C). Interestingly, ER localization of Far11-GFP was disrupted by the deletion of any of the other five Far complex components (Fig. 3D), suggesting that Far11 is the most peripheral component of this complex at the ER. These data also suggest that Far3, Far7, Far8, and Far11 are peripheral membrane proteins since their ER localization requires the tail-anchored proteins Far9 and Far10. This possibility was supported by my initial

observation early in my studies that the localization of GFP-tagged Far3, Far7, Far8, and Far11 became more cytoplasmic when they were expressed in wild-type cells in comparison to respective deletion mutant cells, suggesting that these four GFP-tagged Far proteins compete with their non-tagged counterparts for Far9/10-dependent ER localization (data not shown). The interdependence of Far3, Far7, and Far8 for ER localization also suggests that they might form a subcomplex before their ER recruitment. Together, these data suggest that the Far complex assembles at the ER in the spatial order of Far9/10, Far3/7/8, and then Far11.

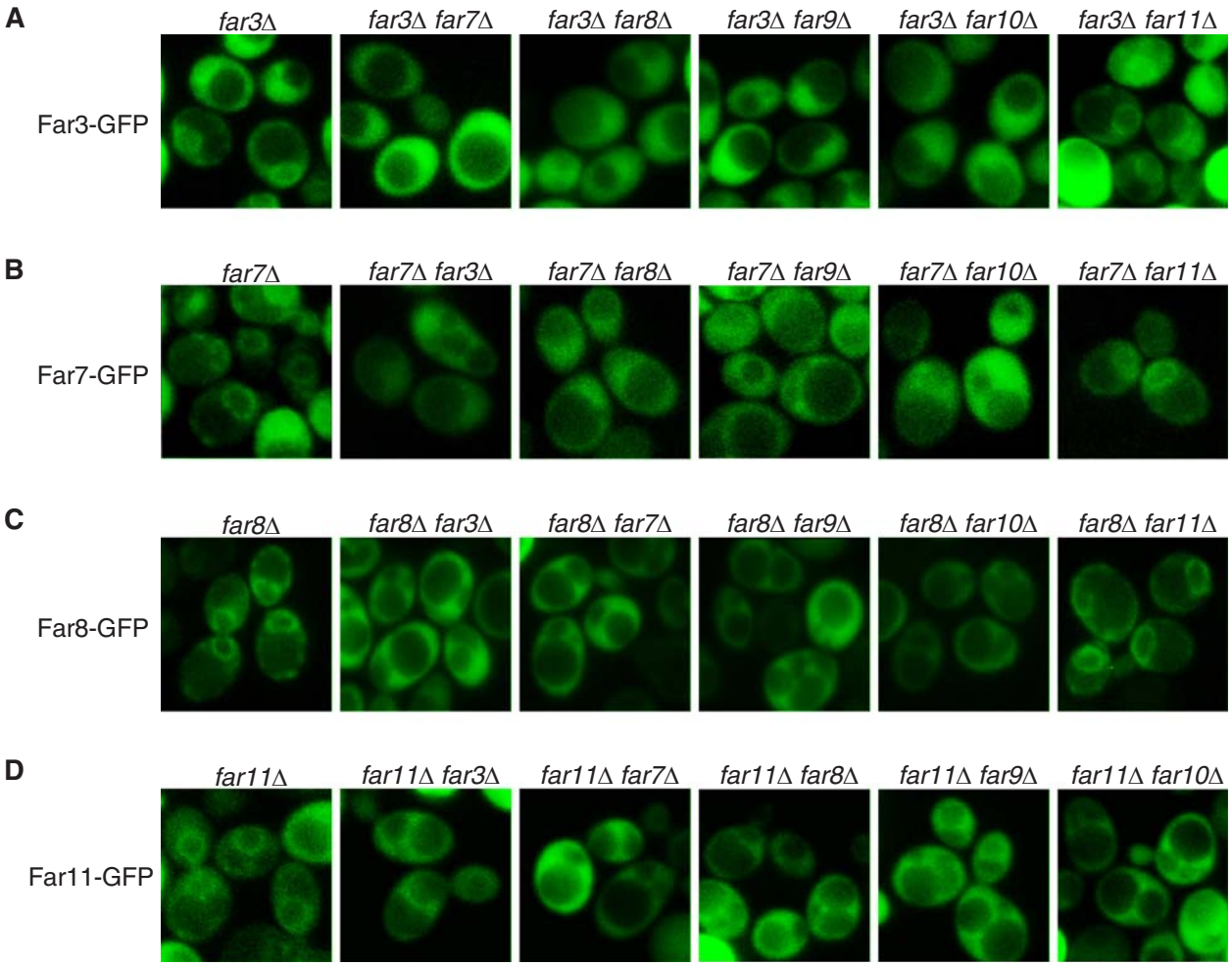

Figure 3. Cellular localization of GFP-tagged Far3, Far7, Far8 or Far11 in the absence of individual components of the Far complex.

(A) Localization of Far3-GFP in the mutant strains as indicated (*far3Δ,* TPY1010; *far3Δ far7Δ*, TPY1358; *far3Δ far8Δ*, TPY1361; *far3Δ far9Δ*, TPY1348; *far3Δ far10Δ*, TPY1363; *far3Δ far11Δ* TPY1402). (B) Localization of Far7-GFP in the mutant strains as indicated (*far7Δ,* TPY1013; *far7Δ far3Δ*, TPY1408; *far7Δ far8Δ*, TPY1366; *far7Δ far9Δ*, TPY1350; *far7Δ far10Δ*, TPY1368; *far7Δ far11Δ* TPY1352). (C) Localization of Far8-GFP in the mutant strains as

indicated (*far8Δ*, TPY1015; *far8Δ far3Δ*, TPY1369; *far8Δ far7Δ*, TPY1370; *far8Δ far9Δ*, TPY1351; *far8Δ far10Δ*, TPY1373; *far8Δ far11Δ* TPY1405). (D) Localization of Far11-GFP in the mutant strains as indicated (*far11Δ*, SY4064; *far11Δ far3Δ*, TPY1374; *far11Δ far7Δ*, TPY1377; *far11Δ far8Δ*, TPY1406; *far11Δ far9Δ*, TPY1410; *far11Δ far10Δ*, TPY1379). All cells were grown in SD medium and observed by fluorescence microscopy.

3.4.4. Far3, Far7, and Far8 form a subcomplex

To test whether Far3, Far7, and Far8 are able to form a subcomplex independent of Far9, Far10 and Far11, I determined whether Far3, Far7 and Far8 could form pair-wise interactions in *far3/7/8/9/10/11Δ* sextuple mutant cells by co-immunoprecipitation. Accordingly, Far3-GFP was coexpressed with either 3xHA epitope-tagged Far7 or Far8 and Far7-GFP was coexpressed with either 3xHA epitope-tagged Far3 or Far8 in *far3/7/8/9/10/11Δ* sextuple mutant cells. HA-tagged proteins from cell lysates were immunoprecipitated with anti-HA antibody and immunoprecipitates were probed with anti-GFP antibody to detect GFP-tagged proteins via Western blotting. I found that Far7-HA, but not Far8-HA, was able to pull down Far3-GFP (Fig. 4A, lane 1-3). Similarly, Far3-HA, but not Far8-HA, was able to pull down Far7-GFP (Fig. 4A, lane 4-6). Together, these data indicate that Far3 and Far7 are able to interact with each other in the absence of the other Far complex components.

Far8 has been reported to interact with Far3 and Far7 by yeast two-hybrid and co-immunoprecipitation analyses in wild-type strains (68, 73). Although I carried out the interaction analysis between Far8 and Far3 or Far7 in sextuple mutant cells, which were not used in previous studies, the failure to detect their interactions in such cells was still surprising because these three proteins appear to require each other to for ER

localization as shown in Figure 3. One possibility is that Far8 may only bind to the Far3-7 complex. To test this hypothesis, I first confirmed whether Far8 interacts with Far3 or Far7 in respective double deletion mutant cells. I generated a *far3Δ far8Δ* double mutant carrying plasmids encoding *FAR3-HA* and *FAR8-GFP*. Figure 4B shows that Far8-GFP was co-immunoprecipitated specifically with Far3-HA (compare lane 1 and 2). Similarly, I found that Far8-GFP specifically interacts with Far7-HA in a *far7Δ far8Δ* double mutant (Fig. 4B, lane 3-4). I next examined whether Far8 interacts with the Far3-Far7 complex in the sextuple mutant. I coexpressed Far3-HA, Far8-GFP and non-tagged Far7 in *far3/7/8/9/10/11Δ* sextuple mutant cells and found that expression of Far7 in the sextuple mutant was sufficient for Far3-HA to interact with Far8-GFP (Fig. 4C, compare lane 1-2). Similarly, reintroduction of Far3 into sextuple mutant cells coexpressing Far7-HA and Far8-GFP also enabled an interaction between Far7 and Far8 (Fig. 4C, compare lane 3-4). These data together indicate that Far3, Far7, and Far8 form a subcomplex in the absence of the other components of the Far complex.

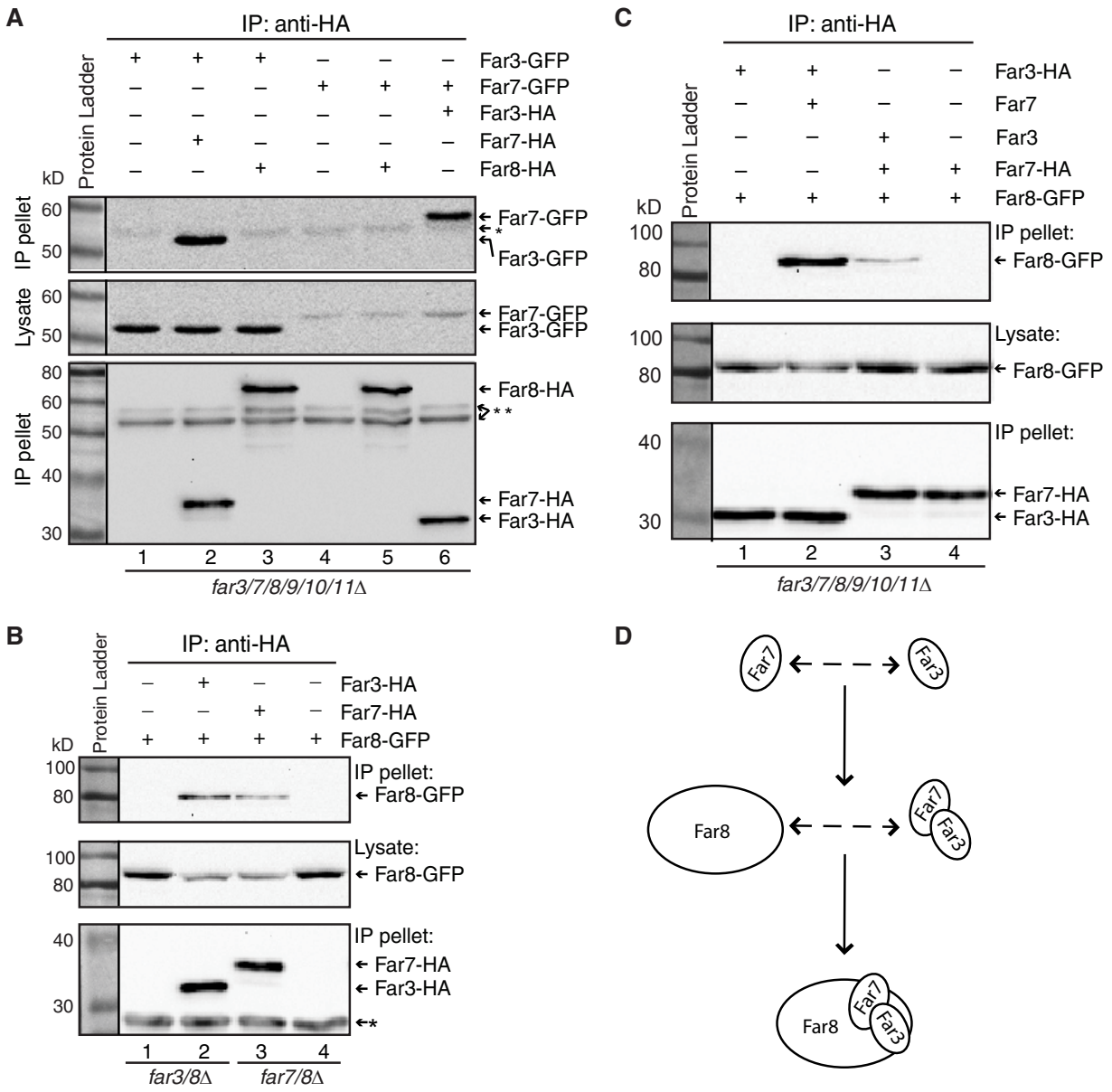

Figure 4. Far3, Far7, and Far8 form a subcomplex.

(A) Far3 and Far7 are able to interact in the absence of Far8, Far9, Far10, and Far11. Cell lysates of sextuple *farΔ* mutant cells (TPY845) coexpressing Far3-GFP (pTP143) and Far7-HA (pTP646) or Far8-HA (pTP658), Far7-GFP (pTP164) and Far3-HA (pTP655) or

Far8-HA (pTP658) as indicated were subjected to immunoprecipitation with anti-HA antibody and epitope-tagged proteins were detected by immunoblotting. * and ** indicate the heavy chain of the anti-HA antibody used for immunoprecipitation that was detected by goat anti-mouse IgG light chain specific and standard secondary antibody, respectively.

(B) Far8 interacts with Far3 or Far7 in the presence of the other Far complex components. *far3/8Δ* mutant cells expressing Far8-GFP (TPY1369) without or with Far3-HA and *far7/8Δ* mutant cells expressing Far8-GFP (TPY1370) without or with Far7-HA were analyzed for interactions between Far8-GFP and Far3-HA or Far7-HA by immunoprecipitation and immunoblotting.

(C) Far8 interacts with the Far3-7 complex. Cell lysates of sextuple *farΔ* mutant cells expressing epitope-tagged and non-tagged proteins as indicated were subjected to immunoprecipitation with anti-HA antibody. GFP- and HA- tagged proteins were detected by immunoblotting.

(D) Model of assembly of the Far3-7-8 subcomplex.

3.4.5. Interaction between Far9 and Far11 requires the Far3-7-8 subcomplex

ER localization of Far11-GFP was disrupted by deletion of any of the other Far complex components as shown in Figure 3D. These findings along with the findings that Far3, Far7, and Far8 form a subcomplex suggest that the Far3-7-8 subcomplex may bridge the interaction of Far11 and Far9/10 at the ER. To test this possibility, interaction between myc-tagged Far9 and HA-tagged Far11 was analyzed in *far9Δ far11Δ* double mutant cells without (WT) or with an additional mutation of *far3Δ*, *far7Δ*, or *far8Δ*. Far9-myc was immunoprecipitated from cell lysates and immunoprecipitates were probed with anti-HA antibody to detect Far11-HA via Western blotting. Figure 5 shows that Far11-HA was co-immunoprecipitated with Far9-myc and deletion of *FAR3, FAR7,* or *FAR8* greatly reduced their interaction. This data indicates that ER recruitment of Far11 by Far9 requires the Far3-7-8 subcomplex.

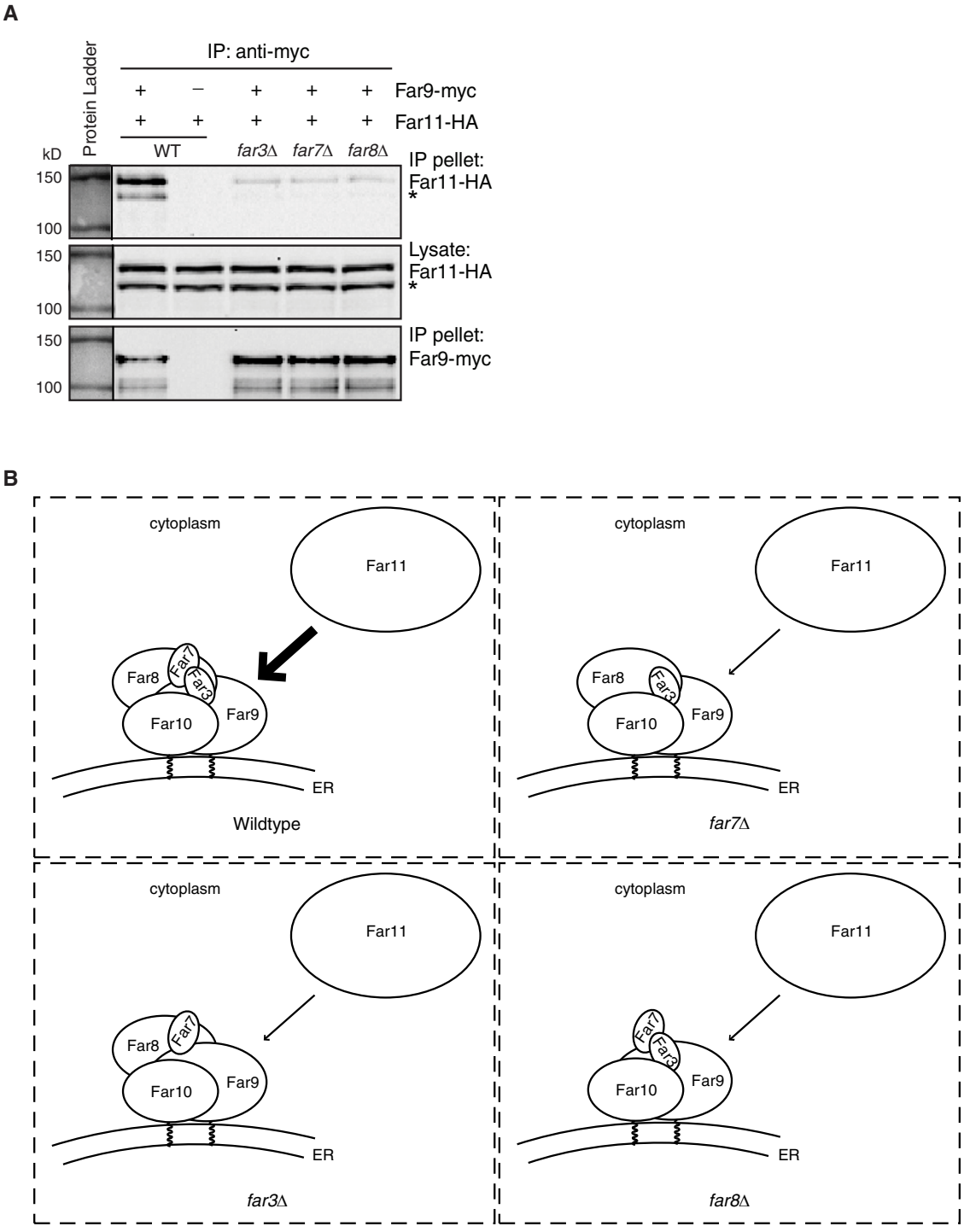

Figure 5. Interaction between Far9 and Far11 is greatly reduced in the absence of Far3, Far7, or Far8.

(A) Cell lysates of strains TPY1411 (WT), TPY1412 (*far3Δ*), TPY1413 (*far7Δ*), and TPY1416 (*far8Δ*) coexpressing Far9-myc and Far11-HA (pZL2762) and the strain SY4064 (WT) expressing Far11-HA alone were subjected to immunoprecipitation with anti-myc antibody. HA- and myc-tagged proteins were detected by immunoblotting. An asterisk denotes a proteolytic product of Far11-HA (93).

(B) Model depicting interaction between Far11 and Far9 in wildtype versus *far3Δ far7Δ* or *far8Δ* mutants.

3.4.6. ER localization of Far9 is required for its optimal function in TORC2 signaling

Yeast Far9 and Far10 and their human and fly orthologs all contain a tail-anchor domain and a forkhead-associated (FHA) domain (Fig. 6A). Tail-anchored proteins utilize the tail-anchor domain for membrane association (17). The finding that Far9 and Far10 are able to localize to the ER in the absence of the other Far complex components prompted us to determine the role of Far9's tail-anchor in the ER localization of Far9. Accordingly, I constructed a GFP-tagged C-terminal truncation mutant of Far9, GFP-Far9ΔC and examined its location in *far9Δ* mutant cells. Unlike GFP-tagged wild-type Far9, GFP-Far9ΔC localized diffusely in the cytoplasm (Fig. 6B), indicating that the tail-anchor domain of Far9 is required for its ER localization.

Recently, I proposed that the Far complex antagonizes TORC2 signaling by showing that a *far9Δ* mutation or loss of other Far complex components are able to bypass a *tor2* temperature sensitive (*tor2-21)* mutation (93). I sought to test whether ER localization of the Far complex is required for its function. To that end, I introduced a *far9ΔC* mutation, which results in the synthesis of Far9 without the tail-anchored domain, at the genomic *FAR9* locus in *tor2-21* mutant cells. I then tested whether the *far9ΔC* mutation could bypass the *tor2-21* mutation and found that *far9ΔC* was able to

partially mimic *far9Δ* in suppressing the growth defect of *tor2-21* mutant cells grown at 36 °C and 37 °C (Fig. 6C). To exclude the possibility that the removal of the tail anchor domain of Far9 may reduce the steady-state level of Far9 by reducing its stability, which could explain the partial suppression of the *tor2-21* growth defect at high temperatures, I examined the levels of GFP-tagged Far9 and Far9ΔC in *tor2-21 far9Δ* cells and found that Far9ΔC was expressed to similar levels as full length Far9 (Fig. 6D). Together these data suggest that the suppression of the *tor2-21* mutation by *far9ΔC* results from the loss of ER localization of Far9 and that ER localization of Far9 is required for its optimal function.

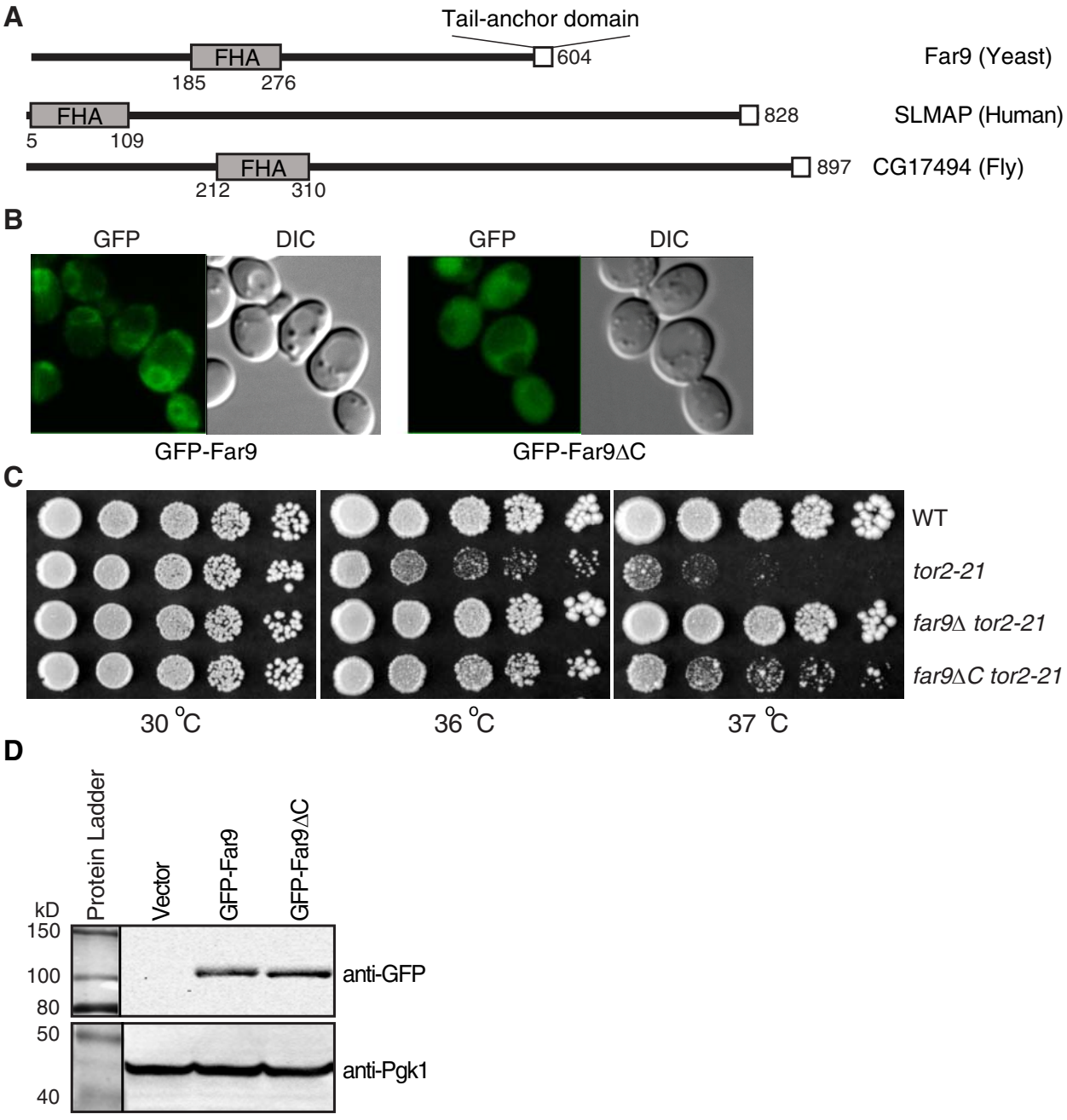

Figure 6. The tail-anchor domain of Far9 is required for its ER localization.

(A) Diagrammatic representations of Far9 and its orthologs in flies and humans. A conserved FHA domain and the tail-anchor domain are indicated by gray and white rectangles, respectively.

(B) ER Localization of Far9 requires the tail-anchor domain. *far9Δ* mutant cells (TPY1048) expressing GFP-tagged Far9 (pTP179) or Far9ΔC (pTP554) were grown in SD medium and observed by fluorescence microscopy.

(C) The tail-anchor domain of Far9 is required for the optimal function of Far9 in TORC2 signaling. Serial dilutions of indicated cells (WT, SH100; *tor2-21*, SH121; *tor2-21 far9Δ*, TPY357; *tor2-21 far9ΔC*, TPY1341) were grown on YPD medium at 30 °C, 36 °C, and 37 °C for 3-4 days.

(D) Loss of the tail-anchor domain of Far9 does not reduce its steady-state level. Total cellular proteins of *far9Δ* mutant cells (TPY357) expressing GFP-Far9 or GFP-Far9ΔC were prepared and separated by SDS-PAGE and GFP-tagged proteins were detected by immunoblotting. 3-Phosphoglycerate kinase (Pgk1) was included as a loading control.

3.5. Discussion

3.5.1. ER/nuclear envelope localization of STRIPAK complex components: a universal theme

The Far complex is part of the yeast striatin interacting phosphatase and kinase (STRIPAK) complex which is conserved in eukaryotes (14, 42, 48, 67, 93, 96). Cellular localization of the Far complex proteins has been reported previously (9, 61, 76). However, these studies report some inconsistent and conflicting results. While consistent with data from a genome-wide study on the localization of yeast proteins and a study on cellular localization of tail-anchored proteins showing ER localization of Far3, Far7, and Far8, and Far9, and Far10 (9, 61), this study provides a comprehensive look into the localization of the Far Complex at the ER including the order of assembly of the complex in an effort to rectify the discrepancies. Using fluorescence microscopy, I found that functional Far-GFP fusions localize to the nuclear and plasma membrane periphery indicative of endoplasmic reticulum localization. Co-localization of the Far-GFP fusions with the ER packaging chaperone Shr3-RFP tagged protein confirm ER localization of the Far complex. By systematically examining the localization of Far-GFP fusions in sextuple *far3/7/8/9/10/11Δ* and various double *farΔ* mutant cells I determined the order by which the Far complex organizes itself on the ER: Far9/10 establish a foot

hold on the ER utilizing the tail-anchor domain, and Far3/7/8 form a subcomplex that bridges Far11 to Far9/10 at the ER (Fig. 7).

Inconsistencies in the localization of the Far proteins in the previous studies may be explained by several possibilities. Cytoplasmic localization of Far9 in the genome-wide study on yeast protein localization is most likely to be due to the tagging of GFP at its C-terminus, which is expected to interfere with tail-anchor domain-dependent ER membrane insertion of Far9. The clustering effect of Far10 in Beilharz et al.'s study may result from a higher level of overexpression of Far10 from the relatively strong *MET25* promoter than in my current study (78, 88). My data disagrees with Lisa-Sanatmaria et al.'s study, which reported Far11 as a late-Golgi protein, Far3 as an early Golgi protein, and Far9 on the transport vesicles between ER and the Golgi (76). Although these three cellular compartments are all part of the protein secretion pathway downstream of ER, proteins associated with these three compartments exhibit distinct cellular localization, different from the ER (61, 82, 85). In Lisa-Sanatmaria et al.'s study, the authors added a C-terminal CFP tag to Far9, failing to take into consideration the role of the tail-anchor domain of Far9 on its cellular localization. Furthermore, the functionality of the fusion proteins in the aforementioned study was not reported. If the investigators neglected to confirm the functionality of their fusion proteins and were in fact not functional, this could present another possibility that accounts for the localization differences. This

study has comprehensively confirmed the functionality of the Far-GFP fusion proteins for the analysis of their cellular localization, therefore my data showing ER localization of the Far complex should lie to rest the dispute over which cellular compartment the Far complex is associated with in yeast.

ER/nuclear envelope localization of proteins associated with the STRIPAK complex seems to be a conserved feature. *S. cerevisiae* Far9/10 and their orthologs all contain a tail anchor domain at the extreme C-terminus (Fig. 6A and data not shown). The human ortholog of yeast Far9/10, SLMAP, has been shown to associate with the ER and nuclear envelope (21, 42). Two components of the STRIPAK complex in the fission yeast *S. pombe*, Csc2 (*S. cerevisiae* Far11 ortholog) and Csc3 (*S. cerevisiae* Far8 ortholog) also associate with the nuclear envelope/ER. Csc1, a component of the *S. pombe* STRIPAK complex and the *S. cerevisiae* Far9/10 ortholog, was not found to localize to the nuclear envelope (109). However, this could be due to the addition of GFP at its C-terminus, which includes a tail-anchor domain. A C-terminal GFP tag is expected to interfere with membrane insertion of tail-anchor domain proteins. ER localization of the STRIPAK components appears to be important for their function: In muscle cells, SLMAP is associated with the sarcolemmal membrane, which is derived from the ER and important for muscle cell function (51, 53, 89). Here I show that ER localization of the Far complex is required for its optimal function in TORC2 signaling. How is ER

localization of the yeast Far complex required for its function in TORC2 signaling? Previously, I have shown that the yeast Far complex and PP2A negatively regulate TORC2 signaling by promoting dephosphorylation of the TORC2 substrate Slm1 and possibly Slm2, Ypk1 and Ypk2, all of which associate with the plasma membrane (37, 90). The association with the Far complex could bring PP2A to the periplasmic region to facilitate dephosphorylation of TORC2 substrates (Fig.8).

Unlike *S. cerevisiae* Far proteins, human SLMAP and the *S. pombe* STRIPAK complex also localize to the centrosome and the spindle pole body respectively (42, 52, 109). Consistent with their localization in the centrosome/spindle pole body, the human and *S. pombe* STRIPAK complexes have been proposed to play roles in mitosis (42, 52, 109). Failure to detect localization of the yeast Far complex components and even the Far9 truncation mutant without its tail-anchor domain to the spindle pole body is consistent with Frost et al.'s hypothesis that the function of STRIPAK complex may have been "repurposed" and the *S. cerevisiae* STRIPAK complex has lost its function in mitosis (42).

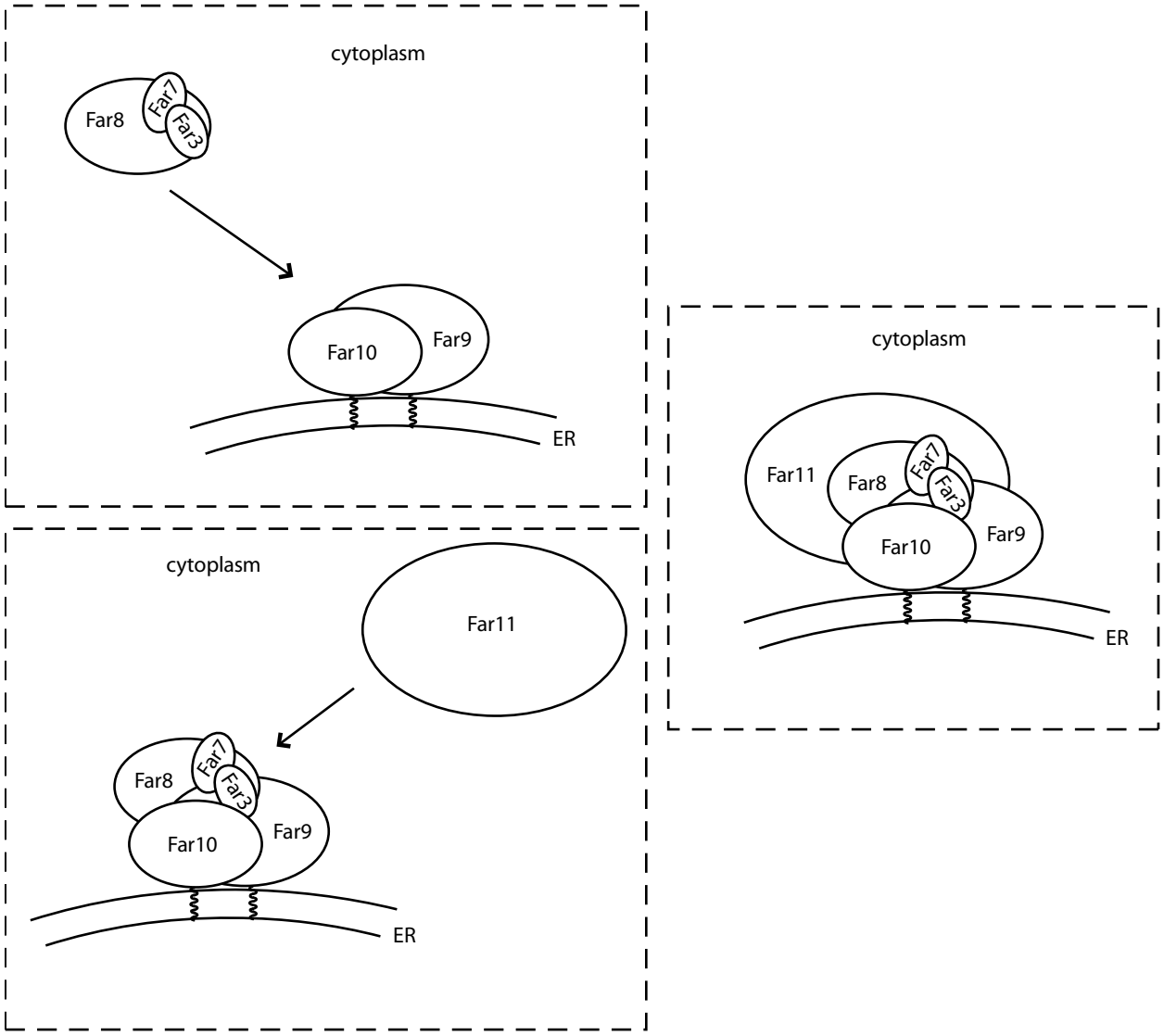

Figure 7. Model of the assembly of the Far complex on the ER.

3.5.2. ER localization of the yeast Far complex has a role in TORC2 signaling

Previously, I reported that mutations in the Far complex suppresses TORC2 deficiency in the order: *far11Δ* > *far8/9Δ* > *far3/7Δ* > *far10Δ* (93). It is interesting to note that Far11, which is the most peripheral component of the complex according to this study, is also the most important among the six Far proteins in TORC2 signaling. Although this result is surprising, it may help understand why ER localization of the Far complex is not absolutely required for its function in TORC2 signaling. Far3 and Far7 are able to form a complex in the absence of the other four Far proteins. Coincidently, mutant effects of *far3Δ* and *far7Δ* on TORC2 signaling are most similar, suggesting that their roles in the Far complex are equal. Far3 and Far7 are only found in a restricted set of fungal species and lack apparent orthologs in animals (42). However, yeast Far3/Far7 and human SIKE/FGFR1OP2 are all relatively small proteins predicted to have a coiled-coil domain (49, 68, 73), suggesting that Far3/Far7 may be the functional or structural counterparts of human SIKE/FGFR1OP2. Interestingly, the STRIPAK complex in *S. pombe* contains a novel protein of 166 residues, Csc4, which is also predicted to have a coiled-coil domain (109). It is possible that these small, coiled-coil domain proteins may play the same structural role in the STRIPAK complex in different species as a result of divergent evolution.

In this report, I found that Far3, Far7, and Far8 are able to form a subcomplex independently of Far9, Far10, and Far11. Far8 shares limited sequence homology to striatins, which are the B''' regulatory subunits of PP2A phosphatase. The PP2A holoenzyme in yeast is a heterotrimer consisting of the scaffolding A subunit Tpd3, the regulatory B subunit Cdc55 or B' subunit Rts1, and one of the two homologous and functionally redundant catalytic C subunits, Pph21 or Pph22 (34). It is not clear whether Far8 is a B type regulatory subunit of PP2A due to my previous finding that an *rts1* mutation has a similar phenotype as mutations in the Far complex components in TORC2 signaling. Human Striatin 3 and its *Sordaria Macrospora* ortholog PRO11 have been reported to contain an N-terminal coiled-coil region and both proteins are critical components in the organization of the respective STRIPAK complexes (14, 67). Like human striatins, yeast Far8 was also predicted to contain an N-terminal coiled-coil domain (68, 73). Interestingly, almost all components of the Far complex are predicted to contain coiled-coil domains (68, 73). These coiled-coil domains may mediate protein-protein interactions and provide a structural framework for the organization of the Far complex. Further research will be conducted to uncover the role of Far8 in the yeast STRIPAK complex and how the Far complex interfaces with PP2A.

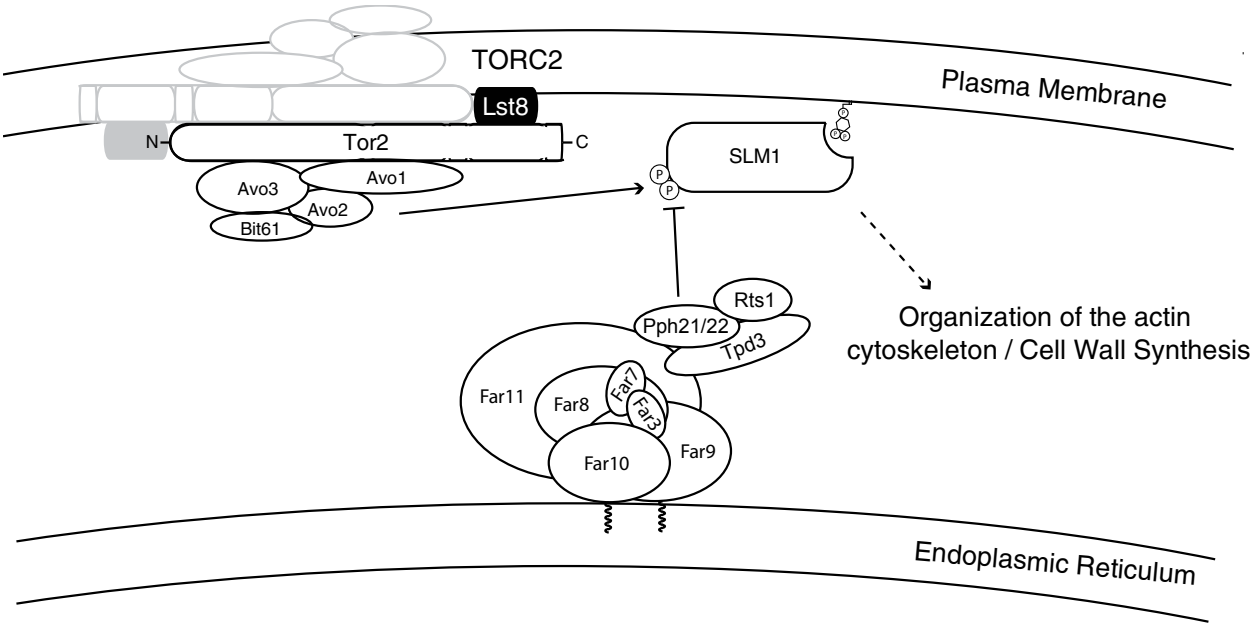

Figure 8. Model of PP2A-Far complex's role in TORC2 signaling *in vivo*.

Table 2. *S. cerevisiae* strains used in Chapter 3.

Strain	Genotype	Source	Application
SY2227 *(WT)*	MATa ade1-1 leu2-2,113 trp1 ura3-52 bar1 HIS3::pFUS1::HIS3 mfa2-1::FUS1-lacZ rad16::pGAL1::STE4	(68)	
TPY1010 *(far3)*	SY2227 *far3::kanMX4*	This study	Fig. 1A, 3A
TPY1013 *(far7)*	SY2227 *far7::kanMX4*	This study	Fig. 1A, 3B
TPY1015 *(far8)*	SY2227 *far8::kanMX4*	This study	Fig. 1A, 3C
TPY1048 *(far9)*	SY2227 *far9::kanMX4*	This study	Fig. 1A, 6B
TPY1072 *(far10)*	SY2227 *far10::kanMX4*	This study	Fig. 1A
SY4064 *(far11)*	SY2227 *far11::kanMX4*	(68)	Fig. 1A, 3D, 5
SH100 *(WT)*	*MATa leu2-3,112 ura3-52 rme1 trp1 his4 HMLa ade2 tor2::ADE2 [YCplac111::TOR2]*	(57)	Fig. 6C
SH121 *(tor2-21)*	*MATa leu2-3,112 ura3-52 rme1 trp1 his4 HMLa ade2 tor2::ADE2 [YCplac111::tor2-21]*	(57)	Fig. 6C
TPY157 *(tor2-21 far3)*	SH121 *far3::kanMX4*	(93)	Fig. 1B
TPY147 *(tor2-21 far7)*	SH121 *far7::kanMX4*	(93)	Fig. 1B
TPY213 *(tor2-21 far8)*	SH121 *far8::kanMX4*	(93)	Fig. 1B
TPY357 *(tor2-21 far9)*	SH121 *far9::kanMX4*	(93)	Fig. 1B, 6C-D
TPY151 *(tor2-21 far10)*	SH121 *far10::kanMX4*	(93)	Fig. 1B
TPY116 *(tor2-21 far11)*	SH121 *far11::kanMX4*	(93)	Fig. 1B

SY4075 *(far sext)*	SY2227 *far3::LEU2 far7::CgTRP1 far8::URA3 far9::HYGB far10::KAN far11::NAT*	(68)	
TPY845 *(far sext ura3)*	SY4075 *ura3::kanMX4*	This study	Fig. 2, 4A, 4C
TPY1358 *(far3 far7)*	SY2227 *far3::kanMX4 far7::TRP1 [pRS416-FAR3-GFP]*	This study	Fig. 3A
TPY1361 *(far3 far8)*	SY2227 *far3::kanMX4 far8::TRP1 [pRS416-FAR3-GFP]*	This study	Fig. 3A
TPY1348 *(far3 far9)*	SY2227 *far3::kanMX4 far9::TRP1 [pRS416-FAR3-GFP]*	This study	Fig. 3A
TPY1363 *(far3 far10)*	SY2227 *far3::kanMX4 far10::TRP1 [pRS416-FAR3-GFP]*	This study	Fig. 3A
TPY1402 *(far3 far11)*	SY2227 *far3::kanMX4 far11::TRP1 [pRS416-FAR3-GFP]*	This study	Fig. 3A
TPY1408 *(far7 far3)*	SY2227 *far7::kanMX4 far3::TRP1 [pRS416-FAR7-GFP]*	This study	Fig. 3B
TPY1366 *(far7 far8)*	SY2227 *far7::kanMX4 far8::TRP1 [pRS416-FAR7-GFP]*	This study	Fig. 3B
TPY1350 *(far7 far9)*	SY2227 *far7::kanMX4 far9::TRP1 [pRS416-FAR7-GFP]*	This study	Fig. 3B
TPY1368 *(far7 far10)*	SY2227 *far7::kanMX4 far10::TRP1 [pRS416-FAR7-GFP]*	This study	Fig. 3B
TPY1352 *(far7 far11)*	SY2227 *far7::kanMX4 far11::TRP1 [pRS416-FAR7-GFP]*	This study	Fig. 3B
TPY1369 *(far8 far3)*	SY2227 *far8::kanMX4 far3::TRP1 [pRS416-FAR8-GFP]*	This study	Fig. 3C, 4B
TPY1370 *(far8 far7)*	SY2227 *far8::kanMX4 far7::TRP1 [pRS416-FAR8-GFP]*	This study	Fig. 3C, 4B
TPY1351 *(far8 far9)*	SY2227 *far8::kanMX4 far9::TRP1 [pRS416-FAR8-GFP]*	This study	Fig. 3C
TPY1373 *(far8 far10)*	SY2227 *far8::kanMX4 far10::TRP1 [pRS416-FAR8-GFP]*	This study	Fig. 3C
TPY1405 *(far8 far11)*	SY2227 *far8::kanMX4 far11::TRP1 [pRS416-FAR8-GFP]*	This study	Fig. 3C

TPY1374 *(far11 far3)*	SY2227 *far11::kanMX4 far3::TRP1 [pRS416-MKS1-FAR11-GFP]*	This study	Fig. 3D
TPY1377 *(far11 far7)*	SY2227 *far11::kanMX4 far7::TRP1 [pRS416-MKS1-FAR11-GFP]*	This study	Fig. 3D
TPY1406 *(far11 far8)*	SY2227 *far11::kanMX4 far8::TRP1 [pRS416-MKS1-FAR11-GFP]*	This study	Fig. 3D
TPY1410 *(far11 far9)*	SY2227 *far11::kanMX4 far9::TRP1 [pRS416-MKS1-FAR11-GFP]*	This study	Fig. 3D
TPY1379 *(far11 far10)*	SY2227 *far11::kanMX4 far10::TRP1 [pRS416-MKS1-FAR11-GFP]*	This study	Fig. 3D
SY4080 *(FAR9-myc)*	SY2227 *FAR9-MYC13-KAN* [pSL2771*, CEN LEU2]*	(68)	
TPY1411 *(FAR9-myc)*	SY4080 without the pSL2771 plasmid	This study	Fig. 5
SY4070 *(FAR9-myc far3)*	SY2227 *far3::LEU2 FAR9-MYC13-KAN* [pSL2784*, 2μ URA3 FAR3-HA]*	(68)	
TPY1412 *(far3 FAR9-myc)*	SY4070 without the pSL2784 plasmid	This study	Fig. 5
TPY1413 *(far7 FAR9-myc)*	TPY1411 *far7::TRP1*	This study	Fig. 5
TPY1416 *(far8 FAR9-myc)*	TPY1411 *far8::TRP1*	This study	Fig. 5
TPY1341 *(far9ΔC)*	SH121 *far9ΔC*	This study	Fig. 6C

Table 3. Plasmids used in Chapter 3

Plasmid	Description	Source	Application
pTP201	pRS414-SHR3-RFP expressing Shr3 from its own promoter with an RFP tag at the C-terminus.	This study	Fig. 1B
pTP143	pRS416-FAR3-GFP, expressing Far3 from its own	This	Fig. 1A-B,

	promoter with a GFP tag at the C-terminus.	study	2, 3A, 4A
pTP164	pRS416-FAR7-GFP, expressing Far7 from its own promoter with a GFP tag at the C-terminus.	This study	Fig. 1A-B, 2, 3B, 4A
pTP131	pRS416-FAR8-GFP, expressing Far8 from its own promoter with a GFP tag at the C-terminus.	This study	Fig. 1A-B, 2, 3C, 4B
pTP179	pRS416-MKS1-GFP-FAR9, expressing Far9 from the *MKS1* promoter with a GFP tag at the N-terminus.	This study	Fig. 1A-B, 2, 6B, 6D
pTP203	pRS416-MKS1-GFP-FAR10, expressing Far10 from the *MKS1* promoter with a GFP tag at the N-terminus.	This study	Fig. 1A-B, 2
pZL2564	pRS416-FAR11-GFP, expressing Far11 from its own promoter with a GFP tag at the C-terminus.	This study	Fig. 1A-B, 2, 3D
pTP646	pRS418-FAR7-HA, expressing Far7 from its own promoter with a 3xHA tag at the C-terminus.	This study	Fig. 4A-C
pTP658	pRS418-FAR8-HA, expressing Far8 from its own promoter with a 3xHA tag at the C-terminus.	This study	Fig. 4A
pTP655	pRS418-FAR3-HA, expressing Far3 from its own promoter with a 3xHA tag at the C-terminus.	This study	Fig. 4A-C
pTP664	pRS418-FAR7-FAR3-HA, expressing non-tagged Far7 from its own promoter and Far3 from its own promoter with a 3xHA tag at the C-terminus.	This study	Fig. 4C
pTP673	pRS418-FAR3-FAR7-HA, expressing non-tagged Far3 from its own promoter and Far7 from its own promoter with a 3xHA tag at the C-terminus.	This study	Fig. 4C
pZL2762	pRS416-FAR11-HA, expressing Far11 from its own promoter with a 3xHA tag at the C-terminus.	(93)	Fig. 5
pTP554	pRS416-MKS1p-GFP-FAR9ΔC, expressing Far9ΔC from the *MKS1* promoter with a GFP tag at the N-terminus.	This study	Fig. 6B, 6D

REFERENCE

1. **Adami, A., B. Garcia-Alvarez, E. Arias-Palomo, D. Barford, and O. Llorca.** 2007. Structure of TOR and its complex with KOG1. Mol Cell **27:**509-16.

2. **Amberg, D. C., D. J. Burke, and J. N. Strathern.** 2005. Methods in Yeast Genetics: A Cold Spring Harbor Laboratory Course Manual. Cold Spring Harbor Laboratory, Cold Spring Harbor, New York.

3. **Araki, T., Y. Uesono, T. Oguchi, and E. A. Toh.** 2005. LAS24/KOG1, a component of the TOR complex 1 (TORC1), is needed for resistance to local anesthetic tetracaine and normal distribution of actin cytoskeleton in yeast. Genes Genet Syst **80:**325-43.

4. **Aronova, S., K. Wedaman, P. A. Aronov, K. Fontes, K. Ramos, B. D. Hammock, and T. Powers.** 2008. Regulation of ceramide biosynthesis by TOR complex 2. Cell Metab **7:**148-58.

5. **Audhya, A., R. Loewith, A. B. Parsons, L. Gao, M. Tabuchi, H. Zhou, C. Boone, M. N. Hall, and S. D. Emr.** 2004. Genome-wide lethality screen identifies new PI4,5P2 effectors that regulate the actin cytoskeleton. Embo J **23:**3747-57.

6. **Bardwell, L.** 2005. A walk-through of the yeast mating pheromone response pathway. Peptides **26:**339-50.

7. **Baryshnikova, A., M. Costanzo, Y. Kim, H. Ding, J. Koh, K. Toufighi, J. Y. Youn, J. Ou, B. J. San Luis, S. Bandyopadhyay, M. Hibbs, D. Hess, A. C. Gingras, G. D. Bader, O. G. Troyanskaya, G. W. Brown, B. Andrews, C. Boone, and C. L. Myers.** 2010. Quantitative analysis of fitness and genetic interactions in yeast on a genome scale. Nat Methods **7:**1017-24.

8. **Beck, T., and M. N. Hall.** 1999. The TOR signalling pathway controls nuclear localization of nutrient-regulated transcription factors. Nature **402:**689-92.

9. **Beilharz, T., B. Egan, P. A. Silver, K. Hofmann, and T. Lithgow.** 2003. Bipartite signals mediate subcellular targeting of tail-anchored membrane proteins in Saccharomyces cerevisiae. J Biol Chem **278:**8219-23.

10. **Berchtold, D., and T. C. Walther.** 2009. TORC2 plasma membrane localization is essential for cell viability and restricted to a distinct domain. Mol Biol Cell **20:**1565-75.

11. **Bickle, M., P. A. Delley, A. Schmidt, and M. N. Hall.** 1998. Cell wall integrity modulates RHO1 activity via the exchange factor ROM2. Embo J **17:**2235-45.

12. **Binda, M., M. P. Peli-Gulli, G. Bonfils, N. Panchaud, J. Urban, T. W. Sturgill, R. Loewith, and C. De Virgilio.** 2009. The Vam6 GEF controls TORC1 by activating the EGO complex. Mol Cell **35:**563-73.

13. **Blagosklonny, M. V.** Progeria, rapamycin and normal aging: recent breakthrough. Aging (Albany NY) **3:**685-91.

14. **Bloemendal, S., Y. Bernhards, K. Bartho, A. Dettmann, O. Voigt, I. Teichert, S. Seiler, D. A. Wolters, S. Poggeler, and U. Kuck.** 2012. A homologue of the human STRIPAK complex controls sexual development in fungi. Mol Microbiol **84:**310-23.

15. **Bloemendal, S., K. M. Lord, C. Rech, B. Hoff, I. Engh, N. D. Read, and U. Kuck.** 2010. A mutant defective in sexual development produces aseptate ascogonia. Eukaryot Cell **9:**1856-66.

16. **Bonangelino, C. J., E. M. Chavez, and J. S. Bonifacino.** 2002. Genomic screen for vacuolar protein sorting genes in Saccharomyces cerevisiae. Mol Biol Cell **13:**2486-501.

17. **Borgese, N., and E. Fasana.** 2011. Targeting pathways of C-tail-anchored proteins. Biochim Biophys Acta **1808:**937-46.

18. **Botstein, D., S. A. Chervitz, and J. M. Cherry.** 1997. Yeast as a model organism. Science **277:**1259-60.

19. **Bultynck, G., V. L. Heath, A. P. Majeed, J. M. Galan, R. Haguenauer-Tsapis, and M. S. Cyert.** 2006. Slm1 and slm2 are novel substrates of the calcineurin

phosphatase required for heat stress-induced endocytosis of the yeast uracil permease. Mol Cell Biol **26:**4729-45.

20. **Burns, N., B. Grimwade, P. B. Ross-Macdonald, E. Y. Choi, K. Finberg, G. S. Roeder, and M. Snyder.** 1994. Large-scale analysis of gene expression, protein localization, and gene disruption in Saccharomyces cerevisiae. Genes Dev **8:**1087-105.

21. **Byers, J. T., R. M. Guzzo, M. Salih, and B. S. Tuana.** 2009. Hydrophobic profiles of the tail anchors in SLMAP dictate subcellular targeting. BMC Cell Biol **10:**48.

22. **Cardenas, M. E., N. S. Cutler, M. C. Lorenz, C. J. Di Como, and J. Heitman.** 1999. The TOR signaling cascade regulates gene expression in response to nutrients. Genes Dev **13:**3271-9.

23. **Cardenas, M. E., and J. Heitman.** 1995. FKBP12-rapamycin target TOR2 is a vacuolar protein with an associated phosphatidylinositol-4 kinase activity. Embo J **14:**5892-907.

24. **Ceccarelli, D. F., R. C. Laister, V. K. Mulligan, M. J. Kean, M. Goudreault, I. C. Scott, W. B. Derry, A. Chakrabartty, A. C. Gingras, and F. Sicheri.** 2011. CCM3/PDCD10 heterodimerizes with germinal center kinase III (GCKIII)

proteins using a mechanism analogous to CCM3 homodimerization. J Biol Chem **286:**25056-64.

25. **Chen, E. J., and C. A. Kaiser.** 2003. LST8 negatively regulates amino acid biosynthesis as a component of the TOR pathway. J Cell Biol **161:**333-47.

26. **Cid, V. J., A. Duran, F. del Rey, M. P. Snyder, C. Nombela, and M. Sanchez.** 1995. Molecular basis of cell integrity and morphogenesis in Saccharomyces cerevisiae. Microbiol Rev **59:**345-86.

27. **Cooper, T. G.** 2002. Transmitting the signal of excess nitrogen in Saccharomyces cerevisiae from the Tor proteins to the GATA factors: connecting the dots. FEMS Microbiol Rev **26:**223-38.

28. **Cybulski, N., and M. N. Hall.** 2009. TOR complex 2: a signaling pathway of its own. Trends Biochem Sci **34:**620-7.

29. **Daniel, J.** 1993. Potentially rapid walking in cellular regulatory networks using the gene-gene interference method in yeast. Mol Gen Genet **240:**245-57.

30. **Daquinag, A., M. Fadri, S. Y. Jung, J. Qin, and J. Kunz.** 2007. The yeast PH domain proteins Slm1 and Slm2 are targets of sphingolipid signaling during the response to heat stress. Mol Cell Biol **27:**633-50.

31. **Donia, M., J. A. McCubrey, K. Bendtzen, and F. Nicoletti.** Potential use of rapamycin in HIV infection. Br J Clin Pharmacol **70:**784-93.

32. **Drubin, D. G., and W. J. Nelson.** 1996. Origins of cell polarity. Cell **84:**335-44.

33. **Durocher, D., and S. P. Jackson.** 2002. The FHA domain. FEBS Lett **513:**58-66.

34. **Duvel, K., and J. R. Broach.** 2004. The role of phosphatases in TOR signaling in yeast. Curr Top Microbiol Immunol **279:**19-38.

35. **Ehninger, D., P. J. de Vries, and A. J. Silva.** 2009. From mTOR to cognition: molecular and cellular mechanisms of cognitive impairments in tuberous sclerosis. J Intellect Disabil Res **53:**838-51.

36. **Fabrizio, P., S. Hoon, M. Shamalnasab, A. Galbani, M. Wei, G. Giaever, C. Nislow, and V. D. Longo.** 2010. Genome-wide screen in Saccharomyces cerevisiae identifies vacuolar protein sorting, autophagy, biosynthetic, and tRNA methylation genes involved in life span regulation. PLoS Genet **6:**e1001024.

37. **Fadri, M., A. Daquinag, S. Wang, T. Xue, and J. Kunz.** 2005. The pleckstrin homology domain proteins Slm1 and Slm2 are required for actin cytoskeleton organization in yeast and bind phosphatidylinositol-4,5-bisphosphate and TORC2. Mol Biol Cell **16:**1883-900.

38. **Ferguson, B., J. Horecka, J. Printen, J. Schultz, B. J. Stevenson, and G. F. Sprague, Jr.** 1994. The yeast pheromone response pathway: new insights into signal transmission. Cell Mol Biol Res **40:**223-8.

39. **Fidalgo, M., M. Fraile, A. Pires, T. Force, C. Pombo, and J. Zalvide.** 2010. CCM3/PDCD10 stabilizes GCKIII proteins to promote Golgi assembly and cell orientation. J Cell Sci **123:**1274-84.

40. **Fingar, D. C., and J. Blenis.** 2004. Target of rapamycin (TOR): an integrator of nutrient and growth factor signals and coordinator of cell growth and cell cycle progression. Oncogene **23:**3151-71.

41. **Frias, M. A., C. C. Thoreen, J. D. Jaffe, W. Schroder, T. Sculley, S. A. Carr, and D. M. Sabatini.** 2006. mSin1 is necessary for Akt/PKB phosphorylation, and its isoforms define three distinct mTORC2s. Curr Biol **16:**1865-70.

42. **Frost, A., M. G. Elgort, O. Brandman, C. Ives, S. R. Collins, L. Miller-Vedam, J. Weibezahn, M. Y. Hein, I. Poser, M. Mann, A. A. Hyman, and J. S. Weissman.** 2012. Functional repurposing revealed by comparing S. pombe and S. cerevisiae genetic interactions. Cell **149:**1339-52.

43. **Fuchs, B. B., and E. Mylonakis.** 2009. Our paths might cross: the role of the fungal cell wall integrity pathway in stress response and cross talk with other stress response pathways. Eukaryot Cell **8:**1616-25.

44. **Galanis, E., J. C. Buckner, M. J. Maurer, J. I. Kreisberg, K. Ballman, J. Boni, J. M. Peralba, R. B. Jenkins, S. R. Dakhil, R. F. Morton, K. A. Jaeckle, B. W. Scheithauer, J. Dancey, M. Hidalgo, and D. J. Walsh.** 2005. Phase II trial of temsirolimus (CCI-779) in recurrent glioblastoma multiforme: a North Central Cancer Treatment Group Study. J Clin Oncol **23:**5294-304.

45. **Giannattasio, S., Z. Liu, J. Thornton, and R. A. Butow.** 2005. Retrograde response to mitochondrial dysfunction is separable from TOR1/2 regulation of retrograde gene expression. J Biol Chem **280:**42528-35.

46. **Goffeau, A., B. G. Barrell, H. Bussey, R. W. Davis, B. Dujon, H. Feldmann, F. Galibert, J. D. Hoheisel, C. Jacq, M. Johnston, E. J. Louis, H. W. Mewes, Y. Murakami, P. Philippsen, H. Tettelin, and S. G. Oliver.** 1996. Life with 6000 genes. Science **274:**546, 563-7.

47. **Gordon, J., J. Hwang, K. J. Carrier, C. A. Jones, Q. L. Kern, C. S. Moreno, R. H. Karas, and D. C. Pallas.** 2011. Protein phosphatase 2a (PP2A) binds within the

oligomerization domain of striatin and regulates the phosphorylation and activation of the mammalian Ste20-Like kinase Mst3. BMC Biochem **12:**54.

48. **Goudreault, M., L. M. D'Ambrosio, M. J. Kean, M. J. Mullin, B. G. Larsen, A. Sanchez, S. Chaudhry, G. I. Chen, F. Sicheri, A. I. Nesvizhskii, R. Aebersold, B. Raught, and A. C. Gingras.** 2009. A PP2A phosphatase high density interaction network identifies a novel striatin-interacting phosphatase and kinase complex linked to the cerebral cavernous malformation 3 (CCM3) protein. Mol Cell Proteomics **8:**157-71.

49. **Grand, E. K., F. H. Grand, A. J. Chase, F. M. Ross, M. M. Corcoran, D. G. Oscier, and N. C. Cross.** 2004. Identification of a novel gene, FGFR1OP2, fused to FGFR1 in 8p11 myeloproliferative syndrome. Genes Chromosomes Cancer **40:**78-83.

50. **Guertin, D. A., D. M. Stevens, C. C. Thoreen, A. A. Burds, N. Y. Kalaany, J. Moffat, M. Brown, K. J. Fitzgerald, and D. M. Sabatini.** 2006. Ablation in mice of the mTORC components raptor, rictor, or mLST8 reveals that mTORC2 is required for signaling to Akt-FOXO and PKCalpha, but not S6K1. Dev Cell **11:**859-71.

51. **Guzzo, R. M., M. Salih, E. D. Moore, and B. S. Tuana.** 2005. Molecular properties of cardiac tail-anchored membrane protein SLMAP are consistent with structural role in arrangement of excitation-contraction coupling apparatus. Am J Physiol Heart Circ Physiol **288:**H1810-9.

52. **Guzzo, R. M., S. Sevinc, M. Salih, and B. S. Tuana.** 2004. A novel isoform of sarcolemmal membrane-associated protein (SLMAP) is a component of the microtubule organizing centre. J Cell Sci **117:**2271-81.

53. **Guzzo, R. M., J. Wigle, M. Salih, E. D. Moore, and B. S. Tuana.** 2004. Regulated expression and temporal induction of the tail-anchored sarcolemmal-membrane-associated protein is critical for myoblast fusion. Biochem J **381:**599-608.

54. **Harold, F. M.** 2002. Force and compliance: rethinking morphogenesis in walled cells. Fungal Genet Biol **37:**271-82.

55. **Harrison, D. E., R. Strong, Z. D. Sharp, J. F. Nelson, C. M. Astle, K. Flurkey, N. L. Nadon, J. E. Wilkinson, K. Frenkel, C. S. Carter, M. Pahor, M. A. Javors, E. Fernandez, and R. A. Miller.** 2009. Rapamycin fed late in life extends lifespan in genetically heterogeneous mice. Nature **460:**392-5.

56. **Heinisch, J. J., A. Lorberg, H. P. Schmitz, and J. J. Jacoby.** 1999. The protein kinase C-mediated MAP kinase pathway involved in the maintenance of cellular integrity in Saccharomyces cerevisiae. Mol Microbiol **32:**671-80.

57. **Helliwell, S. B., I. Howald, N. Barbet, and M. N. Hall.** 1998. TOR2 is part of two related signaling pathways coordinating cell growth in Saccharomyces cerevisiae. Genetics **148:**99-112.

58. **Helliwell, S. B., A. Schmidt, Y. Ohya, and M. N. Hall.** 1998. The Rho1 effector Pkc1, but not Bni1, mediates signalling from Tor2 to the actin cytoskeleton. Curr Biol **8:**1211-4.

59. **Horecka, J., and G. F. Sprague, Jr.** 1996. Identification and characterization of FAR3, a gene required for pheromone-mediated G1 arrest in Saccharomyces cerevisiae. Genetics **144:**905-21.

60. **Huber, A., B. Bodenmiller, A. Uotila, M. Stahl, S. Wanka, B. Gerrits, R. Aebersold, and R. Loewith.** 2009. Characterization of the rapamycin-sensitive phosphoproteome reveals that Sch9 is a central coordinator of protein synthesis. Genes Dev **23:**1929-43.

61. **Huh, W. K., J. V. Falvo, L. C. Gerke, A. S. Carroll, R. W. Howson, J. S. Weissman, and E. K. O'Shea.** 2003. Global analysis of protein localization in budding yeast. Nature **425:**686-91.

62. **Inoki, K., H. Ouyang, Y. Li, and K. L. Guan.** 2005. Signaling by target of rapamycin proteins in cell growth control. Microbiol Mol Biol Rev **69:**79-100.

63. **Jacinto, E., V. Facchinetti, D. Liu, N. Soto, S. Wei, S. Y. Jung, Q. Huang, J. Qin, and B. Su.** 2006. SIN1/MIP1 maintains rictor-mTOR complex integrity and regulates Akt phosphorylation and substrate specificity. Cell **127:**125-37.

64. **Jacinto, E., R. Loewith, A. Schmidt, S. Lin, M. A. Ruegg, A. Hall, and M. N. Hall.** 2004. Mammalian TOR complex 2 controls the actin cytoskeleton and is rapamycin insensitive. Nat Cell Biol **6:**1122-8.

65. **Kamada, Y.** 2010. Prime-numbered Atg proteins act at the primary step in autophagy: unphosphorylatable Atg13 can induce autophagy without TOR inactivation. Autophagy **6:**415-6.

66. **Kamada, Y., Y. Fujioka, N. N. Suzuki, F. Inagaki, S. Wullschleger, R. Loewith, M. N. Hall, and Y. Ohsumi.** 2005. Tor2 directly phosphorylates the AGC kinase Ypk2 to regulate actin polarization. Mol Cell Biol **25:**7239-48.

67. **Kean, M. J., D. F. Ceccarelli, M. Goudreault, M. Sanches, S. Tate, B. Larsen, L. C. Gibson, W. B. Derry, I. C. Scott, L. Pelletier, G. S. Baillie, F. Sicheri, and A. C. Gingras.** 2011. Structure-Function Analysis of Core STRIPAK Proteins: A SIGNALING COMPLEX IMPLICATED IN GOLGI POLARIZATION. J Biol Chem **286:**25065-75.

68. **Kemp, H. A., and G. F. Sprague, Jr.** 2003. Far3 and five interacting proteins prevent premature recovery from pheromone arrest in the budding yeast Saccharomyces cerevisiae. Mol Cell Biol **23:**1750-63.

69. **Kim, D. H., D. D. Sarbassov, S. M. Ali, J. E. King, R. R. Latek, H. Erdjument-Bromage, P. Tempst, and D. M. Sabatini.** 2002. mTOR interacts with raptor to form a nutrient-sensitive complex that signals to the cell growth machinery. Cell **110:**163-75.

70. **Kim, D. H., D. D. Sarbassov, S. M. Ali, R. R. Latek, K. V. Guntur, H. Erdjument-Bromage, P. Tempst, and D. M. Sabatini.** 2003. GbetaL, a positive regulator of the rapamycin-sensitive pathway required for the nutrient-sensitive interaction between raptor and mTOR. Mol Cell **11:**895-904.

71. **Kuehn, M. J., R. Schekman, and P. O. Ljungdahl.** 1996. Amino acid permeases require COPII components and the ER resident membrane protein Shr3p for packaging into transport vesicles in vitro. J Cell Biol **135:**585-95.

72. **Kunz, J., U. Schneider, I. Howald, A. Schmidt, and M. N. Hall.** 2000. HEAT repeats mediate plasma membrane localization of Tor2p in yeast. J Biol Chem **275:**37011-20.

73. **Lai, F., R. Wu, J. Wang, C. Li, L. Zou, Y. Lu, and C. Liang.** 2011. Far3p domains involved in the interactions of Far proteins and pheromone-induced cell cycle arrest in budding yeast. FEMS Yeast Res **11:**72-9.

74. **Laplante, M., and D. M. Sabatini.** 2012. mTOR signaling in growth control and disease. Cell **149:**274-93.

75. **Li, X., R. Zhang, H. Zhang, Y. He, W. Ji, W. Min, and T. J. Boggon.** 2010. Crystal structure of CCM3, a cerebral cavernous malformation protein critical for vascular integrity. J Biol Chem **285:**24099-107.

76. **Lisa-Santamaria, P., A. Jimenez, and J. L. Revuelta.** 2012. The protein factor-arrest 11 (Far11) is essential for the toxicity of human caspase-10 in yeast and participates in the regulation of autophagy and the DNA damage signaling. J Biol Chem **287:**29636-47.

77. **Liu, Z., T. Sekito, C. B. Epstein, and R. A. Butow.** 2001. RTG-dependent mitochondria to nucleus signaling is negatively regulated by the seven WD-repeat protein Lst8p. Embo J **20:**7209-19.

78. **Liu, Z., T. Sekito, M. Spirek, J. Thornton, and R. A. Butow.** 2003. Retrograde signaling is regulated by the dynamic interaction between Rtg2p and Mks1p. Mol Cell **12:**401-11.

79. **Liu, Z., J. Thornton, M. Spirek, and R. A. Butow.** 2008. Activation of the SPS amino acid-sensing pathway in Saccharomyces cerevisiae correlates with the phosphorylation state of a sensor component, Ptr3. Mol Cell Biol **28:**551-63.

80. **Loewith, R., and M. N. Hall.** 2011. Target of rapamycin (TOR) in nutrient signaling and growth control. Genetics **189:**1177-201.

81. **Loewith, R., E. Jacinto, S. Wullschleger, A. Lorberg, J. L. Crespo, D. Bonenfant, W. Oppliger, P. Jenoe, and M. N. Hall.** 2002. Two TOR complexes, only one of which is rapamycin sensitive, have distinct roles in cell growth control. Mol Cell **10:**457-68.

82. **Losev, E., C. A. Reinke, J. Jellen, D. E. Strongin, B. J. Bevis, and B. S. Glick.** 2006. Golgi maturation visualized in living yeast. Nature **441:**1002-6.

83. **Marion, R. M., A. Regev, E. Segal, Y. Barash, D. Koller, N. Friedman, and E. K. O'Shea.** 2004. Sfp1 is a stress- and nutrient-sensitive regulator of ribosomal protein gene expression. Proc Natl Acad Sci U S A **101:**14315-22.

84. **Martin, D. E., A. Soulard, and M. N. Hall.** 2004. TOR regulates ribosomal protein gene expression via PKA and the Forkhead transcription factor FHL1. Cell **119:**969-79.

85. **Matsuura-Tokita, K., M. Takeuchi, A. Ichihara, K. Mikuriya, and A. Nakano.** 2006. Live imaging of yeast Golgi cisternal maturation. Nature **441:**1007-10.

86. **McAlister, V. C., K. Mahalati, K. M. Peltekian, A. Fraser, and A. S. MacDonald.** 2002. A clinical pharmacokinetic study of tacrolimus and sirolimus combination immunosuppression comparing simultaneous to separated administration. Ther Drug Monit **24:**346-50.

87. **Mulet, J. M., D. E. Martin, R. Loewith, and M. N. Hall.** 2006. Mutual antagonism of target of rapamycin and calcineurin signaling. J Biol Chem **281:**33000-7.

88. **Mumberg, D., R. Muller, and M. Funk.** 1994. Regulatable promoters of Saccharomyces cerevisiae: comparison of transcriptional activity and their use for heterologous expression. Nucleic Acids Res **22:**5767-8.

89. **Nader, M., B. Westendorp, O. Hawari, M. Salih, A. F. Stewart, F. H. Leenen, and B. S. Tuana.** 2012. Tail-anchored membrane protein SLMAP is a novel regulator of cardiac function at the sarcoplasmic reticulum. Am J Physiol Heart Circ Physiol **302:**H1138-45.

90. **Niles, B. J., H. Mogri, A. Hill, A. Vlahakis, and T. Powers.** 2012. Plasma membrane recruitment and activation of the AGC kinase Ypk1 is mediated by target of rapamycin complex 2 (TORC2) and its effector proteins Slm1 and Slm2. Proc Natl Acad Sci U S A **109:**1536-41.

91. **Peces, R., C. Peces, V. Perez-Duenas, E. Cuesta-Lopez, S. Azorin, and R. Selgas.** 2009. Rapamycin reduces kidney volume and delays the loss of renal function in a patient with autosomal-dominant polycystic kidney disease. Clinical Kidney Journal **2:**133-135.

92. **Powers, R. W., 3rd, M. Kaeberlein, S. D. Caldwell, B. K. Kennedy, and S. Fields.** 2006. Extension of chronological life span in yeast by decreased TOR pathway signaling. Genes Dev **20:**174-84.

93. **Pracheil, T., J. Thornton, and Z. Liu.** 2012. TORC2 signaling is antagonized by protein phosphatase 2A and the Far complex in Saccharomyces cerevisiae. Genetics **190:**1325-39.

94. **Reinke, A., S. Anderson, J. M. McCaffery, J. Yates, 3rd, S. Aronova, S. Chu, S. Fairclough, C. Iverson, K. P. Wedaman, and T. Powers.** 2004. TOR complex 1 includes a novel component, Tco89p (YPL180w), and cooperates with Ssd1p to maintain cellular integrity in Saccharomyces cerevisiae. J Biol Chem **279:**14752-62.

95. **Renner, C., P. L. Zinzani, R. Gressin, D. Klingbiel, P. Y. Dietrich, F. Hitz, M. Bargetzi, W. Mingrone, G. Martinelli, A. Trojan, K. Bouabdallah, A. Lohri, E. Gyan, C. Biaggi, S. Cogliatti, F. Bertoni, M. Ghielmini, P. Brauchli, and N. Ketterer.** A multicenter phase II trial (SAKK 36/06) of single-agent everolimus (RAD001) in patients with relapsed or refractory mantle cell lymphoma. Haematologica **97:**1085-91.

96. **Ribeiro, P. S., F. Josue, A. Wepf, M. C. Wehr, O. Rinner, G. Kelly, N. Tapon, and M. Gstaiger.** 2010. Combined functional genomic and proteomic approaches identify a PP2A complex as a negative regulator of Hippo signaling. Mol Cell **39:**521-34.

97. **Roberg, K. J., S. Bickel, N. Rowley, and C. A. Kaiser.** 1997. Control of amino acid permease sorting in the late secretory pathway of Saccharomyces cerevisiae by SEC13, LST4, LST7 and LST8. Genetics **147:**1569-84.

98. **Sarbassov, D. D., S. M. Ali, D. H. Kim, D. A. Guertin, R. R. Latek, H. Erdjument-Bromage, P. Tempst, and D. M. Sabatini.** 2004. Rictor, a novel binding partner of mTOR, defines a rapamycin-insensitive and raptor-independent pathway that regulates the cytoskeleton. Curr Biol **14:**1296-302.

99. **Sarbassov, D. D., S. M. Ali, and D. M. Sabatini.** 2005. Growing roles for the mTOR pathway. Curr Opin Cell Biol **17:**596-603.

100. **Schmelzle, T., and M. N. Hall.** 2000. TOR, a central controller of cell growth. Cell **103:**253-62.

101. **Schmelzle, T., S. B. Helliwell, and M. N. Hall.** 2002. Yeast protein kinases and the RHO1 exchange factor TUS1 are novel components of the cell integrity pathway in yeast. Mol Cell Biol **22:**1329-39.

102. **Schmidt, A., M. Bickle, T. Beck, and M. N. Hall.** 1997. The yeast phosphatidylinositol kinase homolog TOR2 activates RHO1 and RHO2 via the exchange factor ROM2. Cell **88:**531-42.

103. **Schmidt, A., J. Kunz, and M. N. Hall.** 1996. TOR2 is required for organization of the actin cytoskeleton in yeast. Proc Natl Acad Sci U S A **93:**13780-5.

104. **Schwertz, D. W., and P. Vaitkus.** 2003. Drug-eluting stents to prevent reblockage of coronary arteries. J Cardiovasc Nurs **18:**11-6.

105. **Sekito, T., Z. Liu, J. Thornton, and R. A. Butow.** 2002. RTG-dependent mitochondria-to-nucleus signaling is regulated by MKS1 and is linked to formation of yeast prion [URE3]. Mol Biol Cell **13:**795-804.

106. **Shamji, A. F., F. G. Kuruvilla, and S. L. Schreiber.** 2000. Partitioning the transcriptional program induced by rapamycin among the effectors of the Tor proteins. Curr Biol **10:**1574-81.

107. **Shaw, R. J., and L. C. Cantley.** 2006. Ras, PI(3)K and mTOR signalling controls tumour cell growth. Nature **441:**424-30.

108. **Simonin, A. R., C. G. Rasmussen, M. Yang, and N. L. Glass.** 2010. Genes encoding a striatin-like protein (ham-3) and a forkhead associated protein (ham-4) are required for hyphal fusion in Neurospora crassa. Fungal Genet Biol **47:**855-68.

109. **Singh, N. S., N. Shao, J. R. McLean, M. Sevugan, L. Ren, T. G. Chew, A. Bimbo, R. Sharma, X. Tang, K. L. Gould, and M. K. Balasubramanian.** 2011. SIN-inhibitory phosphatase complex promotes Cdc11p dephosphorylation and propagates SIN asymmetry in fission yeast. Curr Biol **21:**1968-78.

110. **Spilman, P., N. Podlutskaya, M. J. Hart, J. Debnath, O. Gorostiza, D. Bredesen, A. Richardson, R. Strong, and V. Galvan.** Inhibition of mTOR by rapamycin

abolishes cognitive deficits and reduces amyloid-beta levels in a mouse model of Alzheimer's disease. PLoS One **5:**e9979.

111. **Sprague, G. F., Jr.** 1991. Assay of yeast mating reaction. Methods Enzymol **194:**77-93.

112. **Stallone, G., A. Schena, B. Infante, S. Di Paolo, A. Loverre, G. Maggio, E. Ranieri, L. Gesualdo, F. P. Schena, and G. Grandaliano.** 2005. Sirolimus for Kaposi's sarcoma in renal-transplant recipients. N Engl J Med **352:**1317-23.

113. **Sturgill, T. W., A. Cohen, M. Diefenbacher, M. Trautwein, D. E. Martin, and M. N. Hall.** 2008. TOR1 and TOR2 have distinct locations in live cells. Eukaryot Cell **7:**1819-30.

114. **Sun, S. Y., L. M. Rosenberg, X. Wang, Z. Zhou, P. Yue, H. Fu, and F. R. Khuri.** 2005. Activation of Akt and eIF4E survival pathways by rapamycin-mediated mammalian target of rapamycin inhibition. Cancer Res **65:**7052-8.

115. **Tabuchi, M., A. Audhya, A. B. Parsons, C. Boone, and S. D. Emr.** 2006. The phosphatidylinositol 4,5-biphosphate and TORC2 binding proteins Slm1 and Slm2 function in sphingolipid regulation. Mol Cell Biol **26:**5861-75.

116. **Tee, A. R., and J. Blenis.** 2005. mTOR, translational control and human disease. Semin Cell Dev Biol **16:**29-37.

117. **Torres, J., C. J. Di Como, E. Herrero, and M. A. De La Torre-Ruiz.** 2002. Regulation of the cell integrity pathway by rapamycin-sensitive TOR function in budding yeast. J Biol Chem **277:**43495-504.

118. **Toutouzas, K., C. Di Mario, R. Falotico, T. Takagi, G. Stankovic, R. Albiero, N. Corvaja, and A. Colombo.** 2002. Sirolimus-eluting stents: a review of experimental and clinical findings. Z Kardiol **91 Suppl 3:**49-57.

119. **Uetz, P., L. Giot, G. Cagney, T. A. Mansfield, R. S. Judson, J. R. Knight, D. Lockshon, V. Narayan, M. Srinivasan, P. Pochart, A. Qureshi-Emili, Y. Li, B. Godwin, D. Conover, T. Kalbfleisch, G. Vijayadamodar, M. Yang, M. Johnston, S. Fields, and J. M. Rothberg.** 2000. A comprehensive analysis of protein-protein interactions in Saccharomyces cerevisiae. Nature **403:**623-7.

120. **Vezina, C., A. Kudelski, and S. N. Sehgal.** 1975. Rapamycin (AY-22,989), a new antifungal antibiotic. I. Taxonomy of the producing streptomycete and isolation of the active principle. J Antibiot (Tokyo) **28:**721-6.

121. **Wedaman, K. P., A. Reinke, S. Anderson, J. Yates, 3rd, J. M. McCaffery, and T. Powers.** 2003. Tor kinases are in distinct membrane-associated protein complexes in Saccharomyces cerevisiae. Mol Biol Cell **14:**1204-20.

122. **Wei, H., D. G. Ashby, C. S. Moreno, E. Ogris, F. M. Yeong, A. H. Corbett, and D. C. Pallas.** 2001. Carboxymethylation of the PP2A catalytic subunit in Saccharomyces cerevisiae is required for efficient interaction with the B-type subunits Cdc55p and Rts1p. J Biol Chem **276:**1570-7.

123. **Wendel, H. G., E. De Stanchina, J. S. Fridman, A. Malina, S. Ray, S. Kogan, C. Cordon-Cardo, J. Pelletier, and S. W. Lowe.** 2004. Survival signalling by Akt and eIF4E in oncogenesis and cancer therapy. Nature **428:**332-7.

124. **Wielowieyski, P. A., S. Sevinc, R. Guzzo, M. Salih, J. T. Wigle, and B. S. Tuana.** 2000. Alternative splicing, expression, and genomic structure of the 3' region of the gene encoding the sarcolemmal-associated proteins (SLAPs) defines a novel class of coiled-coil tail-anchored membrane proteins. J Biol Chem **275:**38474-81.

125. **Wullschleger, S., R. Loewith, and M. N. Hall.** 2006. TOR signaling in growth and metabolism. Cell **124:**471-84.

126. **Wullschleger, S., R. Loewith, W. Oppliger, and M. N. Hall.** 2005. Molecular organization of target of rapamycin complex 2. J Biol Chem **280:**30697-704.

127. **Xiang, Q., C. Rasmussen, and N. L. Glass.** 2002. The ham-2 locus, encoding a putative transmembrane protein, is required for hyphal fusion in Neurospora crassa. Genetics **160:**169-80.

128. **Xie, M. W., F. Jin, H. Hwang, S. Hwang, V. Anand, M. C. Duncan, and J. Huang.** 2005. Insights into TOR function and rapamycin response: chemical genomic profiling by using a high-density cell array method. Proc Natl Acad Sci U S A **102:**7215-20.

129. **Yaffe, M. P., and G. Schatz.** 1984. Two nuclear mutations that block mitochondrial protein import in yeast. Proc Natl Acad Sci U S A **81:**4819-23.

130. **Yang, Q., K. Inoki, T. Ikenoue, and K. L. Guan.** 2006. Identification of Sin1 as an essential TORC2 component required for complex formation and kinase activity. Genes Dev **20:**2820-32.

131. **Zheng, X., C. Xu, A. Di Lorenzo, B. Kleaveland, Z. Zou, C. Seiler, M. Chen, L. Cheng, J. Xiao, J. He, M. A. Pack, W. C. Sessa, and M. L. Kahn.** 2010. CCM3 signaling through sterile 20-like kinases plays an essential role during zebrafish cardiovascular development and cerebral cavernous malformations. J Clin Invest **120:**2795-804.

132. **Zoncu, R., A. Efeyan, and D. M. Sabatini.** 2011. mTOR: from growth signal integration to cancer, diabetes and ageing. Nat Rev Mol Cell Biol **12:**21-35.

133. **Zurita-Martinez, S. A., and M. E. Cardenas.** 2005. Tor and cyclic AMP-protein kinase A: two parallel pathways regulating expression of genes required for cell growth. Eukaryot Cell **4:**63-71.

APPENDIX

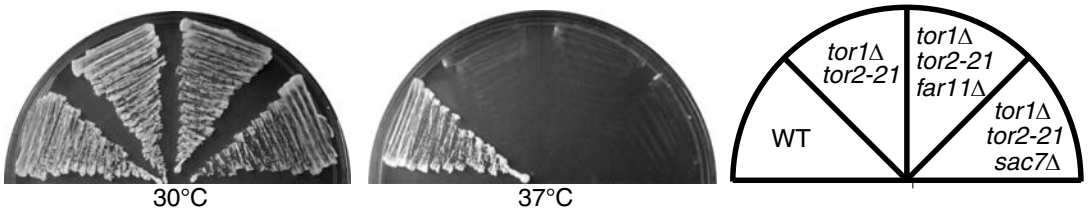

Figure A1. *sac7Δ* and *far11Δ* do not suppress the temperature sensitive growth phenotype of a *tor1Δtor2-21* double mutant.

Wild-type (SH100), *tor1Δ tor2-21* (SH221), *tor1Δ tor2-21 sac7Δ* (TPY112), and *tor1Δ tor2-21 far11Δ* (TPY118) cells were grown on YPD plates at 30 °C and 37 °C.

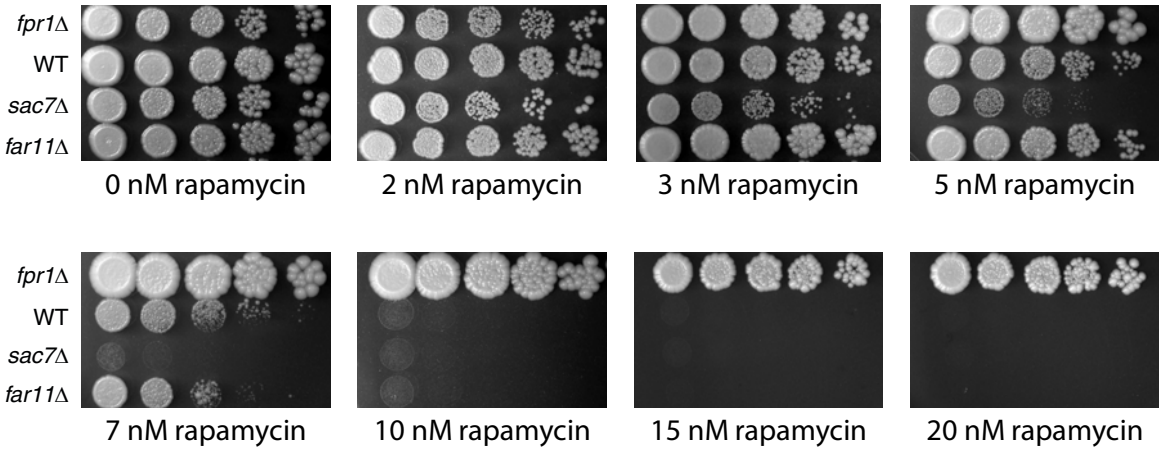

Figure A2. The effect of rapamycin on the growth of *sac7Δ* and *far11Δ* mutant cells.

Cultures of wild-type (ZLY423), *fpr1Δ* (TPY122), *sac7Δ* (ZLY2404), and *far11Δ* mutant (TPY114) cells were serially diluted and spotted on YPD plates supplemented with different concentrations of rapamycin.

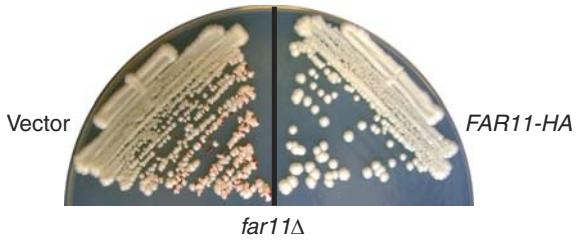

Figure A3. A *FAR11-HA* fusion construct is functional.

far11Δ mutant cells (*lst8Δ ade2-1 far11Δ*, TPY114) carrying plasmid pRS412-LST8 and either pRS416 empty vector (Vector) or pRS416-FAR11-HA (*FAR11-HA*, pZL2762) were grown on YNBcasD medium supplemented with adenine.

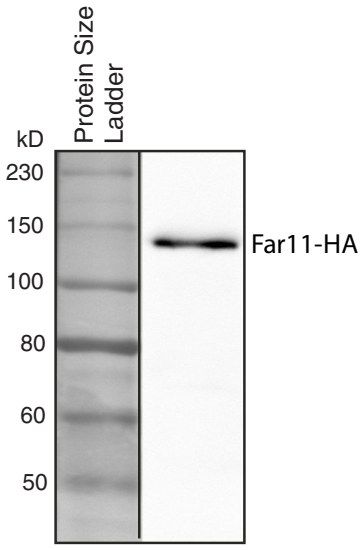

Figure A4. Far11-HA in total cellular proteins prepared by trichloroacetic acid precipitation exists as a single band on Western blots.

Total cellular proteins were prepared from the yeast strain SY4078 carrying a centromeric plasmid encoding *FAR11-HA* (pZL2762) using the NaOH-β mercaptoethanol-trichloroacetic acid method as described (129) and separated by SDS-PAGE. Far11-HA was detected by immunoblotting with the high affinity rat monoclonal anti-HA antibody 3F10 (Roche).

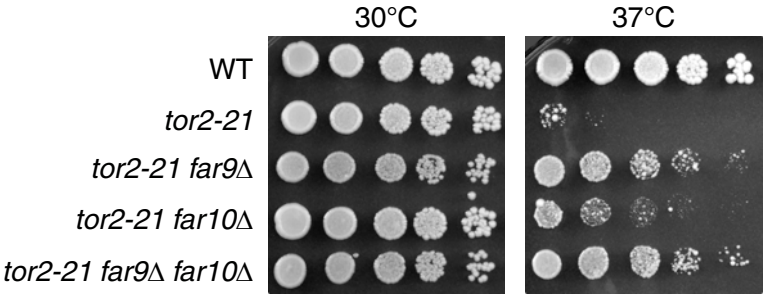

Figure A5. The effect of *far9Δ* and *far10Δ* on suppressing the temperature-sensitive growth phenotype of a *tor2*-21 mutant.

Wild-type (SH100), *tor2-21* (SH121), *tor2-21 far9Δ* (TPY207), *tor2-21 far10Δ* (TPY264) and *tor2-21 far9Δ far10Δ* mutant (TPY220) cells were serially diluted and spotted on YPD plates and grown at 30 °C and 37 °C.

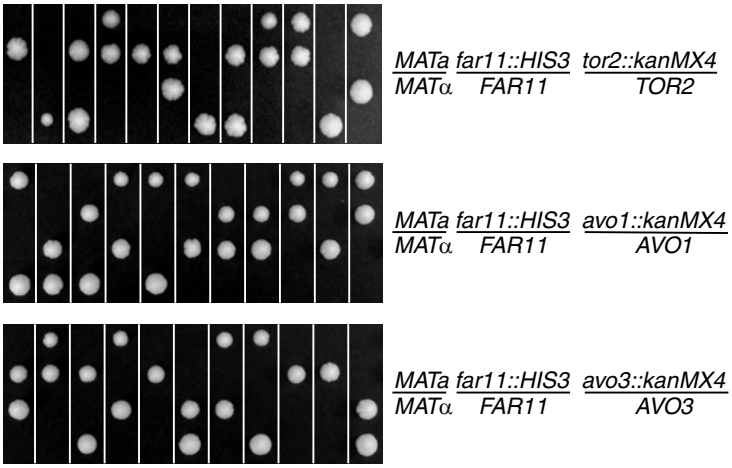

Figure A6. Tetrad analysis of sporulated diploid cells heterozygous for mutations in *FAR11* and *TOR2, AVO1,* or *AVO3*.

None of the colonies were geneticin (G418) resistant, indicating that no viable *tor2Δ*, *avo1Δ*, or *avo3Δ* mutant haploid cells were generated.

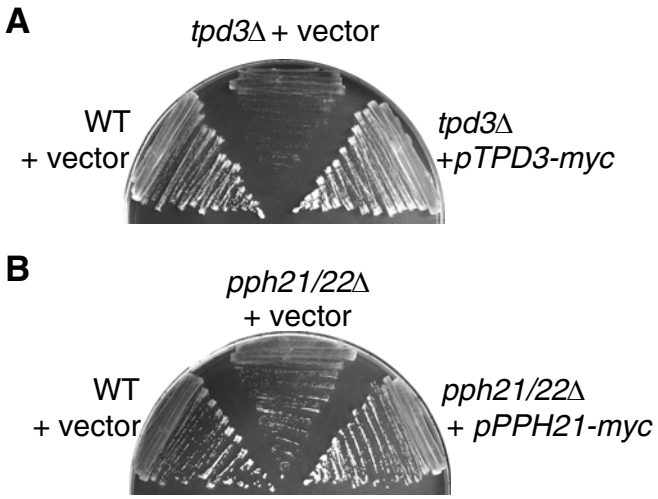

Figure A7. Tpd3-myc and Pph21-myc are functional.

(A) Wild type (BY4741) and isogenic *tpd3Δ* mutant (BY4741 tpd3) cells carrying an empty vector (pRS415) or *TPD3-myc* plasmid (pTP242) as indicated were grown on leucine-dropout medium and the picture was taken after 3 days.

(B) Wild type (BY4741) and isogenic *pph21/22Δ* mutant (BY4741 pph21/22) cells carrying an empty vector (pRS415) or *PPH21-myc* plasmid (pTP244) were analyzed for cell growth as described for panel A.

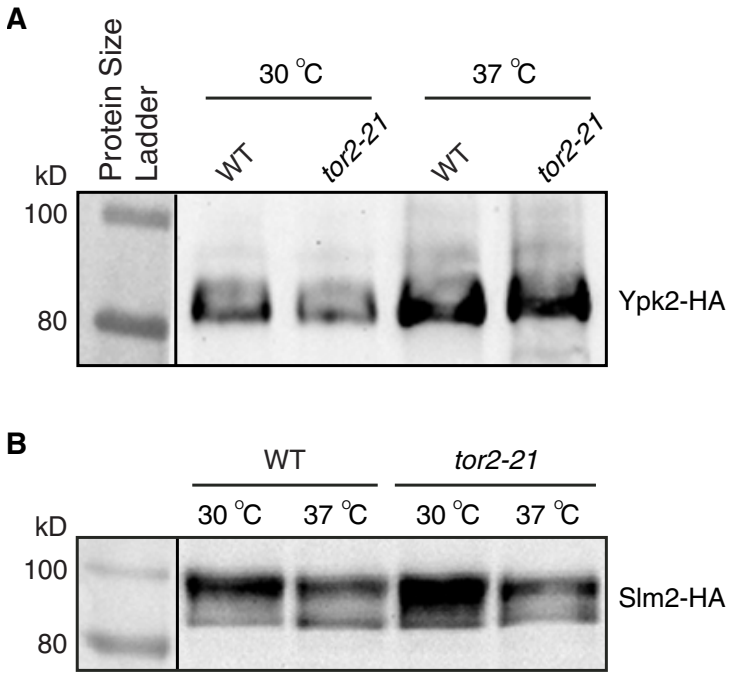

Figure A8. Immunoblot analysis of HA-tagged Ypk2 (A) and Slm2 (B).

Wild-type (WT, SH100) and temperature-sensitive *tor2-21* mutant cells (SH121) expressing C-terminal 3xHA-tagged Ypk2 or Slm2 from a centromeric plasmid (*YPK2-HA*, pTP271; *SLM2-HA*, pTP377) were grown in YNBcasD medium at 30 °C to mid-log phase and switched to 37 °C for 3h before cellular proteins were processed for Western blotting.

Table 1. Supplemental Strains used in Chapter 2.

Strain	Genotype	Source	Application
TPY114 (*far11*)	*MATa ade2-1 ura3 his3-11,15 leu2 lst8::LEU2 far11::kanMX4 [pRS412-LST8]*	This study	Fig, A2, A3
SY4078	SY2227 *FAR7-myc13-KAN <pSL2771>*	(68)	Fig. A4
SH100 (WT)	*MATa leu2-3,112 ura3-52 rme1 trp1 his4 HMLa ade2 tor2::ADE2 [YCplac111::TOR2]*	(57)	Fig. A1, A5, A8
SH121 (*tor2-21*)	*MATa leu2-3,112 ura3-52 rme1 trp1 his4 HMLa ade2 tor2::ADE2 [YCplac111::tor2-21]*		Fig. A5, A8
SH221 (*tor1 tor2-21*)	*MATa leu2-3,112 ura3-52 rme1 trp1 his3 HMLa ade2 tor1::HIS3 tor2::ADE2 [YCplac111::tor2-21]*		Fig. A1
TPY110 (*tor2-21 sac7*)	SH121 *sac7::kanMX4*	This study	
TPY311 (*tor2-21 far11*)	SH121 *far11::TRP1*	This study	
TPY301 (*tor2-21 sac7 far11*)	SH121 *sac7::kanMX4 far11::TRP1*	This study	
TPY112	SH221 *sac7::kanMX4*	This study	Fig. A1
TPY118	SH221 *far11::kanMX4*	This study	Fig. A1
TPY207 (*tor2-21 far9*)	SH121 *far9::kanMX4*	This study	Fig. A5
TPY264 (*tor2-21 far10*)	SH121 *far10::URA3*	This study	Fig. A5
TPY220 (*tor2-21 far9 far10*)	SH121 far9::kanMX4 *far10::URA3*	This study	Fig. A5
ZLY423 (WT)	*MATa ade2-1 ura3 his3-11,15 leu2 lst8::LEU2 [pRS412-LST8]*	This study.	Fig. A2
TPY122 (*fpr1*)	*MATa ade2-1 ura3 his3-11,15 leu2 lst8::LEU2 fpr1::kanMX4 [pRS412-LST8]*	This study	Fig. A2
ZLY2404 (*sac7*)	*MATa ade2-1 ura3 his3-11,15 leu2 lst8::LEU2 sac7::kanMX4 [pRS412-LST8]*	This study	Fig. A2
TPY114 (*far11*)	*MATa ade2-1 ura3 his3-11,15 leu2 lst8::LEU2 far11::kanMX4 [pRS412-LST8]*	This study	

BY4741 (*pph21/22*)	*MATa ura3 leu2 his3 met15 pph21::kanMX4 pph22::kanMX4*	This study	Fig. A7
BY4741	*MATa ura3 leu2 his3 met15*	Yeast genome deletion project	Fig. A7
BY4741 *tpd3*	BY4741 *tpd3::kanMX4*		Fig. A7
BY4743	*MATa/MATalpha ura3/ura3 leu2/leu2 his3/his3 lys2/LYS2 met15/MET15*		
BY4743 *tor2/TOR2*	BY4743 *tor2::kanMX4/TOR2*		
BY4743 *avo1/AVO1*	BY4743 *avo1::kanMX4/AVO1*		
BY4743 *avo3/AVO3*	BY4743 *avo3::kanMX4/AVO3*		
TPY654	BY4743 *tor2::kanMX4/TOR2 far11::HIS3/FAR11*	This study	Fig. A6
TPY652	BY4743 *avo1::kanMX4/AVO1 far11::HIS3/FAR11*	This study	Fig. A6
TPY653	BY4743 *avo3::kanMX4/AVO3 far11::HIS3/FAR11*	This study	Fig. A6

Table 2. Supplemental Plasmids used in Chapter 2.

Plasmid	Description	Source
pZL2762	pRS416-FAR11-HA, expressing Far11 from its own promoter with a 3xHA tag at the C-terminus.	This study
pTP377	pRS416-SLM2-HA, expressing Slm2 from its own promoter with a 3xHA tag at the C-terminus.	This study
pTP271	pRS416-YPK2-HA, expressing Ypk2 from its own promoter with a 3xHA tag at the C-terminus.	This study
pZL1255	pRS412-LST8	This study
pTP242	pRS415-ADH1-TPD3-myc, expressing Tpd3 from the *ADH1* promoter with a 3xmyc tag at the C-terminus.	This study
pTP244	pRS415-PPH21-myc, expressing Pph21 from its own promoter with a 3xmyc tag at the C-terminus.	This study

March 15, 2013

James E. Payne, Ph.D.
Interim Provost and VP for Academic Affairs
Executive Director of Graduate Programs
University of New Orleans
Administration Building 205
2000 Lakeshore Dr.
New Orleans, LA 70148

Dear Dr. Payne,

I give permission for the paper in *Genetics* titled "TORC2 Signaling is Antagonized by Protein Phosphatase 2A and the Far Complex in *Saccaromyces cerevisiae*" to be used in Tammy Pracheil's dissertation

Sincerely,

Janet L. Thornton

VITA

Tammy Marie Pracheil, daughter of Francis and Cindy Pracheil, was born in Bridge City, Louisiana. She received her high school diploma from L.W. Higgins Senior High School in Marrero, Louisiana in 2004. In 2008, she graduated Cum Laude receiving her Bachelor of Science in Biological Sciences from the Department of Biology at the University of New Orleans, New Orleans, Louisiana.

In the summer of 2008, she was admitted into the Graduate School of the Department of Chemistry at the University New Orleans to pursue a PhD in Biochemistry, and became a member of Professor Zhengchang Liu's research group. In May 2012, she was awarded a Master of Science from the Department of Chemistry. She will receive her PhD in May 2013.